# Oxidative stress pathways in the pathogenesis of renal fibrosis:

# Multiple cellular stress proteins as regulative molecules and therapeutic targets

Dissertation

for the award of the degree

"Doctor rerum naturalium" (Dr.rer.nat.)

of the Georg-August-Universität Göttingen

within the doctoral program Biology and Psychology

of the Georg-August University School of Science (GAUSS)

Submitted by

**Marwa Eltoweissy**

From Alexandria, Egypt

**Göttingen, 2015**

**Thesis Committee:**

**Prof. Dr. Ernst A. Wimmer**
Head of the Developmental Biology Department,
Johann-Friedrich-Blumenbach Institute for Zoology and Anthropology,
Georg-August-University Göttingen.

**Prof. Dr. med. Uwe Groß**
Head of the Medical Microbiology Department,
Medical Microbiology Institute, University Medical Center Göttingen.

**Members of the Examination Board:**

**Reviewer: Prof. Dr. Ernst A. Wimmer**
Head of the Developmental Biology Department,
Johann-Friedrich-Blumenbach Institute for Zoology and Anthropology,
Georg-August University Göttingen.

**Second Reviewer: Prof. Dr. med. Uwe Groß**
Head of the Medical Microbiology Department,
Medical Microbiology Institute, University Medical Center Göttingen.

**Further members of the Examination Board:**

**Prof. Dr. med. Heidi Hahn**
Head of the Tumor Genetics Department,
Human genetics Institute, University Medical Center Göttingen.

**Prof. Dr. Rolf Daniel**
Head of the Genomic and Applied Microbiology Department,
Microbiology and Genetics Institute, Georg-August University Göttingen.

**PD Dr. Michael Hoppert**
General Microbiology Department,
Microbiology and Genetics Institute, Georg-August University Göttingen.

PD **Dr. Roland Dosch**
Developmental Biochemistry Department,
Developmental Biochemistry Institute, University Medical Center Göttingen.

**Date of the oral examination:** 13.02.2015

**DECLARATION**

I hereby declare that the Ph.D. thesis entitled

"**Oxidative stress pathways in the pathogenesis of renal fibrosis: Multiple cellular stress proteins as regulative molecules and therapeutic targets.**" has been written independently, with no other sources than quoted, and no portion of the work referred to in the thesis has been submitted in support of an application for another degree.

**Marwa Eltoweissy**

*Dedicated to my beloved husband and children,*

*whose love, faith in me, and wishes for my success*

*had helped me in my path.*

# Table of Contents

# List of Abbreviations

**~: Approximately**

**%: Percent**

**°C: Degree Celsius**

**>: Greater than**

**≥: Greater than or equal**

**<: Less than**

**≤: Less than or equal**

**2-DE: Two dimensional gel electrophoresis**

**2-Cys Prx: 2-cysteine peroxiredoxins**

**AGE: Advanced glycoxidation end product**

**ANG II: Angiotensin II**

**$AT_1R$: ANG II type-1 receptor**

**$AT_2R$: ANG II type-2 receptor**

**Å: Angstrom**

**ACN: Acetonitrile**

**ACTB: β-actin**

**ANOVA: Analysis of variance**

**ANXA1: Annexin A1**

**ANXA2: Annexin A2**

**ANXA5: Annexin A5**

**ACTA2: Actin, aortic smooth muscle**

**bFGF: basic fibroblast growth factor**

**BSA: Bovine serum albumin**

**Bis-Tris: [Bis(2-hydroxyethyl)-amino-tris(hydroxymethyl)-methane]**

**CKD: Chronic kidney disease**

**Cu-Zn-SOD: Copper-zinc superoxide dismutase**

**C106, Cys106: Cysteine 106**

**Cys106-$SO_2^-$: Cysteine sulfinic acid**

**Cys106-$SO^-$: Cysteine sulfenic acid**

**Cys46: Cysteine 46**

**Cys53: Cysteine 53**

**Col4a3: Collagen alpha-3(IV) chain**

**cm: Centimeter**

**$cm^2$: Square centimeter**

**$CO_2$: Carbon dioxide**

**CHAPS: 3-[(3-cholamidopropyl)dimethylammonio]-1-propanesulfonate**

**c-myc: a regulator gene that codes for a transcription factor**

**COL1A1: Collagen alpha-1(I) chain**

**COL4A1: Collagen alpha-1(IV) chain**

**CPI: Isoelectric point**

**CFL1: Cofilin-1**

**DNA: Deoxyribonucleic acid**

**DMEM: Dulbecco's modified Eagle's medium**

**DTT: Dithiothreitol**

**Da: Dalton**

**DAPI: 3,3-diaminobenzidine**

**DAVID: Database for Annotation Visualization and Integrated Discovery**

**DAVID IDs: DAVID identifiers**

**DES: Desmin**

**DHR-123: Dihydrorhodamine-123**

**DMSO: Dimethyl sulfoxide**

**ESRD: End-stage renal disease**

**ECM: Extracellular matrix**

**E18Q: Glutamine side chain**

**E18D: Aspartic acid side chain**

**EMT: Epithelial mesenchymal trans differentiation**

**ER: Endoplasmic reticulum**

**ENO1: Alpha-enolase**

**e.g.: Example**

**ESI-MS: Electrospray ionization mass spectrometry**

**E18: Glutamic acid side chain or carboxylic acid side chain**

**ECL: Enhanced chemiluminescence**

**FCS: Fetal calf serum**

**FN1: Fibronectin 1**

**GRF: Glomerular filtration rate**

**Glu18: Glutamic acid side chain or carboxylic acid side chain**

**g: Gravitational (unit of centrifugation)**

**GRP78: 78 kDa glucose-regulated protein**

**G-418: Geneticin**

**GO: Gene Ontology**

**GAPDH: Glyceraldehyde-3-phosphate dehydrogenase**

**GDIA1: Rho GDP-dissociation inhibitor 1**

**GDIA2: Rho GDP-dissociation inhibitor 2**

**GAT: Sodium- and chloride-dependent GABA transporter**

**$H_2O_2$: Hydrogen peroxide**

**His-126: Histidine 126**

**h: Hour**

**HCl: Hydrochloric acid**

**HSPA5: 78 kDa glucose-regulated protein**

**HSPA9: 75 kDa glucose-regulated protein**

**HRP: Horse radish peroxidase**

**His tag: a polyhistidine-tag**

**HE: Hematoxylin and eosin**

**HSP90B1: Endoplasmin**

**HSP: Heat shock proteins**

**HYOU1: Hypoxia up-regulated protein 1**

**IGF: Insulin-like growth factor**

**IEF: Iso-electric focusing**

**IPG: Immobilized pH gradient**

**IgG: Immunoglobulin-G**

**IP: Immunoprecipitation**

**K/DOQI: The Kidney Disease Outcomes Quality Initiative**

**kDa: Kilo Dalton**

**kV: kilovolt**

**K130: Lysine 130**

**KRT: Keratin-like protein**

**LDH: Lactate dehydrogenase**

**Mn-SOD: Manganese superoxide dismutase**

**MS/MS: Tandem mass spectrometry**

**ml: Milliliter**

**min: Minute**

**M: Molarity**

**mM: Millimolar**

**mg/ml, mg $ml^{-1}$: Milligram per milliliter**

**mol/L: Mole per liter**

**Myc tag: a polypeptide protein tag derived from the c-myc gene product**

**Mol. wt.: Molecular weight**

**MS: Mass spectrometry**

**Max-Prob: Maximum probability**

**Min Count: Minimum count**

**MTT: [3-(4,5-dimethylthiazol-2-yl)-2,5-diphenyltetrazolium bromide]**

**NAD(P)H: Nicotinamide adenine dinucleotide phosphate**

**NF-kappaB, $NF_KB$: Nuclear factor-kappa B**

**mRNA: messenger ribonucleic acid**

**ng/µl, ng $µl^{-1}$: Nanogram per microliter**

**nM: Nanomole**

**Nrf2: Nuclear erythroid 2 related factor**

**N, nr: Number**

**Ni-NTA: Nitrilotriacetic acid**

**OS: Oxidative stress**

**$O^{2-}$: Superoxide anion**

**Opti-MEM: Reduced serum media**

**$OH^{\cdot}$: Hydroxyl radical**

**PDGF: Platelet derived growth factor**

**PARK7: Protein DJ-1**

**PD: Parkinson's disease**

**PKM2: Pyruvate kinase**

***pI*: Isoelectric point**

**p*Ka*: Acid dissociation constant**

**PRDXs: Peroxiredoxins**

**PRDX1: Peroxiredoxin-1**

**PRDX2: Peroxiredoxin-2**

**PRDX5: Peroxiredoxin-5**

**PRDX6: Peroxirodoxin-6**

**PBS: Phosphate buffered saline**

**PAGE: Polyacrylamide gel electrophoresis**

**pH: preponderance of Hydrogen ions**

**PMF: Peptide mass fingerprint**

**PMSF: phenylmethanesulfonylfluoride or phenylmethylsulfonyl fluoride**

**ppm: parts-per-million**

**$PQ^{2+}$: Paraquat**

**P: probability**

**Q-TOF: Electrospray ionization time of flight**

**RAS: Renin-angiotensin system**

**ROS: Reactive oxygen species**

**RNA: Ribonucleic acid**

**rpm: rotation per minute**

**SODs: Superoxide dismutases**

**SOD1: Copper-zinc superoxide dismutase**

**SOD2: Manganese superoxide dismutase**

**siRNA: small interfering RNA**

**SD: Standard deviation**

**SDS: Sodium dodecyl sulfate**

**STD: Standard**

**sec: Second**

**STRING: Search Tool for the Retrieval of Interacting Genes/proteins**

**Seq. Cov.: Sequence coverage**

**SV40: Simian vacuolating virus 40**

**STIP1: Stress-induced-phosphoprotein 1**

**TGFß1: Transforming growth factor beta 1**

**TNFα: Tumor necrosis growth factor alpha**

**TNFR1: TNF-αreceptor 1**

**TNFR2: TNF-αreceptor 2**

**Tris: Trihydroxymethyl aminomethane**

**TFA: Trifluoroacetic acid**

**TBST: Tris boric acid-tween**

**TRAIL: Tumor necrosis factor-related apoptosis-inducing ligand**

**µg: Microgram**

**µl: Microliter**

**µM: Micromole**

**UV: Ultraviolet**

**UBC: Ubiquitin**

**VCAM-1: Vascular cell adhesion molecule 1**

**V: Volt**

**VCL: Vinculin**

**VIM: Vimentin**

**WT: Wild type**

**WB: Western blot**

**wk: Week**

**w/v: weight/volume**

# List of Tables

# List of Figures

# 1. General Introduction

## 1.1 Chronic kidney disease (CKD)

One of the key functions of the kidneys is to filter waste products that build up in the blood. Renal failure determines that waste products are not removed completely or sufficiently. This can occur quickly (acute kidney injury) often as the result of ischemia, toxins or mechanical trauma (1). More often, however, the development of renal failure is gradual and insidious, with resultant chronic kidney disease (CKD) (1). CKD is a common and serious problem that adversely affects human health, limits longevity, and increases costs to health-care systems worldwide (1). It is often many years before noticeable loss of renal function occurs. People with CKD have a high risk of death from stroke or heart attack (2).

CKD is characterized by a progressive decline in the glomerular filtration rate (GFR); the diagnosis is made on the basis of a reduced GFR for a minimum of 3 months (3). The Kidney Disease Outcomes Quality Initiative of the National Kidney Foundation K/DOQI (4) has proposed a classification scheme for CKD that has been widely adopted (Fig. 1.1). Stage 4 CKD denotes a severe decline in the GFR. Patients with stage 3-4 CKD are at risk for progression of kidney disease and development of end-stage renal disease (ESRD) (5, 6). Moreover, these patients appear to be at even greater risk for the development of cardiovascular disease and associated morbidity and mortality (2, 5, 7). Dialysis or transplantation is then necessary, with loss of quality of life, decreased individual life expectancy and increased costs to healthcare systems (1).

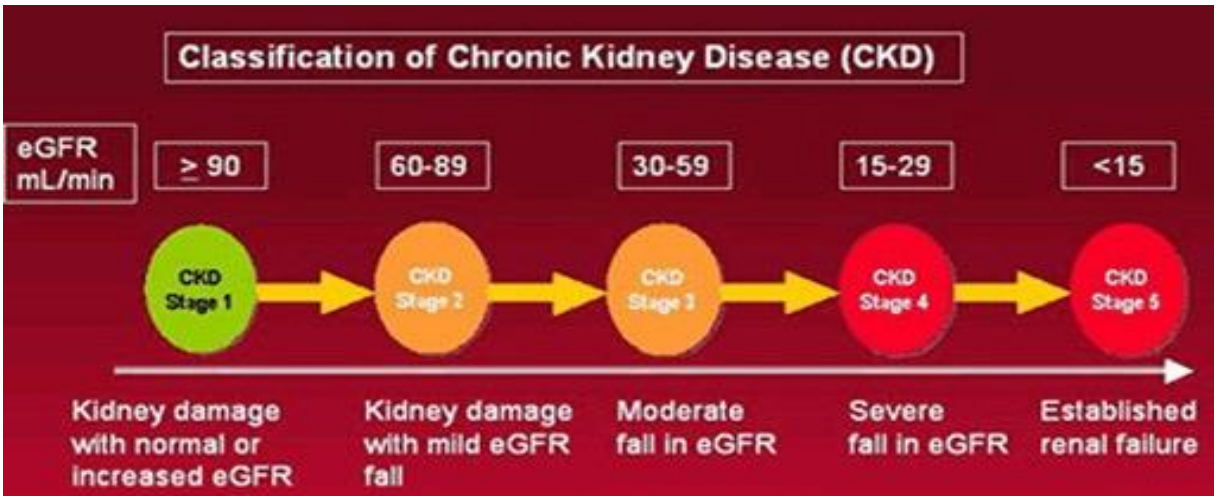


**Figure 1.1: Classification of chronic kidney disease**

National Kidney Foundation. K/DOQI, 2002 (4). Clinical practice guidelines for chronic kidney disease: Evaluation, classification, and stratification.

CKD has increasing incidence and prevalence in developed and developing nations. The kidneys show the greatest age-associated chronic pathology compared with brain, liver, and heart (8), and one in six adults over 25 years of age has some degree of CKD (9), with incidence increasing with age.

The structural characteristics of CKD include increased tubular atrophy, interstitial fibrosis, glomerulosclerosis, renal vasculopathy, peritubular capillary rarefaction, reduced renal regenerative capability, and inflammation (10, 11). These characteristics may be caused, at least inpart, by the gradual loss of renal energy through development of mitochondrial dysfunction and resultant increasing oxidative stress (OS) (1). OS is prevalent in CKD patients and is considered to be an important pathogenic mechanism (1, 12, 13).

## 1.2 Oxidative stress (OS)

Oxygen is the primary oxidant in metabolic reactions designed to obtain energy from the oxidation of a variety of organic molecules. OS results from the metabolic reactions that use oxygen, and it has been defined as a disturbance in the equilibrium status of pro-oxidant/anti-oxidant systems in intact cells (13). During these processes, small amounts of partially

reduced reactive oxygen forms are produced as an unavoidable by-product of mitochondrial respiration. Some of these forms are free radicals referred to as reactive oxygen species (ROS) (13). In addition, other extracellular factors such as hormones, growth factors, and proinflammatory cytokines also affect the production of OS (13-19). Further, systemic diseases such as hypertension, diabetes mellitus, and hypercholesterolemia; infection; antibiotics, chemotherapeutics, radiocontrast agents; and environmental toxins, occupational chemicals, radiation, smoking, as well as alcohol consumption also induce OS (13).

OS has been identified and proven to be the root cause of more than 70 chronic degenerative diseases such as heart disease, cancer, stroke, diabetes, Alzheimer's dementia, Parkinson's disease, macular degeneration and other serious ailments, according to Dr Ray D. Strand, an expert in nutritional medicine (20). In the kidney, OS has been reported to play a critical role in the pathology of acute renal failure (21) and as a common pathway to chronic tubulointerstitial injury (22). The collective information on the role of oxidants that is derived from models of glomerular disease as well as progressive renal failure is impressive (6, 21-25).

### 1.2.1 Reactive oxygen species (ROS)

In physiological conditions, ROS produced in the course of normal conditions are completely inactivated by intact pro-oxidant/anti-oxidant processes that continuously generate and detoxify oxidants during normal aerobic metabolism (26-28). This means that normally there is a balance between pro-oxidant (or oxidant) and antioxidant defense systems. An imbalance between free radical-generating and radical scavenging systems in intact cells has been associated with the cell injury seen in numerous pathologic conditions ultimately leading to cellular damage in severe OS (26-28). The effects of these reactive species are wide-ranging,

but three reactions are particularly relevant to cell injury: lipid peroxidation of membranes, oxidative modification of proteins, and oxidative damage to DNA (29).

Exacerbated production of ROS and/or depletion of antioxidant defense system results from a myriad of different oxidative challenges that influence downstream cellular signaling thus inducing cellular damage or fibrogenic responses through stress-sensitive pathways and, in the kidney, promote renal cell fibrosis and senescence, decrease regenerative ability of cells, affect expression of inflammatory and extracellular matrix (ECM) genes and transduce cell migration and apoptosis. These factors have a stochastic deleterious effect on kidney function (30-34).

The exact sources of ROS generated in biological systems under different disease states are always elusive as they are also a part of physiological processes. The principal intracellular sources of ROS include the mitochondrial electron transport system (cytochrome c oxidase enzyme), peroxisomes, 5′-lipoxygenase, and NAD(P)H oxidase enzymes (35, 36) whereas, commonly described exogenous factors involved in the generation of ROS are represented by inflammatory cytokines, chemotherapeutic drugs, and toxins (36).

## 1.3 OS in promoting CKD

OS is a constant feature and major mediator of CKD progression. Oxidants may contribute to progressive renal disease by virtue of their renal haemodynamic actions, by impairing glomerular selective properties, by inducing inordinate or aberrant growth responses, by inducing loss of cellular phenotype and apoptosis, and by promoting acute and chronic inflammatory responses and certain adhesion molecules and proinflammatory mediators (37). Traditional risk factors such as hypertension, diabetes, obesity, metabolic syndrome (38), as well as acute kidney injury (39), can damage the kidney directly or by enhancing intrarenal atherogenesis. Evidence indicates that increased OS may mediate most of the effects of risk

factors on the kidney (38). Metabolic factors such as elevated free fatty acids, high glucose levels or advanced glycoxidation end products (AGEs) induce ROS in vascular cells, leading to ongoing AGE formation and to gene induction of proinflammatory cytokines. Vice versa, numerous cytokines found elevated in obesity and diabetes may also induce OS thus a 'circulus vitiosus' may be initiated and accelerated (40). Because all factors involved form a highly interwoven network of interactions, the blockade of ROS or AGE formation at different sites may interrupt the vicious cycle. Reduction in renal OS by dietary or pharmacological approaches provides an appealing target for therapies directed towards the retardation of progressive renal injury. Most important to clinical practice, a number of drugs commonly used in the treatment of diabetes, hypertension, or cardiovascular disease, such as angiotensin-converting enzyme inhibitors, $AT_1$ receptor blockers, 3-hydroxy-3-methyl-glutaryl-CoA reductase inhibitors (statins), and thiazolidindiones have shown promising preventive intracellular antioxidant activity in addition to their primary pharmacological actions (40).

## 1.4 OS triggering factors

### 1.4.1 Hydrogen peroxide ($H_2O_2$)

A reactive oxygen metabolite formed by the spontaneous or catalytic dismutation of superoxide anions ($O^{2-}$), produced by the partial reduction of oxygen during aerobic respiration and following the exposure of cells to a variety of physical, chemical, and biological agents (Fig. 1.2). The ROS that are generated by mitochondrial respiration, including $H_2O_2$, are potent inducers of oxidative damage (1). Moreover, various stimuli including cytokines and growth factors generate $H_2O_2$ in target cells by stimulating the activation of NAD(P)H oxidases (41, 42). $H_2O_2$ has been implicated in the pathogenesis of

renal injury (29). $H_2O_2$-induced renal cell damage and tissue necrosis is associated with lipid peroxidation in renal cell membranes (1, 43, 44).

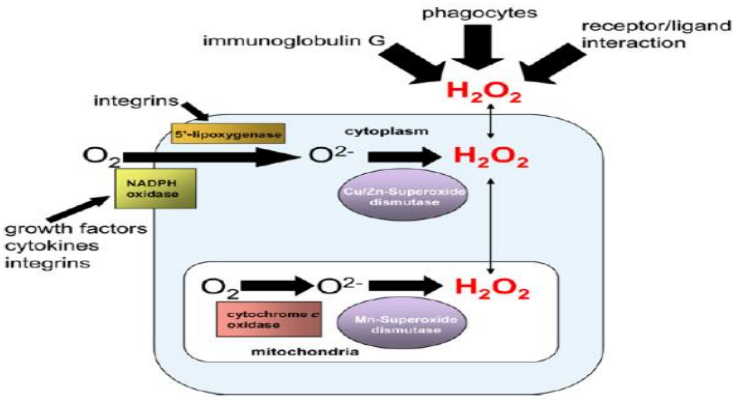


**Figure 1.2: Different sources of hydrogen peroxide**

Hydrogen peroxide can be produced extracellularly by the immunoglobulin G-catalyzed oxidation of water, by receptor/ligand interactions, and by phagocytic immune cells. Superoxide anions ($O^{2-}$), which are produced by the partial reduction of oxygen by cytochrome c oxidase in mitochondria, by membrane associated NAD(P)H oxidase, or by 5′-lipoxygenasein the cytoplasm, are rapidly converted to $H_2O_2$ by the action of cytoplasmic and mitochondrial superoxide dismutase enzymes. Growth factors, cytokines, and integrins stimulate the activation of NAD(P)H oxidase and/or 5′-lipoxygenase. $H_2O_2$ can diffuse across membranes as indicated by the finer arrows. *Adapted from reference 45.*

### 1.4.2 Angiotensin II (ANG II) and platelet derived growth factor (PDGF)

Angiotensin II is considered the major physiological active component of the renin-angiotensin system (RAS). Originally, ANG II was identified as a vasoconstrictor and potent stimulus of aldosterone release from the suprarenal gland (46, 47), yet intensive research over the past two decades has provided convincing evidence for its active role as a true renal growth factor and proinflammatory cytokine, participating in various steps of the inflammatory response by a host of fibrotic pathways including, the upregulation of profibrotic cytokines, inflammation, modulation of renal cell proliferation and tubular epithelial hypertrophy, and ECM biosynthesis and degradation thereby contributing in

progression of renal fibrosis (34,48-55). Beyond this, ANG II also incites OS in renal system, by direct induction of ROS generation (34, 56-61), (Fig.1.3).

#### 1.4.2.1 Mechanism of action of ANG II

All the components of RAS, including substrate angiotensinogen, enzymes involved in the synthesis and degradation of angiotensins, as well as receptors for angiotensins are present in the kidney (62). ANG II binds to two high-affinity receptors, the ANG II type-1 receptor ($AT_1R$) and the ANG II type-2 receptor ($AT_2R$). Signaling through the $AT_1R$ results in vasoconstriction, stimulation of growth, and activation of fibroblasts and myocytes. Signaling through the $AT_2R$ receptor results in vasodilatation and anti-proliferative responses (63). In addition, ANG II binds to its $AT_1R$ activating NAD(P)H oxidase, which in turn increases ROS generation in several tissues (64, 65) (Fig. 1.3). The NAD(P)H oxidase is a multi-subunit enzyme and is one of the enzymatic sources of superoxide production (64).

The angiotensinogen gene, which provides the precursor for ANG II production, is stimulated by NF-$_K$B activation (65-67). Interestingly NF-$_K$B is activated by ANG II in the kidney (68) through both $AT_1$ and $AT_2$ receptors (69). This provides an autocrine reinforcing loop that up-regulates ANG II production. Further, nuclear extracts obtained from the cortex of kidneys with ureteral obstruction contained proteins that bind to an NF-$_K$B-like sequence contained in the rat TNF-α gene promoter (69). TNF-α itself stimulates NF-$_K$B activation (67), which again creates an autocrine reinforcing loop for enhanced TNF-α formation (Fig. 1.3). Because the NF-$_K$B family of transcription factors have many potential combinations, it is possible that different NF-$_K$B isotypes are activated by ANG II at different phases of the progression of renal disease. Transcription factors of the NF-$_K$B family can influence directly or indirectly cellular events leading to tissue fibrosis (Fig. 1.3). ANG II stimulates NF-$_K$B activation leading to increased TNF-α synthesis, which in turn can activate further NF-$_K$B. Resident

renal cells (glomerular mesangial cells and tubular epithelial cells) are also sources of TNF-α production in renal injury (70, 71). Two TNF-α receptors have been described: one with a molecular weight of 55 kD (TNFR1) and the other with a molecular weight of 75 kD (TNFR2) (72). Binding of TNF-α to its receptors activates a number of signal transduction pathways that result in the expression of a variety of transcription factors, cytokines, growth factors, receptors, cell adhesion molecules, mediators of inflammatory processes, acute phase proteins, and major histocompatibility complex proteins (72, 73) (Fig. 1.3). Moreover, increasing levels of ANG II may up-regulate the expression of several other proliferative factors including PDGF, TGFß1, VCAM-1, bFGF, and IGF. Most of these compounds have a major role in matrix protein overproduction thereby promoting cell growth and fibrosis (74) (Fig. 1.3). PDGF stimulates synthesis of fibronectin and type III collagen (75, 76). Also, stimulates TGFß mRNA and its protein in rat kidney fibroblasts, mouse macrophages and human renal proximal tubular cells (75-77).

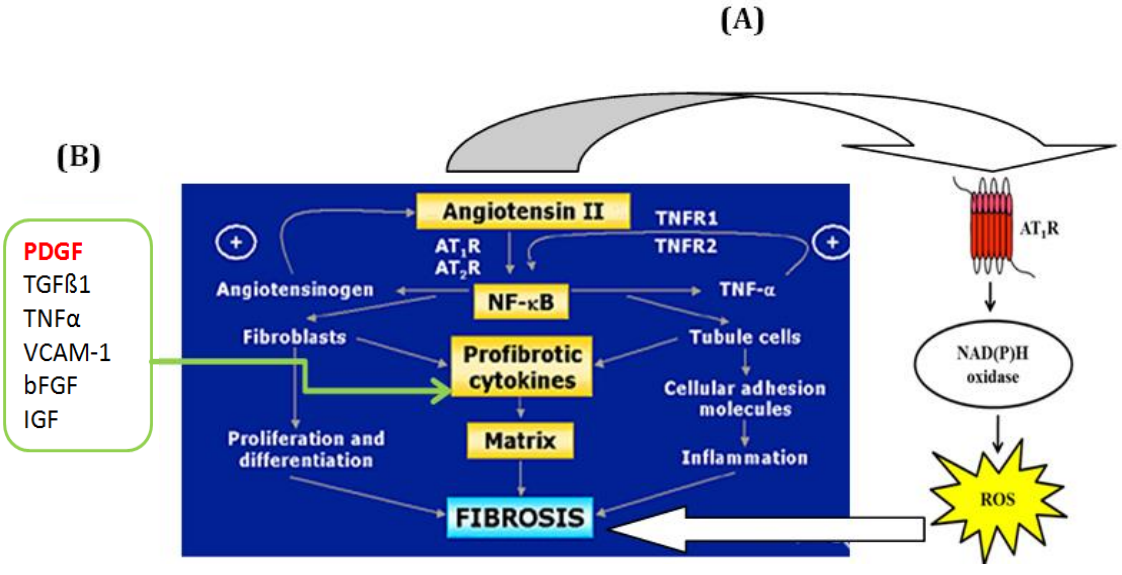


**Figure 1.3: Angiotensin II: Role in renal injury**

**(A):** Angiotensin II binds to its receptor ($AT_1R$) activating the cystolic subunits of NAD(P)H oxidase, which in turn increases ROS generation. **(B):** Increasing levels of ANG II up-regulate the expression of a large array of

cytokines, including PDGF. Most of these compounds participate in stimulating intracellular ROS formation and promote cell growth and fibrosis. *Modified from references 62 and 64.*

## 1.5 Antioxidant systems

In addition to non-enzymatic antioxidants such as vitamins C and E, carotenoids and flavonoids, cells contain a portfolio of antioxidant enzymes whose activities are directed at reducing oxidants. These enzymes can be distinguished by their catalytic mechanisms, cellular localization, and regulation. The major antioxidant enzymes involved in the catalytic breakdown of superoxide and/or peroxide anion radicals are superoxide dismutase (Cu-Zn-SOD and Mn-SOD), catalase, glutathione peroxidase, and thioredoxin peroxidase (peroxiredoxins) (1, 78-81). They are highly efficient enzymes performing their catalytic reduction by dismutation (superoxide dismutase) or by utilizing: a heme prosthetic group (catalase), a cyclic oxidation/reduction of catalytic cysteine or seleno-cysteine residues (glutathione peroxidases), or an oxidation of catalytic cysteine residues (thioredoxin peroxidases). Peroxiredoxins have been subdivided into classes based on protein similarities and the mechanism of reduction of the oxidized protein (for a review see 82). For example, the typical 2-cysteine peroxiredoxins (2-Cys Prx) contain two highly conserved cysteine residues, which are both involved in the thioredoxin-coupled catalytic reduction of $H_2O_2$.

The balance between pro- and antioxidant molecules determines the OS profile. A cell is able to overcome small perturbations and regain its original state. The formation and detoxification of ROS is tightly controlled by a homeostatic mechanism that entails a cellular protective response aiming at neutralizing the damage effect (29, 83). The previously mentioned antioxidant enzymes are examples of key players in that task.

To measure the delicate balance that exists between OS and the system in place has given rise to several tools for adequate detection and quantification (29). Emphasis is now being placed

on biomarkers of OS, which are objectively measured and evaluated as indicators of normal biological processes or pathologic responses to therapeutic intervention.

The localization and effects of OS, as well as information regarding the nature of the OS, may be gleaned from the analysis of discrete biomarkers of OS damage.

## 1.6 OS biomarkers

### 1.6.1 Protein DJ-1 (PARK7)

Protein DJ-1 is also known as the neuroprotective or Parkinson's disease-related protein. Genetic mutations that eliminate the expression of the putative neuroprotective protein DJ-1 are known to cause the familial Parkinson's disease (PD) the most common neurodegenerative disorder (84-94). An accumulating body of evidence pinpointed the important role of DJ-1 in PD (84-94).The mechanisms by which loss of DJ-1 function promotes PD have been most associated with management of ROS and the oxidative damage (for review see 95-99). Recently, we highlighted in our laboratory, the powerful role of protein DJ-1 for renal cell resistance and survival under OS triggered by $H_2O_2$ (Chapter 2) and by ANG II and PDGF (Chapter 3).

#### DJ-1structure

DJ-1 is a 20 kDa small protein with a sequence length of 189 amino acids. Ubiquitously expressed but found at higher levels in the testis, brain and kidney. Located predominantly in the cytoplasm and to a lesser extent in the nucleus and mitochondrion (89). Crystallization studies showed that wild type (WT) DJ-1 protein exists as dimers in solution (100) (Fig. 1.4A). The structure of each monomer is represented in Figure 1.4B.

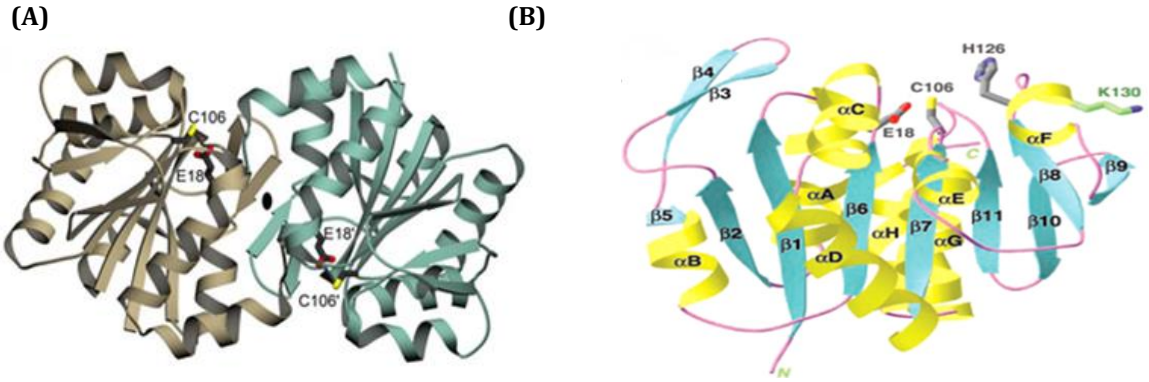


**Figure 1.4: Structure of the wild type DJ-1**

**(A):** A ribbon representation of dimeric DJ-1 is shown with the molecular two fold axis perpendicular to the plane of the page, with one monomer in brown and other in green. The oxidation prone cysteine (C106) and the interacting glutamic acid (E18) are represented in each monomer. **(B):** Structure of the DJ-1 monomer consisting of an α/β-fold with 11 ß-strands (blue) and 8 α-helices (yellow), loops (magenta), and the different side chain residues (Cys106, His126, E18, and K130). C: carboxy terminus, N: amino terminus. *Adapted from references 100 and 101*.

## DJ-1 functions

Elucidating the function and regulation of DJ-1 has been an active field of study for over a decade. Human DJ-1 has been primarily reported as an oncogene (102, 103). Later several diverse cellular roles have been ascribed to protein DJ-1: modulates transcription (104, 105) and androgen-receptor signaling (106), controls fertility (107, 108), acts as a protein chaperone (109, 110) and as a protease (111), required for correct mitochondrial morphology and function (112-114), required for autophagy of dysfunctional mitochondria (115), alters dopamine receptor signaling (116), suppresses apoptosis via interaction with kinases (117, 118), upregulates glutathione synthesis or heat shock proteins (119, 120), and of prime interest its role as an OS sensor (121-128). The function of DJ-1 protein appears to be multifaceted, the current view is that DJ-1 is a multifunctional OS response protein that

defends cells against ROS and mitochondrial damage, although the details of its biochemical function remain obscure.

## DJ-1 mutations

Numerous reports, including our own, utilizing *in vitro* and *in vivo* models in both mammalian and *Drosophila* systems support the idea that DJ-1 plays a protective role under pathological conditions where OS predominates (101, 121, 123, 124, 126, 128-134). With a shift of *pI* from 6.2 to 5.8 (135, 136), Mitsumoto *et al.,* (2001) (135) have suggested that DJ-1 may be directly oxidized by free radicals, because the *pI* shift after oxidation is consistent with formation of cysteine sulfinic acid (Cys106-$SO_2^-$) (135). Hence, formation of Cys106-$SO_2^-$ has been recognized as an important reversible posttranslational modification of proteins (101, 126, 129, 137-142). If the *pI* shift of DJ-1 represents a formation of cysteine sulfinic acid, then mutating these cysteine residues will block oxidation. Cysteine106 (Cys106) has been identified as the prime candidate for this modification (88, 100, 101, 107, 126, 129, 143-148). Phylogenetic analysis has also underscored the significance of Cys106, as human DJ-1 contains three cysteine residues (Cys46, Cys53, and Cys106) of which Cys106 is by far the best conserved (149, 150). Many studies have since shown that Cys106 is required for DJ-1 to confer cellular protection against OS (101, 126, 129, 133, 141, 148, 151-155). Moreover, Cys106 has a low thiol p*Ka* value of ~5 and therefore exists almost exclusively as highly reactive thiolate anion at physiological pH (156). Bond length analysis using atomic resolution X-ray crystallography demonstrates that a neighboring protonated carboxylic acid sidechain residue (Glu18), also known as E18, donates a hydrogen bond to Cys106 and facilitates ionization of the thiol, thereby depressing its p*Ka* value and stabilizing the Cys106-$SO_2^-$ (156). Replacement of Cys106 with other amino acids in DJ-1 resulted in a loss of protective activity against oxidative stressors in a number of systems (101, 126, 129, 133,

146, 154, 156). Whereas modifying the environment around the sidechain of Cys106 could decouple the oxidation propensity and p*Ka* of Cys106 without changing the cysteine residue itself. In 2009, Blackinton *et al.,* (101) designed several Glu18 mutations (E18N, E18D, E18Q) that altered the oxidative propensity of Cys106 (Fig. 1.5) and characterized the effect of Glu18 mutations on cytoprotective activity of Cys106. Results demonstrated that the formation of Cys106-$SO_2^-$ is indeed critical for DJ-1 to regulate its ability to protect neuronal cells against OS and mitochondrial damage. In contrast, the oxidatively impaired E18D mutant where Cys106 was oxidized to the easily reduced sulfenic acid (Cys106-$SO^-$) behaved as an inactive mutant and failed to protect cells.

The influence of WT-DJ-1 mutation by superseding the glutamic acid E18 sidechain residue with an E18Q mutant possessing a glutamine sidechain or an E18D owning an aspartic acid substitution on the oxidative manner of DJ-1 in renal fibroblasic and epithelial cells is discussed in Chapter 3.

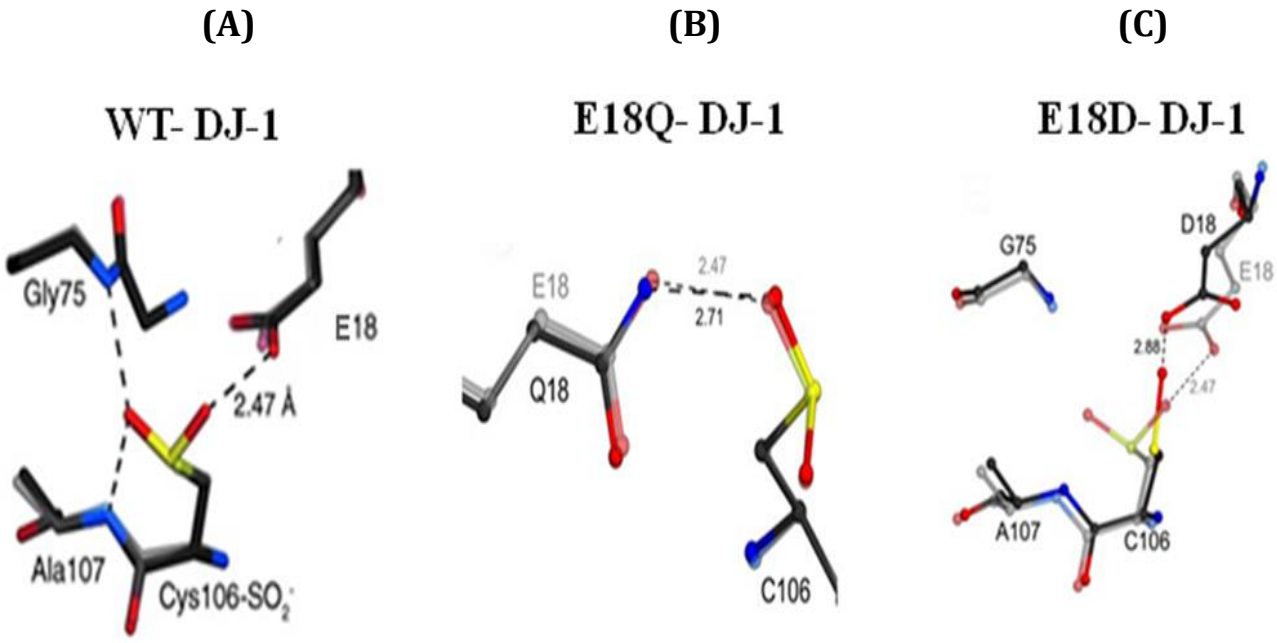

**Figure 1.5: Structural effects of wild type DJ-1 designed mutations**

**(A):** Views of the stable Cys106 sulfinic acid oxidized form of DJ-1 (Cys106-$SO_2^-$). The region around Cys106 from the crystal structure of Cys106-$SO_2^-$ DJ-1 is superimposed over the structure of reduced Cys106-$SO_2^-$ DJ-1. Stabilizing hydrogen bonds between the Cys106-$SO_2^-$ and surrounding residues are shown in dashed lines, with the key interaction between E18 and Cys106-$SO_2^-$ labeled. **(B):** A superposition of oxidized E18Q (*darker model*) and WT- DJ-1 (*lighter model*) shows that the key stabilizing hydrogen bond between residue E18 and Cys106-$SO_2^-$ is lengthened in E18Q-DJ-1, weakening this interaction. In E18Q-DJ-1, Cys106 is oxidized to the Cys106-$SO_2^-$. **(C):** A superposition of residues of Cys106 in E18D-DJ-1 (*darker model*) and the corresponding region in oxidized WT-DJ-1 (*lighter model*). The E18D substitution results in structural perturbations at Cys106 that stabilize the Cys106-$SO^-$ oxidation product and hinder further oxidation.Cys106 is oxidized to the easily reduced Cys106-$SO^-$ oxidation product in this variant. Distances given in Å. *Adapted from references 101 and 126.*

## 1.7 Objectives

OS is one of the major motifs in our substantial renal fibrosis project, where we are endeavoring to understand potential molecular mechanisms associated with the pathogenesis of renal disease. In this regard, the use of proteomic-based strategy was undertaken in the present study to screen out and identify novel molecular biomarkers of OS in renal cell line models exposed to different OS incites. A comprehensive comparison of proteome derived from control renal cells and $H_2O_2$ treated cells **(Chapter 2)**, or cytokines (ANG II and PDGF) treated cells **(Chapter 3)** are represented.

The distinctive observation for the involvement of protein DJ-1 (PARK7) in OS pathway by acquiring a *pI* shift, in addition to its high expression in cells treated with $H_2O_2$ **(Chapter 2)**, prompted us to define in depth its physiological functional importance in renal cells challenging OS. For this our work further focused on the following aims:

i) To explore the renal cell proteome alteration that accompanied the cellular adaptation to OS and identify potential key proteins in renal cell resistance to OS.

ii) To investigate and document PARK7 vital role in renal cells' resistance and adaptation under conditions of OS by, utilizing small interfering RNA (siRNA) targeting PARK7 and examining the impact on cell response to OS by employing various assays. These are addressed in **Chapter 2**.

iii) To explore the role of protein DJ-1 (PARK7) in the profibrotic cytokines triggered renal fibrosis. Furthermore to investigate the effect of DJ-1 expression regulation on cell progression towards renal fibrosis.

iv) To sought DJ-1 in renal fibrosis using fibrosis animal model.

v) To exploit wild type DJ-1 and designed mutations to define the role of DJ-1 in balancing OS in renal fibrosis.

vi) To characterize potential mechanism(s) of DJ-1 action by identifying its interaction partners. These are addressed in **Chapter 3**.

# 2. PROTEOMICS ANALYSIS IDENTIFIES PARK7 AS AN IMPORTANT PLAYER FOR RENAL CELL RESISTANCE AND SURVIVAL UNDER OXIDATIVE STRESS

---

In this part of the work we performed a thorough comparison of proteome derived from control renal cells and $H_2O_2$ treated cells to explore the renal cell proteome alteration that resulted as a consequence to the cellular adaptation to OS. Potential key proteins in renal cell resistance to OS were identified, characterized and verified. In another set of experiments using DHR-123 agent, we confirmed the accumulation of ROS derivatives under OS conditions. We further investigated and documented PARK7 vital role in renal cells' resistance and adaptation under conditions of OS by utilizing small interfering RNA (siRNA) targeting PARK7 and testing the impact on cell response to OS by morphological examinations and by employing the MTT viability assay.

**Authors:** Marwa Eltoweissy, Gerhard A. Müller, Asima Bibi, Phuc Van Nguye, Gry H. Dihazi, Claudia A. Müller, and Hassan Dihazi.

**Contribution:** All experiments besides,
Asima Bibi: MTT assay for HK-2 cells (Fig. 9C).

**Status of publication:** *Published in: Mol BioSyst (2011), 7(4): 1277-88.*
*(Impact Factor: 4.02)*

**Congress presentations:**

1. **Kongress der Gesellschaft für Nephrologie (GfN), 27-29 September 2009, Göttingen, Deutschland.**

2. **90th Annual Meeting of the German Physiological Society (DPG) 26-29 March 2011, Regensburg, Germany.**

3. **10th HUPO World Congress 4-7 September 2011, Geneva, Switzerland.**

Molecular BioSystems

Dynamic Article Links View Online

Cite this: DOI: 10.1039/c0mb00116c

www.rsc.org/molecularbiosystems

PAPER

# Proteomics analysis identifies PARK7 as an important player for renal cell resistance and survival under oxidative stress

Marwa Eltoweissy,[a] Gerhard A. Müller,[a] Asima Bibi,[a] Phuc Van Nguye,[a] Gry H. Dihazi,[a] Claudia A. Müller[b] and Hassan Dihazi*[a]

*Received 26th July 2010, Accepted 18th January 2011*
**DOI: 10.1039/c0mb00116c**



Renal fibrosis is a process that is characterized by declining excretory renal function.The molecular mechanisms of fibrosis are not fully understood. Oxidative stress pathways were reported to be involved in renal tissue deterioration and fibrosis progression. In order to identify new molecular targets associated with oxidative stress and renal fibrosis, differential proteomics analysis was performed with established renal cell lines (TK173 and HK-2). The cells were treated with oxidative stress triggering factor $H_2O_2$ and the proteome alterations were investigated. Two dimensional protein maps were generated and differentially expressed proteins were processed and identified using mass spectrometry analysis combined with data base search. Interestingly the increase of ROS in the renal cell lines upon $H_2O_2$ treatment was accompanied by alteration of a large number of proteins, which could be classified in three categories: the first category grouped the proteins that have been described to be involved in fibrogenesis (e.g. ACTA2, VCL, VIM, DES, KRT, COL1A1, COL4A1), the second category, which was more interesting involved proteins of the oxidative stress pathway (PRDX1, PRDX2, PRDX6, SOD, PARK7, HYOU1), which were highly up-regulated under oxidative stress, and the third category represented proteins, which are involved in different other metabolic pathways. Among the oxidative stress proteins the up-regulation of PARK7 was accompanied by a shift in the pI as a result of oxidation. Knockdown of PARK7 using siRNA led to significant reduction in renal cell viability under oxidative stress. Under $H_2O_2$ treatment the PARK7 knockdown cells showed up to 80% decrease in cell viability and an increase in apoptosis compared to the controls. These results highlight for the first time the important role of PARK7 in oxidative stress resistance in renal cells.

## Introduction

Organisms and cells undergo a variety of molecular and physiological changes resulting from their interaction with the environment. Respiration or exposure to external agents (*e.g.* light, ionizing radiation or some redox drugs) may result in a partial reduction of cellular oxygen leading to serious imbalance between the production of free radicals and the antioxidant defense. Such a situation generates a diverse group of reactive species known collectively as "reactive oxygen species" (ROS).[1] The production of ROS, in turn, leads to the formation of a broad variety of other modified and oxidized cellular molecules resulting in a state of oxidative stress. Despite the diverse number of cellular defenses and pathways to counteract the negative effects, excessive ROS production beyond the organ's scavenging capacity simultaneously attacks and alters other target molecules and causes lipid peroxidation induction, DNA breakdown and/or proteins denaturation.[2]

A growing body of evidence suggests oxidative stress as one of the most relevant pathogenic influences in numerous human diseases, including diabetes, vascular complications,[3] cancer,[4] and neurodegenerative disorders such as Alzheimer's[5] and Parkinson's disease.[6] Oxidative stress has also been reported in association with the occurrence of impaired reproductive function,[7] and as a major cause of liver damage,[8] and cardiac myocyte death.[9] Oxidative stress also plays a fundamental role in cataractogenesis,[10] it contributes to mucosal inflammation of the gastrointestinal tract[11] and is important in aging processes.[12] There is convincing experimental and clinical evidence that ROS generation is an important fibrogenic

[a] *Department of Nephrology and Rheumatology, University Medical Center Goettingen, Georg-August University Goettingen, Robert-Koch-Strasse 40, D-37075 Goettingen, Germany. E-mail: dihazi@med.uni-goettingen.de; Fax: +049-551-3991039; Tel: +049-551-3991221*
[b] *Section for Transplantation-Immunology and Immunohematology, ZMF, University Tuebingen, Waldhörnle Str. 22 Germany*

factor and that most, if not all, progressive renal diseases are the consequence of a deleterious process of destructive interstitial fibrosis.[12]

The molecular pathogenesis of renal interstitial fibrosis correlates with the degree of renal functional loss and predicts the rate of progression to end-stage renal failure.[13]

Different players were described to be involved in the antioxidant response of the cells.[14–17] Among the antioxidant agents PARK7 is a redox-responsive cytoprotective protein with diverse functions. It was first identified as an oncogene that transformed cells.[18] Functional studies showed that PARK7 may become activated in the presence of ROS, produced under conditions of oxidative stress, but also as a part of physiological receptor-mediated signal transduction. As an important regulator of redox signaling kinase pathways, PARK7 can act as a transcriptional modulator of antioxidative gene expression. Activation of PARK7 leads to a shift of the protein to more acidic (oxidized) forms in Parkinson's disease.[19] Thus, PARK7 oxidized modifications are specifically linked to diseases.

ROS are generated through normal cellular processes in aerobic organisms. Besides the normal singlet oxygen, the ROS include the products which are generated during reduction of oxygen to water: superoxide anion ($O_2^{\bullet -}$), hydrogen peroxide ($H_2O_2$), and hydroxyl radical ($OH^{\bullet}$). Hydrogen peroxide ($H_2O_2$) can rapidly be converted into highly oxidizing hydroxyl radicals ($OH^{\bullet}$) and generate oxidative stress by overwhelming the intracellular antioxidant mechanisms thus, modulating intracellular signaling pathways, including apoptosis and cell cycle regulation.[20] While several markers of chronic oxidative stress induced by $H_2O_2$ are well known, evidence for the regulatory mechanisms underlying oxidative renal injury at the proteome level are still lacking. The current work has therefore been designed to define molecular pathways linking $H_2O_2$ induced oxidative stress to cellular dysfunction through proteomic analysis. Using this methodology, it may not only be possible to provide a basic theory and new opportunities for elucidating significant mechanisms by recognizing changes of global protein expression profiles, but will further yield a quantitative evaluation on the expression level of cellular proteins, thus helping in the identification of new diagnostic markers. To achieve this goal, experiments have been conducted using a well-established and characterized renal fibroblast (TK173) and tubular epithelial cell line (HK2) as model systems and potential cellular key-players in renal fibrosis.

## Materials and methods

### Cell line and culture procedure

The human renal fibroblast cell line (TK 173) used in these experiments was derived from a normal human kidney biopsy. The renal cells were immortalized by transfection with the plasmid pSV3gpt which encodes the large T antigen from SV40 and have typical morphological and biochemical properties of renal interstitial fibroblasts.[21]

The TK173 cell line was routinely maintained in 75 $cm^2$ tissue culture flasks (Falcon) in Dulbecco's modified Eagle's medium (Gibco) supplemented with 10% fetal calf serum (FCS, Gibco), 1% L-glutamine (PAA) and 1% penicillin/streptomycin (PAA). A renal epithelial cell line designated HK-2 (human kidney-2) also used in these experiments was derived from normal adult human renal cortex.[22] Cultured cells were exposed to a recombinant retrovirus containing the HPV 16 E6/E7 genes. They show a high degree of differentiation and specialization *in vitro* and provide a suitable model to study the function of renal proximal tubular epithelials *in vitro*. The HK-2 cell line was maintained as a monolayer culture in Quantum 286 medium for epithelial cells (PAA) with 1% penicillin/streptomycin (Gibco). Cells were regularly passaged at 85–90% confluency. Before the start of each experiment, normal growing cells were harvested with trypsin, recultured in 7 ml medium at a density of $5 \times 10^4$ cells per flask and allowed to attach and grow overnight at 37 °C in a humidified atmosphere of 5% $CO_2$ and 95% air.

### Cell viability assay

The Cell Proliferation Kit I (Roche), a colourimetric assay, was used for the non-radioactive quantification of cell proliferation and viability (Roche Applied Science, Mannheim, Germany). The assay is based on the cleavage of the yellow tetra-zolium salt 3-(4,5-dimethylthiazol-2-yl)-2,5 diphenyl-tetrazolium bromide (MTT) to purple formazan crystals by metabolic active cells.[23] The formazan crystals formed are solubilized and the resulting colored solution is quantified using a plate reader. Cells were plated in 200 µl of medium at a concentration of $5 \times 10^3$ cells per flat-bottomed well in 96-well plates (tissue culture grade, Falcon). After overnight incubation, the medium was replaced with standard media containing different hydrogen peroxide ($H_2O_2$) (Merck) concentrations ranging from 0 to 1000 µM for induction of viability changes, the cells were then re-incubated for 24 h. After this incubation period, 10 µl of the MTT labeling reagent (0.5 mg $ml^{-1}$) were added to each well and the 96-well plates were again incubated for 4 h. After the addition of 100 µl of the solubilization solution into each well the plates were kept overnight in the incubator. Thereafter the cell viability was quantified using a plate reader by light absorbance at a wavelength between 550–600 nm with a reference wavelength > 650 nm. Standard curves correlating the absorbance to the cell number were established and used to quantify cell number changes in test wells. For 72 h cell viability experiments, test media were changed every day before undergoing further steps of analysis.

### Oxidative stress induction

To mimic oxidative stress conditions, cells prepared in culture flasks at a concentration of $5 \times 10^3$ cells per flask were allowed to grow overnight and were then treated with culture medium containing 200 µM $H_2O_2$ (maximum concentration was chosen according to the cell viability experiments). This medium was replaced with a freshly prepared stress medium every 24 h throughout a 72 h experimental period. For each experiment, a control group was handled in parallel to the treated culture group under similar experimental conditions with the exception

 

that the culture medium contained no $H_2O_2$ additive. All oxidative stress experiments were repeated three times.

**Detection of reactive oxygen species (ROS) production**

The fibroblast cell line TK173 cells were grown to confluence in 96-well cell culture plates. Cells in several test wells were then stimulated with 200 μM $H_2O_2$ for 2 h in comparison to untreated control wells. Dihydrorhodamine-123 (DHR-123, Sigma) stock (10 μM) solution was made in DMSO, and stored at −20 °C. Oxidative stress as manifested by ROS production was assessed by preloading the cells, both the control and the $H_2O_2$ treated wells with 50 μM DHR-123 and incubated at 37 °C for 30 min. Intracellular DHR-123 oxidation was imaged using a fluorescence microscope (Zeiss) and appropriate filters.[24]

**Cell lysis and protein extraction**

At the end of each experiment, 75% confluent cell culture flaks were scraped and cells were rinsed twice with phosphate-buffered saline (PBS, Gibco). After centrifugation at 1100 rpm for 5 min at 4 °C the supernatant was removed and the cell pellets were treated with 0.3–0.5 ml of lysis buffer containing 9.5 M urea (Sigma), 2% (w/v) CHAPS (Merck), 2% (w/v) ampholytes, 1% DTT (Sigma), and 10 mM PMSF. Aliquots of 500 μl of urea buffer were frozen until use. Ampholytes, DTT, pepstatin (to a final concentration of 1.4 μM), and Complete™ from Roche Diagnostic (according to the manufacturer's protocol) were freshly added. After adding the lysis buffer the samples were incubated for 30 min at 4 °C. For removing the cell debris, sample centrifugation was carried out at 14 000 rpm and 4 °C for 30 min. The supernatant was centrifuged at 14 000 rpm at 4 °C for an additional 30 min to get maximal purity. The resulting samples were used immediately or stored at −20 °C until used. Protein concentration was determined according to Bradford[25] using bovine serum albumin (Roche Applied Science) as a standard.

**Two-dimensional gel electrophoresis (2-DE)**

Each sample was diluted in rehydration buffer (8 M urea, 1% (w/v) CHAPS, 0.2% ampholytes pH 3–10, 1% DTT, and a trace of bromophenol blue) to a final volume of 175 μl. The mixture containing 150 μg of proteins from cell lysate was used for the hydration of one IPG strip. The strips (pH 5–8, 11 cm) were allowed to rehydrate for 30 min before adding mineral oil (Bio-Rad). The passive rehydration of the strips was carried out overnight for at least 12 h at room temperature in a focusing chamber. Isoelectric focusing was performed on the PROTEAN IEF Cell (Bio-Rad) at a controlled temperature of 20 °C using the following multistep voltage setting protocol: 500 V for 1 h, 1000 V for 1 h, 2000 V for 1 h and left at 8000 V until a total of 50 000 Vh was reached. After the first dimension, the individual strips were equilibrated at room temperature in SDS equilibration buffer containing 6 M urea, 30% (w/v) glycerol, 2% SDS (w/v), 0.05 M Tris-HCl (pH 8.8), 2% DTT and a trace of bromophenol blue for 20 min. An additional incubation in the same buffer supplemented with iodoacetamide (2.5%) instead of DTT was subsequently carried out for another 20 min. The second dimension was performed using SDS-PAGE, 12% BisTris Criterion precast gels (Bio-Rad) according to the manufacturer's instructions. The gels were run at 150 V for 10 min followed by 200 V until the bromophenol blue front had reached the bottom of the gel.

**Gel staining**

For image analysis, 2-DE gels were fixed overnight in a solution containing 50% methanol and 12% acetic acid. Gels were then stained with Flamingo fluorescent stain (Bio-Rad) for at least 5 h. After staining, gels were scanned at 50 μm resolution on a Fuji FLA5100 scanner. The digitalized images were analyzed using Delta 2D 3.4 (Decodon, Germany). For protein spot visualization, the 2-DE gels were post-stained with colloidal Coomassie (Roti-Blue, Roth, Germany) overnight, thus enabling manual spot excision for trypsin digestion and mass spectrometry analysis for protein identification.

**In-gel digestion and mass spectrometry analysis of protein spots**

Manually excised protein spots from the gels were washed with distilled water for 15 min. The destaining procedure was carried out by washing the spots alternately with 50% acetonitrile (ACN) and 100 mM ammonium bicarbonate three times for 5 min. After dehydrating the spots with 100% ACN for 15 min, they were dried in a vacuum centrifuge for ~15 min. Thereafter, the gel spots were rehydrated for digestion with 20 μl of trypsin (10 ng $\mu l^{-1}$ in 100 mM ammonium bicarbonate) and incubated at 37 °C overnight. The extraction of the peptide sample was carried out with different concentrations of ACN and trifluoroacetic acid (TFA) under sonication. All supernatants were pooled together, dried in a vacuum centrifuge, and dissolved in 0.3% TFA. The mass spectrometry analysis and protein identification were performed as described previously.[26]

**Western blot analysis**

Proteins (40 μg) were separated by SDS-PAGE and transferred to a Hybond ECL nitrocellulose membrane (GE Healthcare). Immunodetection was performed according to Towbin *et al.*[27] Briefly, membranes were blocked in 5% milk for 2 h at room temperature, followed by overnight incubation at 4 °C with diluted specific primary antibody. Rabbit monoclonal anti-PARK7 (1 : 1000), rabbit polyclonal anti-fibronectin (1 : 5000), mouse monoclonal anti-vinculin (1 : 500) antibodies (Sigma), rabbit polyclonal anti-superoxide dismutase 1 (1 : 2000) antibody (Abnova), rabbit monoclonal anti-peroxiredoxine 6 (1 : 2000) antibody (Abcam), mouse monoclonal anti-vimentin (1 : 5000) antibody (Dako) and mouse monoclonal anti-β-actin (1 : 5000) were used as primary antibodies. Molecular Probes Alexa Fluor 647 goat anti-mouse IgG antibody or Alexa Fluor 647 goat anti-rabbit IgG (1 : 2000) were used as secondary antibodies. Before imaging, the blots were dried in the dark. The blot membranes were scanned at 50 μm resolution on a Fuji FLA5100 scanner (Fuji Photo) with single laser-emitting excitation light at 635 nm.

**Bioinformatics**

The identified protein list was submitted according to their official gene symbol (listed in Table 1) to DAVID bioinformatics

**Table 1** Identification of the proteins found to be differentially regulated upon oxidative stress. The name, gene name, SwissProt accession number, molecular weight, ESI MS/MS score and the sequence coverage are given

| | Protein name | Gene name | Swiss-prot accession nr. | MW | ESI MS/MS score | Sequence coverage |
|---|---|---|---|---|---|---|
| 1 | Protein DJ-1, Parkinson's disease protein 7 | PARK7 | Q99497 | 20050 | 166 | 22 |
| 2 | Superoxide dismutase [Cu-Zn] | SOD 1 | P00441 | 16154 | 80 | 11 |
| 3 | Peroxiredoxin-2 | PRDX2 | P32119 | 22049 | 188 | 24 |
| 4 | Ubiquitin carboxyl-terminal hydrolase isozyme L1 | UCHL1 | P09936 | 25151 | 166 | 18 |
| 5 | Eukaryotic translation initiation factor 5A-1 | EIF5A | P63241 | 17049 | 71 | 9 |
| 6 | Enhancer of rudimentary homolog | ERH | P84090 | 12422 | 74 | 10 |
| 7 | Thioredoxin | TXN | P10599 | 12015 | 59 | 8 |
| 8 | Rho GDP-dissociation inhibitor 1 | GDIA1 | P52565 | 23250 | 110 | 17 |
| 9 | Calpain small subunit 1 | CAPNS 1 | P04632 | 28469 | 60 | 11 |
| 10 | Rho GDP-dissociation inhibitor 2 | GDIA2 | P52566 | 23031 | 72 | 12 |
| 11 | Ubiquitin | UBC | P62988 | 8560 | 81 | 14 |
| 12 | 40S ribosomal protein S12 | RPS12 | P25398 | 14859 | 74 | 13 |
| 13 | UPF0556protein C19 or f10 | C19 or f10 | Q969H8 | 18897 | 78 | 13 |
| 14 | Transcription factor BTF3 | BTF3 | P20290 | 22211 | 64 | 11 |
| 15 | Confilin 1 | CFL1 | P23528 | 18719 | 110 | 20 |
| 16 | Peroxiredoxin-6 | PRDX6 | P30041 | 22324 | 118 | 19 |
| 17 | Triosephosphate isomerase | TPI1 | P60174 | 26938 | 208 | 26 |
| 18 | *S*-formylglutathione hydrolase | ESD | P10768 | 31956 | 82 | 7 |
| 19 | Heterogeneous nuclear ribonucleoprotein H3 | HNRNPH3 | P31942 | 36960 | 111 | 15 |
| 20 | Glyceraldehyde-3-phosphate dehydrogenase | GAPDH | P04406 | 36202 | 139 | 16 |
| 21 | Annexin A2 | ANXA2 | P07355 | 38808 | 63 | 8 |
| 22 | Calponin-2 | CNN2 | Q99439 | 34074 | 60 | 8 |
| 23 | Actin, cytoplasmic 1 | ACTB | P60709 | 42052 | 117 | 14 |
| 24 | Alpha-enolase | ENO1 | P06733 | 47481 | 182 | 23 |
| 25 | Stress-induced-phosphoprotein 1 | STIP1 | P31948 | 63227 | 294 | 32 |
| 26 | Far upstream element-binding protein 1 | FUBP1 | Q96AE4 | 67690 | 62 | 11 |
| 27 | Stress-70 protein, mitochondrial | HSPA9 | P38646 | 73920 | 72 | 14 |
| 28 | 78 kDa glucose-regulated protein | HSPA5 | P11021 | 72402 | 192 | 24 |
| 29 | Vimentin | VIM | P06870 | 53676 | 349 | 36 |
| 30 | Vinculin | VCL | P18206 | 123591 | 231 | 32 |
| 31 | Fibronectin | FN1 | P02751 | 262607 | 225 | 28 |
| 32 | Collagen alpha-1(1) chain | COL1A1 | P02452 | 139853 | 102 | 22 |

(www.david.abcc.ncifcrf.gov). By applying the gene ID conversion tool, all proteins were identified by DAVID ID. The new converted list was used to analyze and categorize the gene ontology ((GO)-annotations cellular components and molecular function). To limit annotations, *Homo sapiens* was chosen as the background.

### siRNA construct and transfection

siRNA oligonucleotides specific for the knockdown of PARK7 expression (sense strand: 5′-ACCTCGAAGGCTC-CACTGTTCTTAATCAAGAGTTAAGAACAAGTGGAG-CCTTCTT-3′), (antisense strand: 3′-CAAAAAGAAGGCT-CCACTTGTTCTTAACTCTTGATTAAGAAACAAGTGGA-GCCTTCG-5′), were designed in our laboratory and synthesized by Eurofins MWG Operon. The siRNA vector was constructed by ligating oligonucleotides in the psiRNAh7SK neo vector (Invitrogen). All constructs were verified by sequencing. TK173 and HK-2 cells cultured to approximately 80% confluence were transfected with the siRNA containing vector for the knockdown of PARK7 using the transfection reagent Lipofectamine 2000™ (Invitrogen) according to the standard protocol of the manufacturer, non-transfected cells and cells transfected with psiRNAh7SK empty plasmid only were kept as controls. After 24 h the transfection media were changed to normal culture media supplemented with 0.5 mg $ml^{-1}$ G-418 (Invitrogen) as selection criteria for stable transfection. Cells were maintained in the selective medium for 14 days to achieve stable transfection. Cells were assessed for PARK7 expression by immunoblotting. The PARK7 knockdown cells were then subjected to oxidative stress for different times and the cell viability was assessed as described above.

### Statistical analysis

All values are presented as mean ± SD ($n = 3$). Statistical analysis was performed with GraphPad Prism 4 software. Comparisons of two groups were conducted using paired two-tailed *t*-test. Statistical analyses among three or more groups were performed using one-way analysis of variance (ANOVA). Differences among groups were declared statistically significant if $p < 0.05$.

## Results

### Effects of oxidative stress on kidney fibroblast viability

We attempted to assess the response of renal fibroblast cells stimulated with $H_2O_2$ over 24 h using the MTT cell viability assay. TK173 cells were initially seeded in 96-well plates and grown in normal cell culture medium. A group of cells were then stimulated with various concentrations of $H_2O_2$ (50–1000 μM) and the percent viability was compared to control cultures after 24 h. As shown in Fig. 1, cell survival was strongly correlated with the $H_2O_2$ concentration. No significant

 

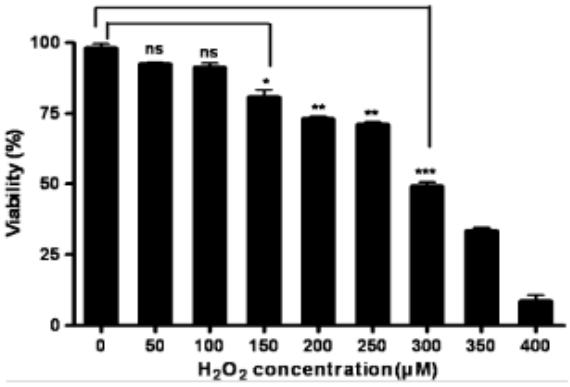


**Fig. 1** MTT assay results showing cell viability under different $H_2O_2$ concentrations over 24 h. Results are represented as a mean of 12 readings ± SD. Statistical analysis were performed using Graph Pad Prism 4 software and one way ANOVA test. Statistical significance was assumed for *p*-values <0.05: $*P < 0.05$, $**P < 0.01$, $***P < 0.001$.

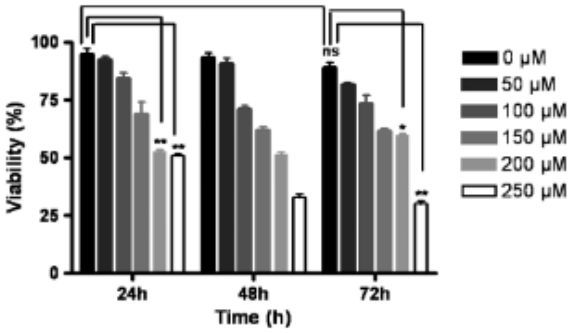


**Fig. 2** MTT assay showing time dependent cell viability under different $H_2O_2$ concentrations over 72 h. Results are represented as a mean of 12 readings ± SD. Statistical analysis were performed using Graphpad Pad Prism 4 software and one way ANOVA test. Statistical significance was assumed for *p*-values <0.05: $*P < 0.05$, $**P < 0.01$.

changes were observed between the control cells and with low $H_2O_2$ dose (50–100 μM) treated cells. Cell death was more pronounced ($p < 0.001$) at 300 μM of $H_2O_2$. Moreover, our first attempts showed that $H_2O_2$ concentrations of 600 μM and higher led to direct cell apoptosis. These findings suggested that cells lost their ability to counteract oxidative stress induced by $H_2O_2$ at a concentration higher than 300 μM. Consequently, for optimal oxidative stress experimental conditions, incubation times of 72 h and $H_2O_2$ maximal concentration of 250 μM were chosen. After overnight incubation at 37 °C in a 5% $CO_2$ incubator, the medium was replaced with 200 μl of the standard medium, and various amounts of 10 mM $H_2O_2$ were added to achieve the required concentration. The medium change was performed every 24 h for both the treated cells and the control. Cell viability assay revealed that the stress effect of $H_2O_2$ was significant at 200 μM. Despite a pronounced death rate observed during the first 24 h of treatment (Fig. 2), cells showed partial recovery after 48 h. After 72 h the cells seemed to develop resistance and grew with less significant difference in their growth rate compared to the controls ($P < 0.05$). In contrast, cells exposed to 250 μM $H_2O_2$ showed non-significant recovery after 48 h, but proceeded with significant cell death after 72 h. To counterbalance the negative effects of oxidative injury, the cells triggered a series of intracellular responses that could ultimately lead to protection against the stress stimulus. Using DHR-123, an uncharged, nonfluorescent agent that can be converted by oxidation to the fluorescent laser dye rhodamine 123, we confirmed that the treatment of renal cells with 200 μM $H_2O_2$ resulted in accumulation of hyperactive ROS derivatives as visualized by excess fluorescence intensity in the treated group of cells (Fig. 3A and B). DHR-123 is often used to detect the production of reactive nitrogen and oxygen species in cells *via* its oxidation into their respective fluorescent products. ROS *e.g.* peroxynitrite, hypochlorous acid, and $H_2O_2$ oxidize DHR-123 to varying degrees. Based on these results, we suggested that a treatment of the renal cells for 72 h with 200 μM $H_2O_2$ would provide a good system to study the impact of oxidative stress on cell proteome in renal cells. These incubation conditions were chosen because they allow an optimal time period for the cells to recover from oxidative stress.

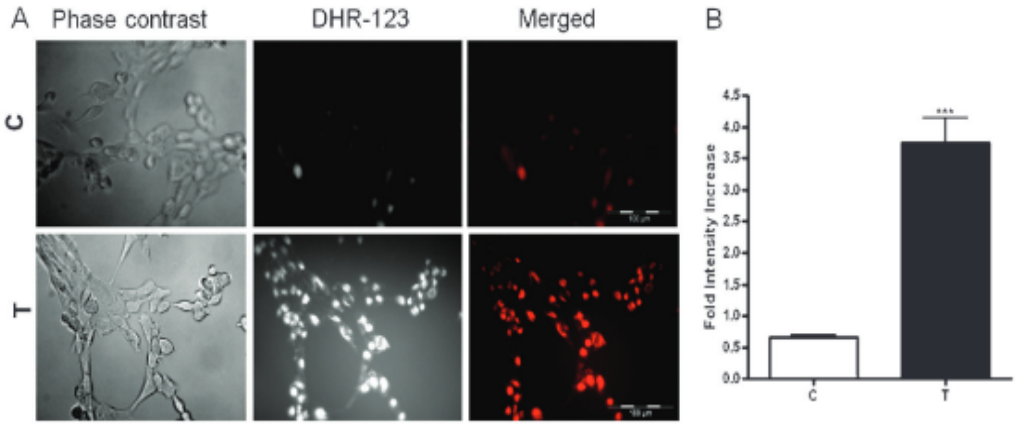


**Fig. 3** Fluorescence microscopy comparing DHR-123 stained control and treated TK173 cells with 200 μM $H_2O_2$. Cells were stained with DHR-123 for 2 hours and visualized using specific filter sets for phase contrast and rhodamine. The obtained images were merged to observe cell morphology. Scale bar = 100 μm.

### Impact of oxidative stress on renal cell protein pattern

To detect and identify altered protein expression induced by $H_2O_2$ exposure, we employed conventional 2-DE coupled with mass spectrometry analysis. This approach allows the identification of novel proteins that have not been previously described to be implicated in the process of oxidative stress induced by $H_2O_2$ in renal fibroblasts and tubular epithelial cells. Simultaneously it offered the possibility to directly analyze the complex biological processes involved.

To establish gel-based reference maps allowing the investigation of the effects of $H_2O_2$ exposure on the renal cells proteome and meanwhile to ensure that results will not be influenced by spot mismatches, the 2-D gel images produced from three independent experiments for both the control and the treated groups were further overlapped using the DECODON software. Well-resolved, reproducible patterns of total protein expression profiles were obtained illustrating differentially expressed protein spots with high reproducibility. The comparison of the gels of the $H_2O_2$ treated cells with those of the control cells showed that $H_2O_2$ exerted toxic effects and altered proteins with higher expression and/or caused pI shifts. For mass spectrometry analysis, preparative 2D gels were stained with Coomassie brilliant blue to visualize all protein spots. Subsequently, differently expressed protein spots were cut out manually and digested for mass spectrometric analysis. In this report, we have restricted our list of proteins identified by mass spectrometry to those spots with MASCOT confidence interval scores of >95%.

Peptide mass fingerprint analysis and non-redundant sequence database matching allowed the identification of diverse groups of proteins. All of the identified proteins, which showed difference in expression under $H_2O_2$ treatment, are numbered and shown in Fig. 4. Spot numbers on 2-DE image matches are listed in Table 1 with further information about the identified protein.

### Bioinformatics analysis of the identified proteins

Using gene ontology resources, such as the DAVID database, and conventional searches of the literature we were able to assign the identified proteins according to their molecular function (Fig. 5A) and cellular location (Fig. 5B) into different categories. Of particular interest, a major functional group responding to the stress stimulus consisted of 37.1% of the cellular proteins. Among them were various antioxidant proteins playing a role in the cell redox homeostasis (PRDX2, PRDX6), or in hydrogen peroxide biosynthetic processes (SOD1). Others are known to act as chaperones or chaperone binding proteins (PARK7, HSPA5, HSPA9, STIP1, SOD1). This diversity of proteins seems to be essential as a positive regulator and sensor for oxidative stress thus enhancing mechanisms that can generate ROS in the oxidative environment, where there are high oxygen levels and where host defense elements are constantly dealing with pathogenic and toxic threats. Moreover, anti-apoptosis functioning proteins (GDIA1, GDIA2, ACTB, CFL1, UBC, VIM, VCL, FN1, COL1A1) involved either in cell adhesion, in the attachment of the actin-based microfilaments to the plasma membrane, in binding cell surfaces with various compounds, in cell motility, opsonisation, locomotion, and/or maintenance of cell morphology were stimulated. The percentage of all molecular functions of the identified proteins is traced in a pie chart represented in Fig. 5A. These include cellular, metabolic, biological, developmental and multi-cellular processes, cellular component organization and cell death. It is noteworthy mentioning that a number of proteins are included in more than one group. These results support the view that the cellular adaptation to oxidative stress is accompanied by modulation of diverse cellular functions. Proteins involved in these cellular adaptations are also located according to their subcellular distribution analysis in a variety of compartments with the majority (97.1%) being intracellular. The rest of the terms were intracellular organelle, membrane-bounded organelle, intracellular organelle part, non-membrane bounded organelle,

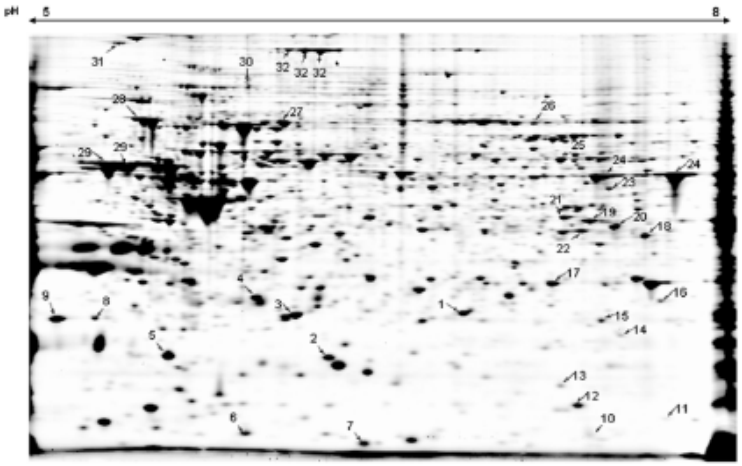


**Fig. 4** 2-DE protein map of total proteins isolated from control and treated cells. 150 μg proteins were loaded on an 11 cm IPG strip with a linear pH 5–8 gradient for isoelectric focusing, and a 12% SDS polyacrylamide gel was used for SDS-PAGE. Proteins were stained with flamingo. Selected proteins, that were found to be differently expressed in both groups, were assigned a number corresponding to their number in Table 1.

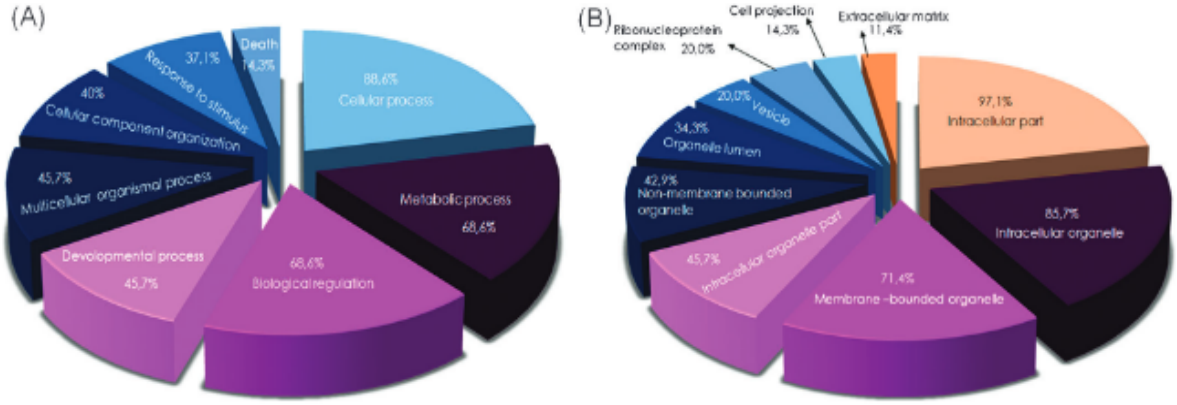


**Fig. 5** Assignment of identified proteins into groups using **DAVID** Bioinformatics database resource. The list of genes to be analyzed was uploaded into Gene list Manager Window and *Homo sapiens* was chosen as the background. The gene list was then submitted for **DAVID** conversion tool. Based on the corresponding **DAVID** gene IDs and thresholds adjustment (Max-Prob $\leq 0.1$ and Min Count $\geq 2$) in Chart Option section, functional annotations associated with each gene were displayed in a chart. **(A)** GO analysis of molecular functions. **(B)** GO analysis of sub cellular locations. Both analyses are represented as pie charts showing the different categories.

organelle lumen, vesicle, ribonucleoprotein complex, cell projection and extracellular matrix (Fig. 5B).

For quantitative evaluation of the amount of some oxidative stress-related proteins namely, PARK7, SOD1, PRDX6, VIM, VCL and FN1, the difference in spot volume for each protein was analyzed using the DECODON and Graph Pad Prism 4 software. Fig. 6A represents enlarged gel sections of parallel gel runs for the control and the treated cell groups pointing to the protein in concern. The expression quantification of each specific protein is presented in Fig. 6B as a grouped bar chart with error bars. Each bar represents the volume means ± SD of gels from three independent experiments. In addition to their significant up-regulation in response to oxidative injury, PARK7 and SOD1 were also observed to acquire a different pI value (Fig. 6A).

### Western blot analysis

In order to highlight the protein expression changes after oxidative stress and to verify the data from proteomic analysis, Western-blot analysis was performed using specific antibodies. Spot intensities were quantified using the Image J and Graph

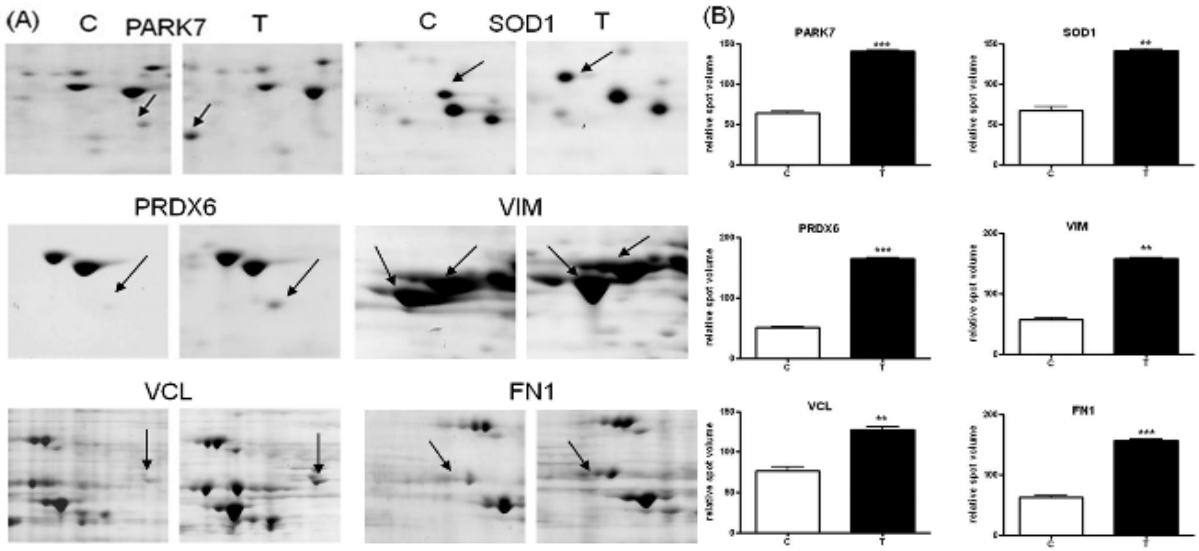


**Fig. 6** **(A)** Graphs represent enlargement of the gel regions of interest showing protein spots found to be differentially expressed in the $H_2O_2$ treated **(T)** group of cells compared to their respective control **(C)**. **(B)** The protein expression quantification for the selected proteins is given in the form of bar diagrams. On the *y*-axis the relative volume of spot, on the *x*-axis the corresponding gene name. Labeling of the graph boxes corresponds to control and treated cells. Results are given as the means ± SD of the percentage volume of spots from at least three independent experiments. $^{**}P < 0.01$, $^{***}P < 0.001$.

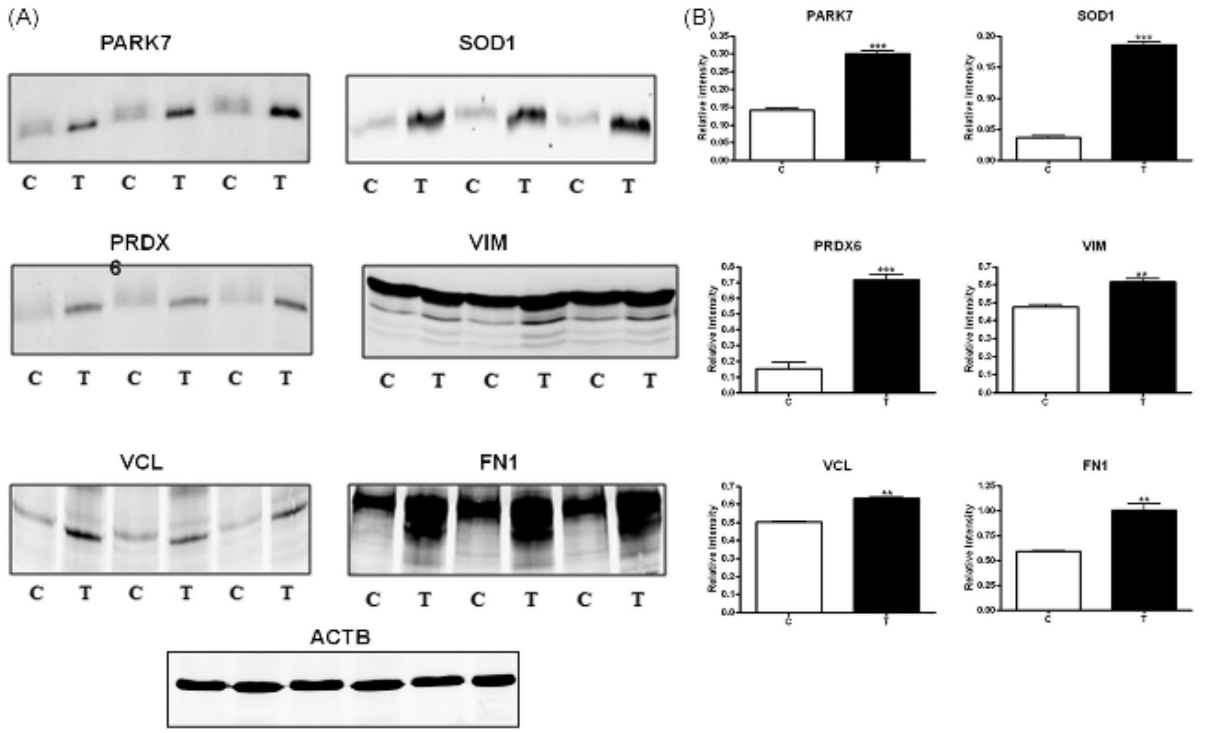


**Fig. 7** Western blot analysis of selection of proteins found to be up-regulated. Control (C) and treated (T) samples were tested for protein expression changes against the appropriate proteins. A: blots probed with antibodies against the appropriate proteins. B: blots quantification. The degree of differential protein expression is shown in the histogram. The expression quantification is presented as a grouped bar chart with error bars. Each bar represents the intensity means ± SD of blots from three independent experiments. $^{**}P < 0.01$, $^{***}P < 0.001$.

Pad Prism 4 software. Histograms depict comparative levels of the specific protein expression. Consistent with 2-DE data, oxidative stress marker proteins (PARK7, SOD1 and PRDX6) were significantly up-regulated after $H_2O_2$ stimulation compared with the corresponding untreated controls (Fig. 7A and B). In addition to these proteins certain fibrosis marker proteins (VIM, VCL, and FN1) were also significantly over-expressed under $H_2O_2$ treatment compared to the controls when β-actin was kept as standard (Fig. 7A and B).

### PARK7 plays an important role in oxidative stress resistance of renal cells

To assess whether PARK7 plays an important role in kidney cells under oxidative stress, we performed knockdown experiments in the human fibroblast kidney cell line TK173. Western blot analysis showed a >90% efficiency in the reduction of endogenous PARK7 protein levels, when β-actin was kept as standard (Fig. 8A). Interestingly, knockdown of PARK7 also led to a significantly reduced viability of TK173 under oxidative stress conditions. MTT assay revealed that the viability of PARK7 knockdown cells compared to both controls (untransfected and transfected with empty plasmid) was decreased by more than 80% upon treatment with $H_2O_2$ (Fig. 8B). In addition, morphological evaluation by microscopy showed that PARK7 knockdown had no significant effect on cell morphology under normal conditions, whereas the reduced level of PARK7 expression caused marked changes in morphological characters finally leading to cell death upon treatment with $H_2O_2$ in comparison to controls (Fig. 8C).

To further evaluate the role of PARK7 in oxidative stress in renal cells, we suppressed the PARK7 expression with siRNA vector transfection in renal tubular cell line HK-2. Western blot of HK-2 cells transfected with PARK7 siRNA showed a significantly reduced expression of PARK7 of >60% compared to their untreated controls with β-actin as internal standard (Fig. 9A and B). Moreover, cell viability assay showed a highly significant decrease in cell viability in PARK7 knockdown cells treated with different concentrations of $H_2O_2$ (Fig. 9C). These findings suggest that the knockdown of PARK7 compromised the oxidative stress resistance not only of the TK173 cells but also of HK-2 cells.

## Discussion

The observations reported in the present work provide evidence for the injury potential of $H_2O_2$ as a stress mediator to renal fibroblastic and epithelial cells. $H_2O_2$ caused cell death after 24 h in a concentration dependent manner. Yanagida and co-workers[6] observed similar effects of $H_2O_2$ using human neuroblastoma cells. Treatment of cells with lower $H_2O_2$ concentrations, in the present work, was sufficient to evoke oxidative stress and affect cell viability. The rate of decline in

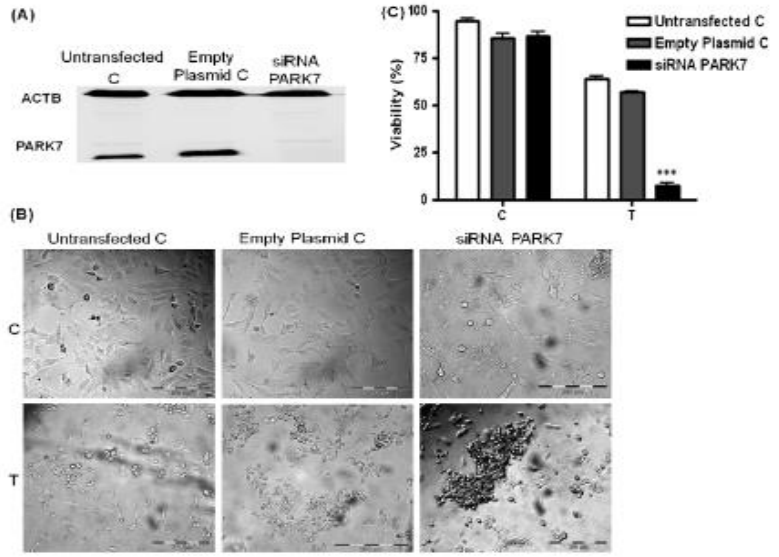


**Fig. 8** (A) Expression of PARK7 in TK173 untransfected, with empty plasmid transfected and siRNA PARK7 transfected cells. A representative Western blot with anti-PARK7 antibody showing expression levels in TK173 cells (untransfected), in cells transfected with empty plasmid only and in cells transfected with siRNA vector targeting PARK7 (siRNA PARK7). Almost 100% knockdown of PARK7 was achieved in siRNA PARK7 transfected cells. (B) The morphological changes induced by PARK7 knockdown and $H_2O_2$ exposure on TK173 cells. Morphological examination conducted after 24 h exposure to $H_2O_2$: the cell growth was dramatically inhibited in the siRNA PARK7 transfected cells, these became irregular shapes and show high apoptosis reflected in increased floating cells (scale bar = 100 μm). (C) MTT assay results comparing the percent viability of the siRNA PARK7 to control set groups, untransfected and with empty plasmid transfected TK173 under normal and treated conditions. Results are represented as a mean of 12 readings ± SD. $^{**}P < 0.01$, $^{***}P < 0.001$.

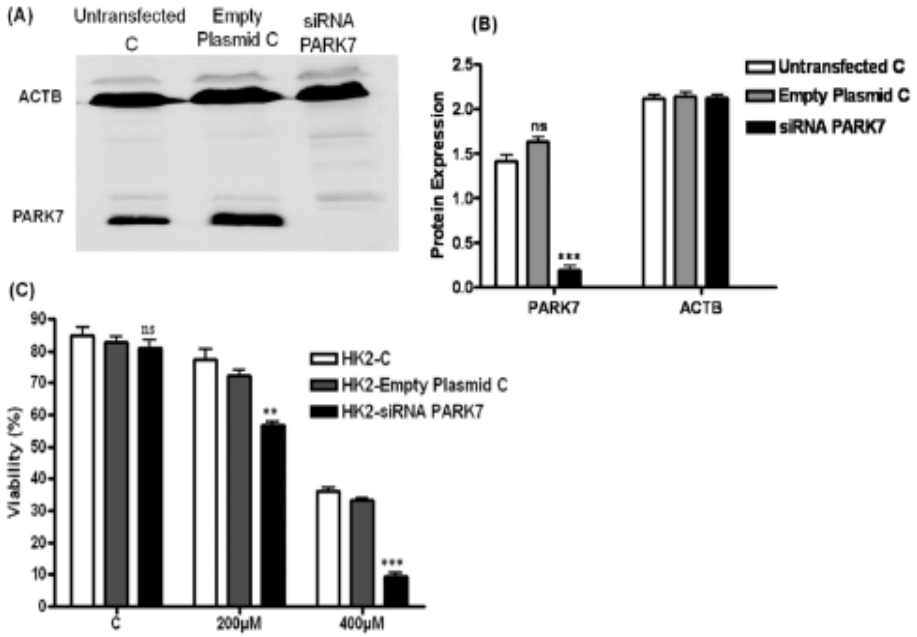


**Fig. 9** (A) Western blot analysis for the efficiency of PARK7 knockdown at protein levels in renal epithelial cells after siRNA vector transfection: siRNA PARK7 transfected HK-2 cells were compared to untransfected controls and to cells transfected with empty plasmid, β-actin was kept as standard. (B) Quantification of Western blot: The degree of differential protein expression is shown in the histogram. The expression quantification is presented as a grouped bar chart with error bars. Each bar represents the intensity means ± SD of blots from three independent experiments. $^{**}P < 0.01$, $^{***}P < 0.001$. (C) MTT assay results comparing the percent viability of the siRNA PARK7 transfected HK-2 cells to control under normal and treated conditions. Results are represented as a mean of 12 readings ± SD. $^{**}P < 0.01$, $^{***}P < 0.001$.

cell number was not only concentration but also time dependent. Similarly Andreucci *et al.*[28] demonstrated that short time incubation of human renal proximal tubular cells (HK-2) with $H_2O_2$ resulted in a significant decrease in cell viability.[28] Moreover, in a recent comparison of the same cells with the renal distal tubular cells (MCDK) demonstrated that apoptosis, loss of cell adhesion and cell death were more obvious in the HK-2 cell line after application of the same stress mediator.[29] These observations indicate that $H_2O_2$ as the oxidative stress agent dramatically impacts the renal cells. However the exact molecular mechanisms underlying the effect of $H_2O_2$ on cell viability and survival and the mechanisms involved in antioxidant defenses are still not completely understood. Hence, there is compelling need to elucidate the molecular mechanisms associated with the subtle lesions caused by $H_2O_2$ that eventually may be of major consequence in the development of renal fibrosis. Our proteomic signatures powerfully explored global changes with respect to regulation and expression of stress responsive proteins in TK173 cells after exposure to $H_2O_2$ stress. Using 2D-gel electrophoresis and mass spectrometry numerous proteins showed high expression in response to $H_2O_2$ treatment.

As reaction on the oxidative insult, renal cells reacted with alteration in the expression of large number of oxidative stress, cytoskeleton and fibrosis marker proteins. Oxidative stress proteins include peroxiredoxins (PRDXs). These are a ubiquitous family of antioxidant enzymes. As redox regulators, they appear to play a key role in homeostatic cellular survival processes; consequently, the changes in the status of these proteins in the cell can alter significantly the cellular responses to various stimuli. The important physiological functions of PRDXs are emphasized by the wide tissue expression of the corresponding family members. In fact, a major common function of PRDXs is the enzymatic degradation of $H_2O_2$.[30] Multiple mammalian PRDXs (I through VI) often coexist in the same cell in various intracellular locations and function as scavengers of endogenous $H_2O_2$ free radicals released after stimulation with growth factors during proliferation, apoptosis or oxidative stress.[31] This is in consistence with our observation of an alteration in different PRDXs detected in our 2D electrophoresis. Especially PRDX6 was significantly increased in renal cells subjected to oxidative stress using $H_2O_2$. PRDX6 was found to be expressed in all major mammalian organs.[32] PRDX6 knockout mice were observed to have lower survival rates, as well as higher protein oxidation levels with more severe tissue damage in organs such as kidney, liver and lung.[33] Over-expression of PRDX6 as a fusion construct with green fluorescent protein in H441 cells, an epithelial cell line that does not express PRDX6, protected this cell against $H_2O_2$. Over-expressing cells showed less lipid peroxidation and decreased damage to cellular plasma membranes.[34] Our data confirmed previous observations, where PRDX6 was qup-regulated in $H_2O_2$-induced cells and acted in antioxidant defense by facilitating repair of damaged cells.

Beside PRDXs other oxidative stress proteins like super-oxide dismutases (SODs) were found to be up-regulated. SODs are metalloenzymes that have been described to exist in humans in three forms with distinctive cellular distribution and metal requirements. Particularly SODs as further antioxidants have clearly proven to be effective both in terms of inhibiting and in reversing established fibrosis.[35] Under normal circumstances, the free radicals burden is controlled by SOD enzymes in the mitochondria (homotetrameric Mn-based)[36] or in the cytosol (homodimetric Cu/Zn).[37] The development of nonpeptidyl SOD mimics,[38] and of $H_2O_2$ scavengers that influence profibrogenic mediators expression[39] offer promise of improved clinical therapies for ROS-mediated injury. The abundant expression of Cu/Zn SOD together with the pI shift acquired in our $H_2O_2$ stressed cells may have important effect on the diverse functions of this protein as an antioxidant. The data demonstrate that the stressed cells react with increased expression of antioxidant enzymes. These results are in harmony with previously reported elevated expression of Cu/Zn SOD in $H_2O_2$ resistant Chinese hamster fibroblasts.[40,41]

As part of oxidative stress response renal cells increased the expression of PARK7, a protein originally discovered as an oncogene,[18] was later found to be responsible for the early onset of Parkinson's disease,[42] to be related to infertility[43] besides its over-expression in multiple tumors.[44] It was also identified as a hydroperoxide-responsive protein.[6] However, the molecular mechanism by which PARK7 exerts these multiple functions remains elusive. Several lines of evidence support a protective role of PARK7 against oxidative stress. Our proteomic analysis extended the above cited investigations and revealed that upon oxidative stress, PARK7 was significantly highly up-regulated and that its pI was shifted to a more acidic point suggesting that PARK7 was oxidized and consequently modified to acquire a slightly lower pI. Conversion of PARK7 into a pI variant in response to $H_2O_2$ had already been reported.[6,44,45] In neuroblastoma cells, PARK7 eliminated $H_2O_2$ by oxidizing itself. The PARK7 oxidation and subsequent activation was a prerequisite for protection of cells against $H_2O_2$-induced cell death.[46] The PARK7 protein induced an immediate antioxidant response by direct trapping of oxygen atoms, oxidizing its cysteine 106 residue and thus quenching reactive oxygen species.[6] PARK7 also induced an indirect response, which was mediated through the stabilization of the nuclear erythroid 2 related factor (Nrf2) which resulted in the activation of antioxidant transcriptional responses.[47] Considering the structural similarity of PARK7 and the GAT superfamily proteins, PARK7 appeared to sense oxidative stress and to gain the protease activity for the digestion of oxidative damaged proteins.[48] Furthermore, in addition to its presence in the cytoplasm, mitochondria, and nucleus, PARK7 protein has been also detected in extracellular spaces[49] suggesting that it may function both intracellular and extracellular. In 2008, Lev *et al.*[50] demonstrated that over-expression of PARK7 in human neuroblastoma cells resulted in increased cellular resistance to $H_2O_2$ and reduced intra-cellular ROS, whereas contrary effects were achieved when PARK7 levels were reduced by siRNA. Using a similar cell model Yanagida *et al.*[6] showed that even a low $H_2O_2$ concentration induced a significant intracellular ROS production and cell death in PARK7 knockdown cells, while this was only slightly induced in normal cells. The effect of oxidative stress on PARK7 in renal cells and the fact that PARK7 knockdown rendered renal cells more susceptible to oxidative stress

 

confirm the pivotal role of PARK7 also in renal cell resistance to oxidative stress and possibly in renal fibrosis.

Parallel to up-regulation of the oxidative stress marker and subsequent activation of antioxidant defense, the renal cells showed an over-expression of cytoskeleton and fibrosis marker proteins indicating potential cell transformation under $H_2O_2$ treatment. Fibrosis markers *e.g.* FN1 and COLIA1 were up-regulated under $H_2O_2$ treatment confirming the pro-fibrotic effect of oxidative stress. Evidence exists linking overexpression of extracellular matrix components such as FN1 and COLIA1 with tubulointerstitial fibrosis.[51,52] As a direct effect of $H_2O_2$, also messenger levels of FN1 were found to be increased in human mesengial cells, suggesting that $H_2O_2$ may have stimulated ECM proteins expression by a direct effect or an indirect effect through activation of the TGF-β system.[53] Similarly, accompanying ROS increase in renal cells, vimentin and vinculin as components and interacting molecules of cytoskeleton were found to be up-regulated after oxidative stress, indicating a role of these proteins in stress protection. The present finding, together with the observation that cytoskeleton proteins[10,54] were also up-regulated in response to oxidative stimuli in other cell systems, strengthens the hypothesis of a protective role of the cytoskeleton as part of the cellular response to oxidative stress.[55]

In conclusion, the up-regulation of the overviewed proteins in renal cells under oxidative stress conditions, in the present work, was found to be a major cellular recovery response after oxidative damage. The proteins identified in the context of renal cell and oxidative stress may provide a new clue on the molecular events leading to cell transformation and renal fibrosis. The regulation of these proteins may present a chief target for protective therapeutic interventions. We further demonstrate the important role of PARK7 in renal cells exposed to an environment that promotes the formation of intracellular ROS. Our data further prove that proteomic techniques can be valuable tools in the study of protein profiling modifications during oxidative stress.

## References


1 B. Halliwell, *Biochem. Pharmacol.*, 1995, **49**, 1341–1348.
2 M. B. Hampton and S. Orrenius, *FEBS Lett.*, 1997, **414**, 552–556.
3 S. M. Son, *Diabetes Res. Clin. Pract.*, 2007, **77**(Suppl 1), S65–S70.
4 T. D. Oberley, *Am. J. Pathol.*, 2002, **160**, 403–408.
5 A. Gella and N. Durany, *Cell Adhes. Migr.*, 2009, **3**, 88–93.
6 T. Yanagida, Y. Kitamura, K. Yamane, K. Takahashi, K. Takata, D. Yanagisawa, H. Yasui, T. Taniguchi, T. Taira, T. Honda and H. Ariga, *J. Pharmacol. Sci.*, 2009, **109**, 463–468.
7 N. Kemal Duru, M. Morshedi and S. Oehninger, *Fertil. Steril.*, 2000, **74**, 1200–1207.
8 L. Cesaratto, C. Vascotto, C. D'Ambrosio, A. Scaloni, U. Baccarani, I. Paron, G. Damante, S. Calligaris, F. Quadrifoglio, C. Tiribelli and G. Tell, *Free Radical Res.*, 2005, **39**, 255–268.
9 T. E. Cullingford, R. Wait, A. Clerk and P. H. Sugden, *J. Mol. Cell. Cardiol.*, 2006, **40**, 157–172.
10 S. Goswami, N. L. Sheets, J. Zavadil, B. K. Chauhan, E. P. Bottinger, V. N. Reddy, M. Kantorow and A. Cvekl, *Invest. Ophthalmol. Visual Sci.*, 2003, **44**, 2084–2093.
11 A. Thomson, D. Hemphill and K. N. Jeejeebhoy, *Dig. Dis.*, 1998, **16**, 152–158.
12 J. Kim, Y. M. Seok, K. J. Jung and K. M. Park, *Am. J. Physiol.: Renal Physiol.*, 2009, **297**, F461–F470.
13 J. Chandra, A. Samali and S. Orrenius, *Free Radical Biol. Med.*, 2000, **29**, 323–333.
14 V. Chavez, A. Mohri-Shiomi, A. Maadani, L. A. Vega and D. A. Garsin, *Genetics*, 2007, **176**, 1567–1577.
15 R. Doonan, J. J. McElwee, F. Matthijssens, G. A. Walker, K. Houthoofd, P. Back, A. Matscheski, J. R. Vanfleteren and D. Gems, *Genes Dev.*, 2008, **22**, 3236–3241.
16 J. M. Van Raamsdonk and S. Hekimi, *PLoS Genet.*, 2009, **5**, e1000361.
17 K. Yen, H. B. Patel, A. L. Lublin and C. V. Mobbs, *Mech. Ageing Dev.*, 2009, **130**, 173–178.
18 D. Nagakubo, T. Taira, H. Kitaura, M. Ikeda, K. Tamai, S. M. Iguchi-Ariga and H. Ariga, *Biochem. Biophys. Res. Commun.*, 1997, **231**, 509–513.
19 P. J. Kahle, J. Waak and T. Gasser, *Free Radical Biol. Med.*, 2009, **47**, 1354–1361.
20 K. Nomura, H. Imai, T. Koumura and Y. Nakagawa, *Biol. Signals Recept.*, 2001, **10**, 81–92.
21 G. A. Muller, J. Frank, H. P. Rodemann and G. Engler-Blum, *Exp. Nephrol.*, 1995, **3**, 127–133.
22 M. J. Ryan, G. Johnson, J. Kirk, S. M. Fuerstenberg, R. A. Zager and B. Torok-Storb, *Kidney Int.*, 1994, **45**, 48–57.
23 M. V. Berridge and A. S. Tan, *Arch. Biochem. Biophys.*, 1993, **303**, 474–482.
24 L. M. Henderson and J. B. Chappell, *Eur. J. Biochem.*, 1993, **217**, 973–980.
25 M. M. Bradford, *Anal. Biochem.*, 1976, **72**, 248–254.
26 H. Dihazi, A. R. Asif, N. K. Agarwal, Y. Doncheva and G. A. Muller, *Mol. Cell. Proteomics*, 2005, **4**, 1445–1458.
27 H. Towbin, T. Staehelin and J. Gordon, *Proc. Natl. Acad. Sci. U. S. A.*, 1979, **76**, 4350–4354.
28 M. Andreucci, G. Fuiano, P. Presta, G. Lucisano, F. Leone, L. Fuiano, V. Bisesti, P. Esposito, D. Russo, B. Memoli, T. Faga and A. Michael, *Cell Proliferation*, 2009, **42**, 554–561.
29 C. J. Percy, B. K. Pat, H. Healy, D. W. Johnson and G. C. Gobe, *Pathology*, 2008, **40**, 694–701.
30 Z. A. Wood, L. B. Poole and P. A. Karplus, *Science*, 2003, **300**, 650–653.
31 S. W. Kang, H. Z. Chae, M. S. Seo, K. Kim, I. C. Baines and S. G. Rhee, *J. Biol. Chem.*, 1998, **273**, 6297–6302.
32 G. Leyens, I. Donnay and B. Knoops, *Comp. Biochem. Physiol., Part B: Biochem. Mol. Biol.*, 2003, **136**, 943–955.
33 X. Wang, S. A. Phelan, K. Forsman-Semb, E. F. Taylor, C. Petros, A. Brown, C. P. Lerner and B. Paigen, *J. Biol. Chem.*, 2003, **278**, 25179–25190.
34 Y. Manevich, T. Sweitzer, J. H. Pak, S. I. Feinstein, V. Muzykantov and A. B. Fisher, *Proc. Natl. Acad. Sci. U. S. A.*, 2002, **99**, 11599–11604.
35 J. L. Lefaix, S. Delanian, J. J. Leplat, Y. Tricaud, M. Martin, A. Nimrod, F. Baillet and F. Daburon, *Int. J. Radiat. Oncol., Biol., Phys.*, 1996, **35**, 305–312.
36 S. L. Marklund, *Proc. Natl. Acad. Sci. U. S. A.*, 1982, **79**, 7634–7638.
37 J. M. McCord and I. Fridovich, *J. Biol. Chem.*, 1969, **244**, 6049–6055.
38 D. Salvemini, Z. Q. Wang, J. L. Zweier, A. Samouilov, H. Macarthur, T. P. Misko, M. G. Currie, S. Cuzzocrea, J. A. Sikorski and D. P. Riley, *Science*, 1999, **286**, 304–306.
39 W. Zhao, D. R. Spitz, L. W. Oberley and M. E. Robbins, *Cancer Res.*, 2001, **61**, 5537–5543.
40 J. A. Keightley, L. Shang and M. Kinter, *Mol. Cell. Proteomics*, 2004, **3**, 167–175.
41 D. R. Spitz, J. H. Elwell, Y. Sun, L. W. Oberley, T. D. Oberley, S. J. Sullivan and R. J. Roberts, *Arch. Biochem. Biophys.*, 1990, **279**, 249–260.
42 V. Bonifati, P. Rizzu, M. J. van Baren, O. Schaap, G. J. Breedveld, E. Krieger, M. C. Dekker, F. Squitieri, P. Ibanez, M. Joosse, J. W. van Dongen, N. Vanacore, J. C. van Swieten, A. Brice, G. Meco, C. M. van Duijn, B. A. Oostra and P. Heutink, *Science*, 2003, **299**, 256–259.
43 M. Okada, K. Matsumoto, T. Niki, T. Taira, S. M. Iguchi-Ariga and H. Ariga, *Biol. Pharm. Bull.*, 2002, **25**, 853–856.
44 J. E. Tillman, J. Yuan, G. Gu, L. Fazli, R. Ghosh, A. S. Flynt, M. Gleave, P. S. Rennie and S. Kasper, *Cancer Res.*, 2007, **67**, 4630–4637.

45 A. Mitsumoto, Y. Nakagawa, A. Takeuchi, K. Okawa, A. Iwamatsu and Y. Takanezawa, *Free Radical Res.*, 2001, **35**, 301–310.
46 P. Jenner, *Ann. Neurol.*, 2003, **53**(Suppl 3), S26–S36.
47 C. M. Clements, R. S. McNally, B. J. Conti, T. W. Mak and J. P. Ting, *Proc. Natl. Acad. Sci. U. S. A.*, 2006, **103**, 15091–15096.
48 K. Honbou, N. N. Suzuki, M. Horiuchi, T. Niki, T. Taira, H. Ariga and F. Inagaki, *J. Biol. Chem.*, 2003, **278**, 31380–31384.
49 M. Waragai, J. Wei, M. Fujita, M. Nakai, G. J. Ho, E. Masliah, H. Akatsu, T. Yamada and M. Hashimoto, *Biochem. Biophys. Res. Commun.*, 2006, **345**, 967–972.
50 N. Lev, D. Ickowicz, E. Melamed and D. Offen, *NeuroToxicology*, 2008, **29**, 397–405.
51 A. A. Eddy, *J. Am. Soc. Nephrol.*, 1996, **7**, 2495–2508.
52 F. Strutz, *Nephrol., Dial., Transplant.*, 1995, **10**, 1526–1532.
53 F. Strutz, M. Zeisberg, A. Renziehausen, B. Raschke, V. Becker, C. van Kooten and G. Muller, *Kidney Int.*, 2001, **59**, 579–592.
54 M. R. Clarkson, M. Murphy, S. Gupta, T. Lambe, H. S. Mackenzie, C. Godson, F. Martin and H. R. Brady, *J. Biol. Chem.*, 2002, **277**, 9707–9712.
55 S. M. Liu and T. Sundqvist, *Exp. Cell Res.*, 1995, **217**, 1–7.



 

# 3. PROTEIN DJ-1 AND ITS ANTI-OXIDATIVE STRESS FUNCTION PLAY AN IMPORTANT ROLE IN RENAL CELLS MEDIATED RESPONSE TO PROFIBROTIC AGENTS

---

In this part of the work we conducted an extensive comparison of proteome derived from control renal cells and cytokines (ANG II and PDGF) treated cells to explore the role of profibrotic cytokines on DJ-1 expression regulation on cell progression towards renal fibrosis. Further, we investigated DJ-1 in renal fibrosis using fibrosis animal model. In an attempt to destine and specify DJ-1 physiological functional importance in balancing OS in renal fibrosis we profited wild type DJ-1 (PARK7) and designed mutations to identify DJ-1 interacting partner proteins in renal cells using affinity purification and mass spectrometry thereby characterizing potential mechanisms of its action.

**Authors:** Marwa Eltoweissy, Abdul Rahman Asif, Gry H. Dihazi, Gerhard A. Müller, and Hassan Dihazi.

**Contribution:** All experiments besides,
Gry H. Dihazi: Plasmids amplification.

**Status of publication:** *Accepted for publication: Mol BioSyst (2016), DOI:10.1039/C5MB00887E (Impact Factor: 3.21)*

**Congress presentations:**

1. **XLVII ERA-EDTA CONGRESS, II DGfN Congress, 25-28 June 2010, Munich, Germany.**

2. **4. Jahrestagung der Deutschen Gesellschaft für Nephrologie, 6-9 Oktober 2012, Hamburg, Deutschland.**

3. **92nd Annual Meeting of the German Physiological Society (DPG), 2-5 March 2013, Heidelberg, Germany.**

## 3.1 Abstract

In the pathogenesis of renal fibrosis, oxidative stress (OS) enhances the production of reactive oxygen species (ROS) leading to sustained cell growth, inflammation, excessive tissue remodelling and accumulation, which results in the development and acceleration of renal damage. In our previous work (128) we established protein DJ-1 (PARK7) as an important ROS scavenger and key player in renal cell response to OS. In the present study we investigated the impact of profibrogenic agonists on DJ-1 and shed light on the role of this protein in renal fibrosis.

Treatment of renal fibroblasts and epithelial cells with the profibrogenic agonist ANG II or PDGF resulted in a significant up-regulation of DJ-1 expression parallel to an increase in the expression of fibrosis markers. Monitoring of DJ-1 expression in kidney extract and tissue sections from renal fibrosis mice model (*Col4a3*-deficient) revealed a disease grad dependent regulation of the protein. Overexpression of DJ-1 prompted cell resistance to OS in both fibroblasts and epithelial cells. Furthermore overexpression of DJ-1 mutant for glutamic acid 18 (E18), involved in ROS scavenging, in which glutamic acid 18 (E18) is mutated to either aspartic acid (D) or glutamine (Q) resulted in a significant increase in cell death under OS in case of E18D mutation. Whereas the E18Q mutation did not impact significantly the cell response to OS, revealing the importance of the acidic group for protein DJ-1 as ROS scavenging more than the nature of amino acid itself. Affinity precipitation of interaction partners of DJ-1 and its mutants revealed both: a consistent proteomic cascade that has substantial physiological and pathological properties in collaboration with protein DJ-1 and, an important role of Annexin A1 and A5 in the mechanism of action of DJ-1 in anti-oxidative stress response. In addition, provided evidence for DJ-1 diverse functions; as an oxidative

sensor, a chaperone and/or its role at the transcriptional and posttranscriptional levels. Consequently, our results support the view that cellular adaptation to OS is accompanied by modulation of coordinated cellular and molecular events, suggest a direct correlation of fibrosis progression and expression of OS proteins, emphasize the current evidence for how the oxidative modification may regulate DJ-1's protective function, and implicate a multistep pathway for the paramount protein DJ-1.

## 3.2 Introduction

Renal fibrosis is considered the final convergent pathway for progressive kidney diseases due to a wide range of pathophysiologically distinct processes (157). Fibrosis progression involves interstitial hyper cellularity, matrix accumulation and atrophy of epithelial structures, resulting in loss of normal function and ultimately organ failure (158-160). Although multiple cell types are capable of producing extracellular matrix (ECM), there is common agreement that renal interstitial fibroblasts are the cell type most responsible for matrix accumulation and consequent structural deformation associated with fibrosis (161, 162). Tubular epithelial cells are also observed to have the capacity to acquire a mesenchymal cell phenotype (i.e, epithelial-to mesenchymal trans differentiation, EMT) in the injured kidney (163).

The pathogenesis of renal fibrosis has been depicted as a continuum of three overlapping phases (164). The induction phase, where cellular stimuli trigger a pro-inflammatory response involving the production of a large array of profibrogenic cytokines and growth factors. A secondary phase manifested by the localized accumulation of cytokines promoting the activation and recruitment of matrix producing cells from different sources to secrete biological active products and increase the synthesis and expression of ECM proteins. The

third phase is an ongoing synthesis and accumulation of matrix despite resolution of the primary stimulus (164).

Angiotensin II (ANG II), the major effector peptide of the renin-aldosterone system (RAS), is a prime agent that has been linked to the progression of renal disease by a host of mechanisms. Compelling evidence suggest that ANG II is an important mediator of OS that stimulates intracellular formation of ROS (22, 165). Over the last decade, many studies described the synergistic relationship between ROS and ANG II signaling (166-168). ROS induced by ANG II are chief signal intermediates in several signal transduction pathways involved in renal pathophysiology (22, 61, 165, 169). ROS oxidize proteins and DNA that promote lipid peroxidation leading to an inflammatory cascade protogonized by inflammatory cytokines including the platelet derived growth factor (PDGF) (170, 171). Hence, ANG II-induced ROS are key events of the fibrogenic response through stress-sensitive pathways (22, 33, 34, 48, 172). Exacerbated production of ROS may also directly incite damage to biologically important macromolecules leading to generation of surrogate markers of OS (56).

Because of the highly reactive nature of ROS, with the potential of deleterious effects on cell integrity, ROS must be neutralized by protective enzymes and endogenous antioxidants (34). Fortunately, living organisms have developed a number of antioxidant defenses to protect against damage from OS. These antioxidants work together in various cell compartments scavenging ROS (78, 79). Hence, one scope of the current study is to use proteomic profiling methods in an effort to characterize in renal fibroblasts (TK-173) and epithelial cells (HK-2) experiencing OS insulted by ANG II or PDGF the expression profiles of the various proteins, thereby highlighting novel molecular mediators in renal fibrosis.

A recent study from our laboratory (128) demonstrated that protein DJ-1 (PARK7), by incorporating as an endogenous antioxidant defense protein, had an added benefit in ameliorating the progression of fibrosis in renal cells exposed to higher OS levels.

DJ-1 is a conserved protein ubiquitously expressed, but found at particularly high levels in the testis, brain and kidney (88). It is reported to be involved in diverse cellular processes. Initially DJ-1 was cloned as a putative oncogene (103). Later, was found to encode the protein involved in male fertility (107, 108, 173), and able to work in transcriptional regulation (104, 105, 174, 175). The responsiveness of DJ-1 to OS has provided a potential functional link to the pathogenesis of Parkinson's disease (PD) (122, 123, 129, 176). Taira *et al.,* 2004 (121) indicated that DJ-1 is an antioxidant capable of self-oxidation. In addition, DJ-1 was also suggested to serve as a redox sensitive molecular chaperone (109). The exact function of DJ-1 has been as yet elusive; however, its pivotal role in OS makes it a candidate to integrate genetic and environmental components critical for sporadic disease (87). Yet the advantage of DJ-1 as a potent nutritional antioxidant protecting renal cells from apoptosis and thereby its implication in the pathogenesis of renal fibrosis did not receive much attention. Evidence supporting DJ-1's beneficial role in kidney are so far not documented. The present study was designed to determine the effect of profibrotic cytokines (ANG II and PDGF) on DJ-1 expression. Moreover, using collagen (*Col4a3*) knockout mice as a fibrosis animal model, we attempted to investigate DJ-1 in renal fibrosis. To further define the role of DJ-1 expression in balancing OS in renal fibrosis, we sought to identify DJ-1 interaction partners in wild-type (WT) and mutant DJ-1 and characterize the mechanism of its action.

## 3.3 Material and Methods

### 3.3.1 Cell line and culture procedure

Human renal fibroblast cell line (TK-173) used in these experiments was derived from a normal human kidney. The cells were immortalized by transfection with the plasmid pSV3gpt from SV40 and have typical morphological and biochemical properties of renal interstitial fibroblasts (177). The TK-173 cell line was routinely maintained as a monolayer culture in 75 $cm^2$ tissue culture flasks (Falcon) in Dulbecco's modified Eagle's medium (DMEM, Gibco), supplemented with 10% fetal calf serum (FCS, Gibco), 1% L-glutamine (Sigma) and 1% penicillin/streptomycin (Gibco). The second cell line culture consisted of renal epithelial cells designated human kidney-2 (HK-2). HK-2 was derived from a normal adult human renal cortex (178). Cultured cells were exposed to a recombinant retrovirus containing the HPV 16 E6/E7 genes. The HK-2 cell line was maintained as a monolayer culture in Quantum 286 medium for epithelial cells (PAA) with 1% penicillin/streptomycin. Cells were passaged at 85-90% confluency. Before the start of each experiment, normal growing cells were harvested with trypsin (Sigma), and cultured in 7 ml medium at a density of $5x10^4$ cells per flask and allowed to attach and grow overnight at 37ºC in a humidified atmosphere with 5% $CO_2$.

### 3.3.2 FCS-free cell culture and cytokine treatment experiments

TK-173 or HK-2 cells were grown to sub-confluency (~70% confluency) in 75 $cm^2$ culture flasks. Medium was removed, and after washing in phosphate buffered saline (PBS, Gibco) the cells were incubated for a further 24 h in 10 ml serum free DMEM with regular change of medium every 2 h. Purified human ANG II (0.5 µM) (Sigma) or, PDGF (10 nM) (R&D Systems), were added to the medium, and the cells were incubated for additional 72 h with the two cytokines separately in separate experiments. The medium with the cytokine was changed every 24 h to avoid any impact of dead cells on cell proteome. A group with no additives was run in parallel serving as the control. Cell extracts were collected, and the proteins were processed as described below for further analyses.

### 3.3.3 Protein extraction and precipitation

The protein extraction was performed as described previously (179). Briefly, the cultured cells were harvested and washed 3 times with PBS. Subsequently the cells were centrifuged at 200xg for 10 min, and the pellet was treated with 0.05-0.1 ml lysis buffer containing 9.5 M urea, 2% (w/v) CHAPS [(3-Cholamidopropyl)dimethylammonio]-1-propanesulfonate] (Sigma), 2% (w/v) ampholytes (MERCK), 1% (w/v) DTT (Sigma). After adding the lysis buffer, the samples were incubated for 30 min at 4ºC. For removing the cell debris, sample centrifugation was carried out at 13,000xg and 4ºC for 45 min. Supernatant was recentrifuged at 13,000xg and 4ºC for an additional 45 min to get maximal purity. The resulting samples were used immediately or stored at -80ºC until use. To reduce the salt contamination and to enrich the proteins, chloroform-methanol precipitation was performed according to Wessel and Fluegge (180). For the Western blot analysis of ECM proteins, the reducing agent (DTT) was avoided in lysis buffer to keep disulfide bridges intact. Total protein concentration was estimated using the Bio-Rad protein assay (Bio-Rad, Hercules, CA, USA) according to Bradford (181). BSA (Roche) was used as a standard.

### 3.3.4 MTT cell viability assay

For the cell viability assay the cell proliferation Kit I (MTT) from Roche was used according to the manufacturer's instructions. To investigate the effect of $H_2O_2$ (MERCK) and cytokines (ANG II and PDGF) on cell viability and proliferation, 5000-6000 cells were grown in a 96 well tissue culture plate (Falcon) in control medium (for $H_2O_2$) or in FCS-free medium (for cytokines). After 24 h the attached cells were treated with $H_2O_2$ (200 µM), ANG II (0.5 µM) or PDGF (10 nM). MTT test was performed 72 h after incubation according to the manufacturer recommendation. For transfection experiments, cells were first transfected with the corresponding plasmid, the transfection success was confirmed (see Plasmids and cellular

transfection) then moved into the 96 well tissue culture plates for MTT analyses. All experiments were performed in triplicate and during each experiment 6 replicate per case were carried out.

### 3.3.5 Two-dimensional gel electrophoresis (2-DE)

2-DE analysis was performed according to Dihazi *et al.*, 2011 (179). Briefly, cell extracts from ANG II, PDGF treated cells or control cells were prepared as described above. A total of 150 μg protein from each experiment was diluted in rehydration buffer [8 M urea, 1% (w/v) CHAPS, 0.2% ampholytes pH 5-8 for 11-cm IPG strips, 15 mM DTT, and a trace of bromophenol blue]. The sample was used for the rehydration of the immobilized pH gradient (IPG) strips (Bio-Rad). The strips were allowed to rehydrate for 1 h before adding mineral oil (Bio-Rad). The passive rehydration was carried out overnight for at least 12 h at room temperature in a focusing chamber. Isoelectric focusing with a Protean IEF (Bio-Rad) was performed at 20ºC using the following multistep protocol: 500 V for 1 h, 1000 V for 1 h, and 8000 V for 6 h. After the first dimension, the individual strips were equilibrated in 6 M urea, 30% (w/v) glycerol, 2% (w/v) SDS, 0.05 M Tris-HCl pH 8.8, and 15 mM DTT for 20 min. An additional incubation in the same buffer, supplemented with iodoacetamide (40 mg/ml), was carried out for another 20 min. After equilibration, the IPG strips were loaded on 12% SDS-PAGE, and run at 200 V for second dimension separation of proteins.

### 3.3.6 Gel staining

For image analysis, 2-D gels were fixed in a solution containing 50% methanol and 12% acetic acid overnight and fluorescently stained with Flamingo fluorescent gel stain (Bio-Rad) for a minimum of 5 h. After staining, gels were scanned at 50 μm resolution on a Fuji FLA5100 scanner (Fuji Photo, Kanagawa, Japan). The digitalized images were analyzed; spot matching across gels and normalization were performed using Delta2D 3.4 (Decodon,

Germany). Delta2D computes a 'spot quality' value for every detected spot. This value shows how closely a spot represents the 'ideal' 3D Gaussian bell shape. Based on the average spot volume ratio, spots whose relative expression is changed at least 2-fold between the compared samples were considered to be significant. 2-D gels were post-stained with colloidal Coomassie blue (Roti-Blue, Carl-Roth, Germany) overnight, and differentially regulated proteins were excised and processed for identification.

### 3.3.7 In-gel digestion and mass spectrometry analysis of protein spots

In-gel digestion and peptide extraction were carried out as described previously (179). Coomassie brilliant blue-stained spots were manually excised from the gels and washed with distilled water for 15 min. The destaining procedure was carried out by washing the spots alternately with 50% acetonitrile (ACN) and 100 mM ammonium bicarbonate 3 times for 5 min. After dehydrating the spots with ACN for 15 min, they were dried in a vacuum centrifuge for approximately 15 min. Thereafter, the gel spots were rehydrated for digestion with 40 µl trypsin (10 ng/µl in 100 mM ammonium bicarbonate) and incubated at 37ºC overnight. The peptide samples were extracted with different concentrations of ACN and trifluoroacetic acid (TFA). Subsequently, the extracted peptides were cocrystallized with the matrix (25 diaminobenzoic acid) on a stainless steel target using 1 µl matrix and 5 µl sample. An Applied Biosystems Voyager-DE STR time-of-flight (TOF) mass spectrometer, operating in delayed reflector mode with an accelerated voltage of 20 kV, was used to generate peptide mass fingerprint (PMF) maps. Mass spectra were obtained by averaging 50 individual laser shots. All samples were externally calibrated with a peptide mix of des-Arg1-bradykinin ([M+H]+904.46), angiotensin I ([M+H]+1296.68), Glu1-fibrinopeptide B ([M+H]+1570.67), ACTH (1-17) ([M+H]+2093.08), and ACTH (18-39) ([M+H]+2465.19), and the resulting mass spectra were internally calibrated with trypsin autolysis products (m/z 842.50 and m/z

2211.10). Monoisotopic peptide masses were assigned, and database searches in the Swiss-Prot primary sequence database, restricted to the taxonomy *Homo sapiens*, were performed using MASCOT Software 2.2 (Matrix Science). Carboxamidomethylation of Cys and oxidation of Met were specified as variable modifications. One missed trypsin cleavage was allowed. Mass tolerance was set to 50 ppm for PMF searches. The minimal requirement for accepting a protein as identified was at least 30% sequence coverage in the PMF. Alternatively, tryptic peptides were subjected to mass spectrometric sequencing using a Q-TOF Ultima Global mass spectrometer (Micromass, Manchester, UK), equipped with a nanoflow ESI Z-spray. For that purpose, gel plugs were excised from 2-D gels and digested as described previously. After digestion, the supernatant was removed and saved, and the additional peptides were extracted with increasing acetonitrile/trifluoroacetic acid solutions under sonication. All supernatants were pooled together, dried in a vacuum centrifuge, and re-dissolved in 0.1% formic acid for injection in the Q-TOF. The mass spectrometric sequencing was performed as described previously. Processed data were searched against the MSDB and Swissprot databases through the Mascot search engine using a peptide mass tolerance and fragment tolerance of 0.5 Da. Protein identifications with at least two peptides sequenced were considered significant.

### 3.3.8 Western blot analysis

Western blot (WB) analysis was performed according to Towbin and colleagues (182, 183). The cell extracts (40 µg per lane) were separated on a 12% SDS-gel. Blotting was performed on nitrocellulose membranes (Amersham Pharmacia Biotech, Buckinghamshire, UK) at 40 V for 24 h in transfer buffer (25 mM Tris-HCl pH 8.4, 192 mM glycine, 0.5% SDS, 20% methanol). The membranes were blocked in 5% non-fat dry milk in PBS buffer containing 0.1% Tween-20 for 2 h at 37ºC. The incubation with the primary antibodies was carried out

overnight at 4ºC. Mouse anti-DJ-1 (Sigma), rabbit anti-PRDX6 (Abcam), rabbit anti-SOD1 (Abnova), rabbit anti-PRDX1 (Abcam) and mouse anti-ACTB (Sigma), were used as primary antibodies. Alexa Fluor 647 goat anti-rabbit IgG antibody, or Alexa Fluor 647 goat anti-mouse IgG antibody were used as secondary antibodies (Molecular Probes). Before imaging, the blots were dried in the dark. The blot membranes were scanned at a resolution of 50 μm on a Fuji FLA5100 scanner with single laser-emitting excitation light at 635 nm and 670 nm, respectively.

In case of *Col4a3* knockout mice, three animals per group were sacrificed at weeks 4.5, 6.5, 7.5, and 9.5, and as control three WT animals were used. The kidneys from all animals were harvested. Aliquots of tissue extracts from three kidneys of different animals (40 μg protein) were dissolved in SDS-sample buffer, separated by electrophoresis in an SDS-polyacrylamide gel (12%) under reducing conditions, transferred to a nitrocellulose membrane, and blocked for 60 min at room temperature with 5% milk-powder in a 0.2 mol/L Tris-HCl buffer, pH 7.6, containing 0.1% Tween 20 solution (TBST buffer). Antibodies against mouse DJ-1, rabbit PRDX6, rabbit SOD1, rabbit PRDX1, rabbit FN1 (Sigma), mouse VCL (Sigma), and rabbit GRP78 (Sigma) as the primary antibodies were diluted in blocking buffer, then added to the membrane and allowed to incubate for 60 min. The addition of secondary antibodies, membrane scanning, and analysis were performed as described above.

### 3.3.9 Immunohistochemical and immunofluorescence analyses of kidney sections

Immunostaining of deparaffinized and rehydrated sections was performed to monitor the expression of DJ-1 and PRDX6 proteins. Following antigen retrieval pretreatment in 0.01 M citric acid using a standard steamer for 25 min, endogenous peroxidase was inactivated with 3% $H_2O_2$ in PBS for 10 min at room temperature in the dark. Sections were blocked with 10% goat serum in PBS for 1 h and incubated with either anti-DJ-1 or anti-PRDX6 primary

antibody overnight at 4ºC. Primary antibodies were detected with HRP labeled secondary antibody for 1 h at room temperature (GE Healthcare). For negative controls tissue sections were incubated only with the secondary antibody. The detection reaction was developed with 3,3-diaminobenzidine (Sigma) for 10 min at room temperature in the dark. Nuclei were counterstained with hematoxylin before examination. All tissue sections were dehydrated in graded alcohols and xylene and embedded in mounting solution Entellan (Merck).

Similar primary antibodies were also detected with fluorescence Alexa 555-conjugated goat anti-rabbit or Alexa 488-conjugated goat anti-mouse secondary antibody (Invitrogen) as recommended. Slides were rinsed and mounted with Vectashield 4,6-diamidino-2-phenylindole (DAPI) (Vector Laboratories) for visualization of nuclei.

### 3.3.10 Plasmids and cellular transfection

Construction of DJ-1 expression vectors (wild type and mutants) has been provided by Addgene ***(https://www.addgene.org/mission/)*** and purchased as ready plasmids: pGW1-Myc-DJ-1-WT (Myc tag protein), pDEST40-DJ-1-E18Q and pDEST40-DJ-1-E18D (6xHis tag proteins). All constructs were amplified in *E-coli* and verified by sequencing. The transfection was performed using transfection reagent Lipofectamine 2000$^{TM}$ (Invitrogen) according to manufacturers' standard protocol. In brief, 2 µg of plasmids and 8 µl of Lipofectamine 2000$^{TM}$ were added to 100 µl OptiMEM (Gibco). The mixture was gently mixed, incubated at room temperature for 20 min, and then added drop-wise to cells (TK-173 or HK-2) cultured to approximately 70% confluence. After 24 h, transfection media were changed with normal culture media supplemented with 0.5 mg/ml G-418 (Invitrogen) as a selection factor for stable transfection. Cells were maintained in the selection medium for 14 days to achieve stable transfection and assessed for protein expression by WB.

### 3.3.11 Protein immunoprecipitation

#### 3.3.11.1 For WT-DJ-1 (Myc tag protein)

To identify the potential interaction partners of DJ-1 WT, immunoprecipitation using anti-DJ-1 coupled to G-protein agarose matrix was performed. The cell lysates were harvested from transfected and control cells as described above. To remove potential backgrounds, the protein samples were adjusted to 1 ml with PBS buffer and 50 µl G-agarose matrix (Roche) were added to each sample. The mixture was incubated for 3 h at room temperature under agitation then centrifuged at 12,000xg for 30 sec. The supernatants were removed to new tubes and 5 µl anti-DJ-1 antibody were added to each sample. The immunoreaction was carried out overnight at 4ºC under agitation. 50 µl protein G-agarose matrix were added to each sample. The mixture was incubated at 4ºC under rotary agitation for 4 h. The samples were centrifuged and the supernatant removed. The G-agarose matrix was washed three times with PBS buffer. The protein elution was performed by incubating the samples in 30 µl of 2xloading buffer at 95ºC for 5 min. Subsequently the samples were centrifuged to remove the G-protein agarose, and the supernatant was used to run SDS-PAGE and identify the binding proteins.

#### 3.3.11.2 For E18Q-DJ-1 and E18D-DJ-1 (6xHis tag proteins)

For the identification of the potential interaction partners of DJ-1 mutants E18Q and E18D, His-tag affinity purification was carried-out. The QIA express Ni-NTA Fast Start Kit (Qiagen) was used and the protein purification was performed according to the provider protocols. Briefly, cells were harvested from transfected and control cells as previously described. Each cell pellet was re-suspended in one ml of the prepared native lysis buffer (Supplied native lysis buffer was supplemented with lysozyme and benzonase nuclease by dissolving the contents of the lysozyme vial in 600 µl of native lysis buffer. For use, 100 µl of

the lysozyme solution were added to a 10 ml aliquot of native buffer). The suspensions were incubated for 30 min on ice with 2-3 gentle swirling then centrifuged at 14,000xg for 30 min at 4ºC. Each sample was allowed to flow in a Fast Start column then washed 2 times each with 500 µl native wash buffer. Bound 6xHis-tagged proteins and their potential interaction partners were then eluted twice using 100 µl native elution buffer for each elution. 5 µl 4xSDS-PAGE sample buffer were added to 20 µl of the last elution sample fraction. SDS-PAGE protein separation and in-gel digestion mass spectrometric analysis of the samples were carried out as described above.

### 3.3.12 Bioinformatics

The classification of the identified proteins according to their main known/postulated functions was carried out using DAVID bioinformatics ***(http://david.abcc.ncifcrf.gov/).***This classification together with the official gene symbol was used to investigate and categorize the gene ontology (GO)-annotations (subcellular location and molecular function).

### 3.3.13 STRING analysis

The types of evidence for the association of the immunoprecipitated proteins suggesting their different functional links were quantitatively integrated using STRING 9.05 database (functional protein-protein interaction networks) ***(http://string-db.org).***

### 3.3.14 Statistical analysis

All blots were quantified using the ImageJ software. For comparison between two measures (in the same group) the paired t-test was used. The unpaired t-test (for comparing two groups) or one-way ANOVA (comparing three or more groups) were used. Graphpad prism software package was used for graphical presentation. Results are expressed as the average (mean±SD) of three or more independent experiments. Differences were considered statistically significant when $p<0.05$.

## 3.4 Results

### 3.4.1 Profibrotic cytokines affect renal cell viability through induction of OS

ANG II has systemic and local effects favoring cell proliferation. In addition, ANG II can induce the expression of different growth factors, which in turn participate in stimulating intracellular ROS formation and contribute to the pathogenesis of renal fibrosis. We attempted to investigate the response of cells stimulated with ANG II or PDGF using MTT cell viability assay. After several trials for different ANG II and PDGF concentrations used in literature, a concentration of 0.5 µM for ANG II and 10 nM for PDGF were found to impact the cell proliferation and induce OS without significant effect on cellular apoptosis in TK-173 and HK-2 cell models (Fig. 3.1A, B). For this reason, the concentrations mentioned were chosen for our further studies. The viability assay revealed that after 72 h incubation with ANG II or PDGF, both cell types showed significant increase ($P<0.05$) in cell growth compared to the control (Fig. 3.1A). When comparing both profibrogenic agonists, treatment with PDGF seems to accelerate the cell proliferation more than ANG II, which may indicate that OS induced by ANG II is more intense than that in case of PDGF.

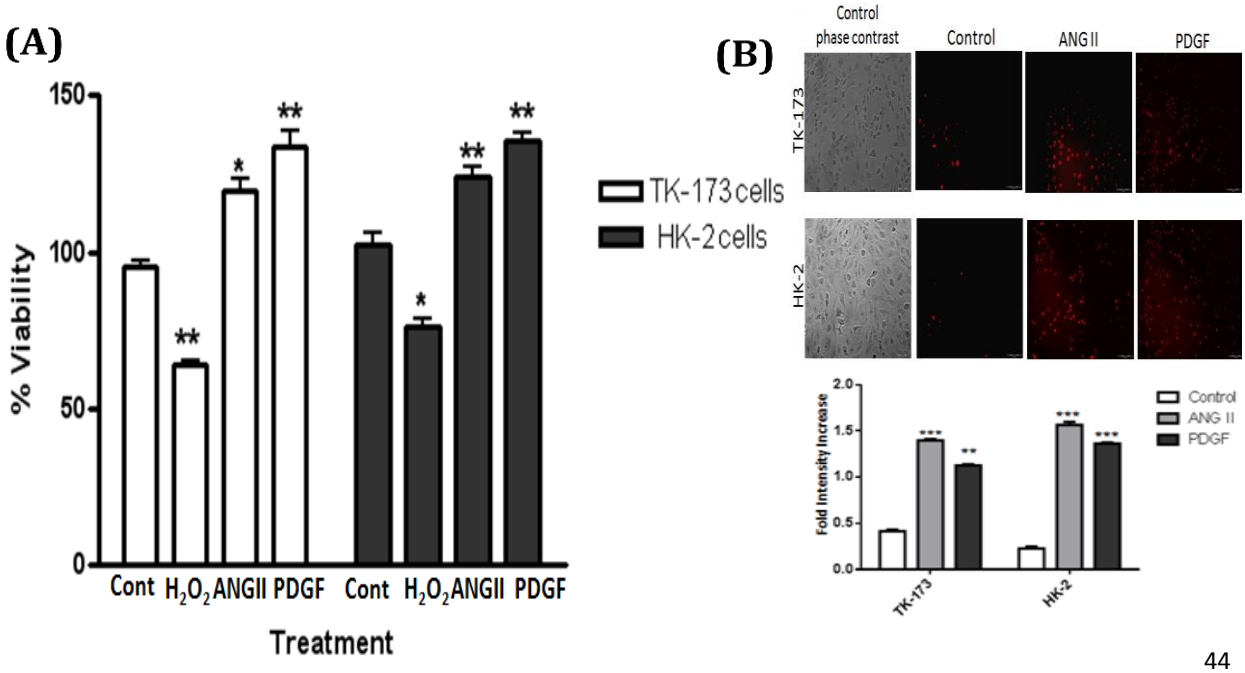

**(A):** 5000 TK-173 or HK-2 cells/well were cultured in 96 well cell culture plates, incubated with $H_2O_2$, ANG II or PDGF stress for 72 h. For ANG II and PDGF treated cells, cells were deprived from FCS in the medium 24 h before treatment. The cell viability was measured and plotted in the form of bar diagrams with the cell treatment on x-axis and cell viability on y-axis. Results are represented as a mean of 12 readings ±SD. **(B):** Fluorescence microscopy comparing DHR-123 stained control and treated (ANG II and PDGF) TK173 and HK-2 cells. Cells were stained with DHR-123 for 30 min and visualized using specific filter sets for phase contrast and rhodamine. The obtained images were merged to observe cell morphology. Scale bar = 100 µm. The fluorescence expression quantification is presented as grouped bar chart under each experimental condition. Results are given as the means ±SD. Statistical significance was assumed for p-values <0.05: *P<0.05, **P<0.01, ***P < 0.001 with respect to their corresponding control.

In confirmation to our previous study (128), the $H_2O_2$ at a concentration of 200 µM significantly inhibited cell viability in both treated cell groups 72 h after stimulation. The quantitative and statistical evaluation results are presented in Figure 3.1A comparing the actual response of TK-173 cells and HK-2 cells to their representative control group. $H_2O_2$ is an OS inducible that confers cellular OS *in vivo*, as we reported previously (128).

### 3.4.2 Mapping of renal cell proteome alteration upon cytokine treatment

Although much has been learned about the molecular mechanisms underlying the pathways by which cytokines activate renal fibrogenesis, an integrated proteomics pattern identifying the altered proteins remains elusive.

One scope of this study is to characterize key specific proteins showing alteration in their expression in cytokine treated cells (TK-173 and HK-2) compared to control ones. For this purpose, proteomic analysis was performed. 2-D protein maps from cell lysate of the different treated groups are presented in Figure 3.2 (A, B). All identified proteins that showed difference in expression under the distinct experimental conditions are numbered and

indicated in Figure 3.2 (A, B) and are listed in Tables 3.1 and 3.2 for TK-173 cells and Tables 3.3 and 3.4 for HK-2 cells.

**(A)**

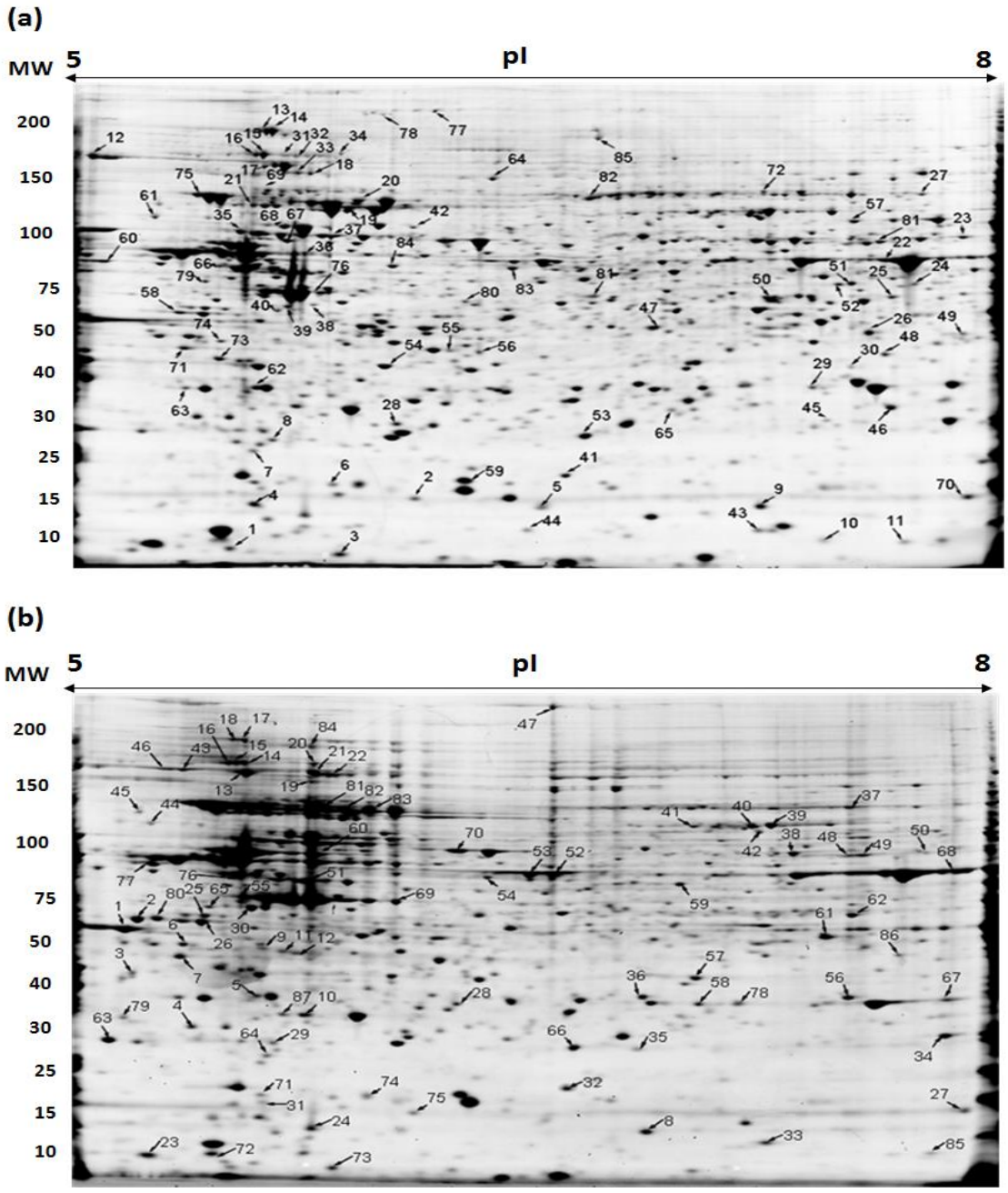


**Figure 3.2B continued**

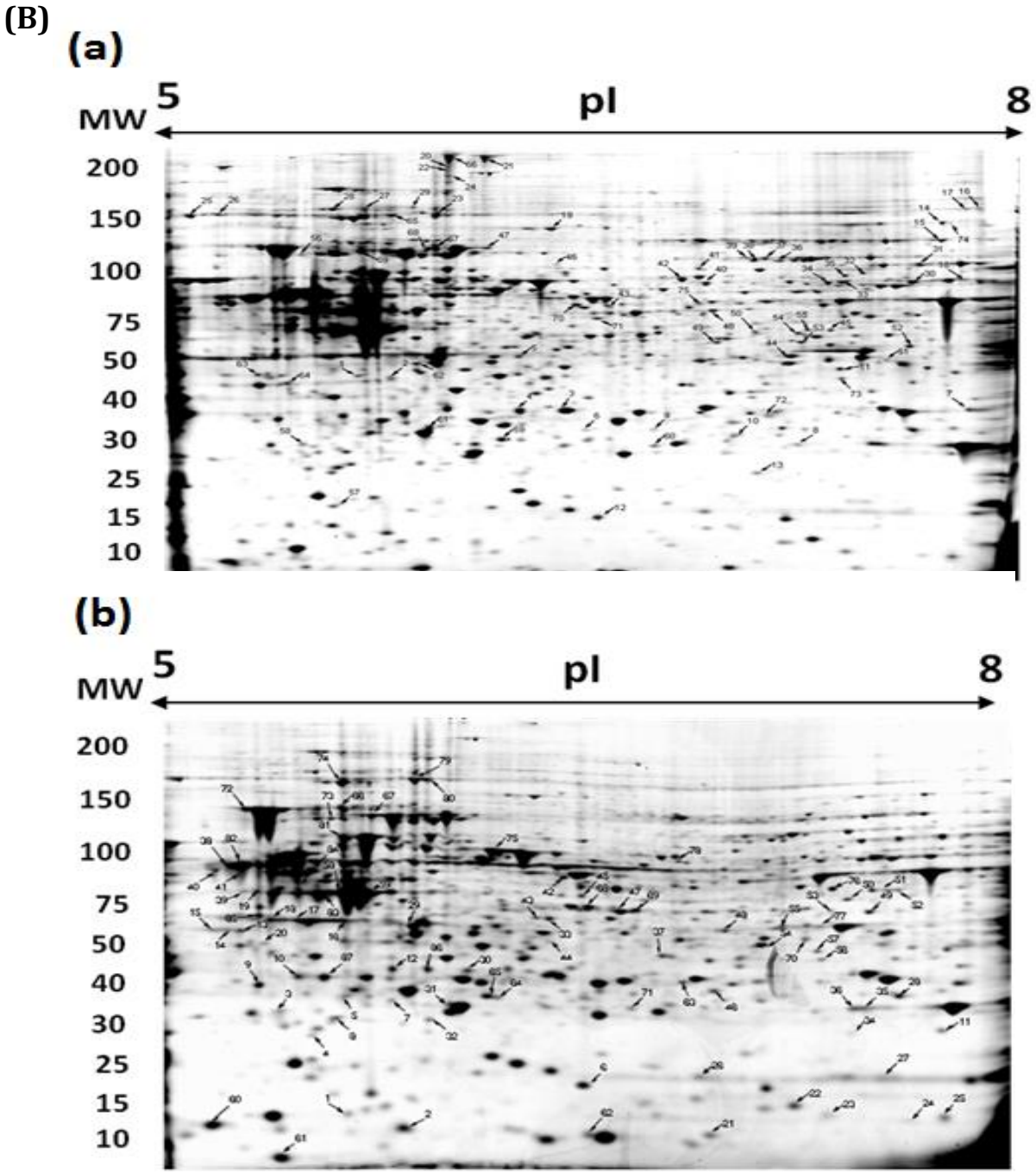


**Figure 3.2: 2-D reference maps of proteins extracted from TK-173 and HK-2 cells**

150 µg proteins were loaded on an 11-cm IPG strip with a linear pH gradient *pI* 5-8 for IEF; 12% SDS-polyacrylamide gels were used for the SDS-PAGE. Proteins were stained with Flamingo fluorescent gel stain. Identified spots were assigned a number corresponding to that in their table. **(A):** For TK-173 cells and **(B):** For HK-2 cells. **(a):** 2-D map under ANG II treatment and **(b):** 2-D map under PDGF treatment.

| Spot Nr. | Protein Name | Gene Name | SwissProt Accession | Mol. Wt. | CPI | PMF Score | PMF Seq. Cov. | MS/MS Score | MS/MS Seq. Cov. |
|---|---|---|---|---|---|---|---|---|---|
| 1 | Translationally controlled tumor protein | TPT1 | P13693 | 19595 | 4.84 | | | 352 | 14 |
| 2 | Microtubule-associated protein RP/EB family member 1 | MAPRE1 | Q15691 | 29999 | 5.02 | 77 | 22 | | |
| 3 | Small ubiquitin-related modifier 2 | JMO2 | P61956 | 10871 | 5.32 | | | 120 | 5 |
| 4 | Myosin regulatory light chain 12A | MYL12A | P19105 | 19794 | 4.65 | | | 111 | 9 |
| 5 | Prefoldin subunit 2 | PFDN2 | Q9UHV9 | 16648 | 6.20 | | | 114 | 5 |
| 6 | Ferritin light chain | FTL | P02792 | 20020 | 5.50 | | | 144 | 7 |
| 7 | Microtubule-associated protein RP/EB family member 1 | MAPRE1 | Q15691 | 29999 | 5.02 | 92 | 24 | | |
| 8 | EF-hand domain-containing protein D2 | EFHD2 | Q96C19 | 26697 | 5.15 | 105 | 9 | | |
| 9 | Peroxiredoxin-1 | PRDX1 | Q06830 | 22110 | 8.27 | | | 201 | 11 |
| 10 | Peptidyl-prolyl cis-trans isomerise A | PPIA | P62937 | 18012 | 7.68 | 176 | 11 | | |
| 11 | Cofilin-1 | CFL1 | P23528 | 18502 | 8.22 | | | 134 | 8 |
| 12 | Endoplasmin | HSP90B1 | P14625 | 92469 | 4.76 | | | 76 | 6 |
| 13 | Fibronectin | FN1 | P02751 | 262607 | 5.46 | | | 574 | 18 |
| 14 | Fibronectin | FN1 | P02751 | 262607 | 5.46 | | | 707 | 27 |
| 15 | Heat shock 70 kDa protein 4 | HSPA4 | P34932 | 94331 | 5.10 | | | 211 | 18 |
| 16 | Heat shock protein HSP 90-alpha | HSP90AA1 | P07900 | 84660 | 4.94 | 115 | 12 | | |
| 17 | Transitional endoplasmic reticulum ATPase | VCP | P55072 | 89322 | 5.14 | | | 322 | 21 |
| 18 | Caprin-1 | CAPRIN1 | Q14444 | 78366 | 5.04 | | | 69 | 7 |
| 19 | Heat shock 70 kDa protein 1 | HSPA1A | P08107 | 70052 | 5.47 | 64 | 11 | | |
| 20 | Stress-70 protein, mitochondrial | HSPA9 | P38646 | 73680 | 5.87 | 114 | 13 | | |
| 21 | Lamin-B1 | LMNB1 | P20700 | 66408 | 5.11 | | | 82 | 3 |
| 22 | Alpha-enolase | ENO1 | P06733 | 47169 | 7.01 | | | 179 | 8 |
| 23 | Fumarate hydratase, mitochondrial | FH | P07954 | 54637 | 8.85 | | | 42 | 7 |
| 24 | 26S protease regulatory subunit 8 | PSMC5 | P62195 | 45626 | 7.11 | | | 291 | 19 |
| 25 | Cytosolic acyl coenzyme A thioester hydrolase | ACOT7 | O00154 | 41796 | 8.85 | | | 261 | 11 |
| 26 | Calponin-2 | CNN2 | Q99439 | 33697 | 6.94 | | | 127 | 6 |
| 27 | Far upstream element-binding protein 2 | KHSRP | Q92945 | 73146 | 6.85 | | | 124 | 6 |
| 28 | Ras-related protein rab-11A | RAB11A | P62491 | 24394 | 6.12 | | | 159 | 7 |
| 29 | LIM and SH3 domain protein 1 | LASP1 | Q14847 | 29717 | 6.61 | | | 146 | 8 |
| 30 | Abhydrolase domain-containing protein 10, mitochondrial | ABHD10 | Q9NUJ1 | 33933 | 8.81 | | | 118 | 9 |
| 31 | Heat shock protein 105 kDa | HSPH1 | Q92598 | 96865 | 5.27 | | | 66 | 7 |
| 32 | Splicing factor 3 subunit 1 | SF3A1 | Q15459 | 88886 | 5.15 | 179 | 18 | | |
| 33 | Caprin-1 | CAPRIN1 | Q14444 | 78366 | 5.04 | | | 64 | 3 |
| 34 | Peroxisome biogenesis factor 1 | PEX1 | O43933 | 142867 | 5.91 | | | 71 | 4 |
| 35 | Serine/threonin protein phosphatase 2A 65 kDa | PPP2R1A | P30153 | 65309 | 5.00 | | | 63 | 5 |
| 36 | Tubulin alpha-1A chain | TUBA1A | Q71U36 | 50136 | 4.94 | | | 70 | 5 |

| | | | | | | | | | |
|---|---|---|---|---|---|---|---|---|---|
| 37 | Tubulin alpha-1B chain | TUBA1B | P68363 | 50152 | 4.94 | | | 125 | 8 |
| 38 | Glutaredoxin-3 | GLRX3 | O76003 | 37432 | 5.31 | 63 | 9 | | |
| 39 | UBX domain-containing protein 1 | UBXN1 | Q04323 | 33325 | 5.23 | | | 136 | 11 |
| 40 | N-myc-interactor | NMI | Q13287 | 35057 | 5.23 | 92 | 14 | | |
| 41 | Protein DJ-1 | PARK7 | Q99497 | 19891 | 6.32 | | | 71 | 5 |
| 42 | Copine-1 | CPNE1 | Q99829 | 59059 | 5.52 | | | 68 | 3 |
| 43 | Peptidyl-prolyl-cis trans isomerase A | PPIA | P62937 | 18012 | 7.68 | | | 80 | 4 |
| 44 | Ubiquitin-conjugating enzymeE2 N | UBE2N | P61088 | 17138 | 6.13 | | | 82 | 7 |
| 45 | GTP-binding nuclear protein Ran | RAN | P62826 | 24423 | 7.01 | | | 66 | 4 |
| 46 | Superoxide dismutase (Mn), mitochondrial | SOD2 | P04179 | 24722 | 8.35 | 116 | 15 | | |
| 47 | Malate dehydrogenase, cytoplasmic | MDH1 | P40925 | 36426 | 6.91 | | | 88 | 6 |
| 48 | Syntenin-1 | SDCBP | O00560 | 32444 | 7.06 | | | 81 | 5 |
| 49 | Glyceraldehyde-3-phosphate dehydrogenase | GAPDH | P04406 | 36053 | 8.57 | | | 104 | 10 |
| 50 | Annexin 1 | ANXA1 | P04083 | 38714 | 6.57 | | | 118 | 6 |
| 51 | Annexin 2 | ANXA2 | P07355 | 38604 | 7.57 | | | 175 | 8 |
| 52 | Fructose-bisphosphate aldolase A | ALDOA | P04075 | 39420 | 8.30 | | | 149 | 9 |
| 53 | BAG family molecular chaperone regulator 2 | BAG2 | O95816 | 23772 | 6.25 | | | 86 | 6 |
| 54 | Annexin A5 | ANXA5 | P08758 | 35937 | 4.93 | 156 | 8 | | |
| 55 | Calponin-3 | CNN3 | Q15417 | 36414 | 5.69 | | | 65 | 2 |
| 56 | Calponin-3 | CNN3 | Q15417 | 36414 | 5.69 | | | 62 | 6 |
| 57 | Pyruvate kinase isozymes M1/M2 | PKM2 | P14618 | 57937 | 7.96 | | | 89 | 6 |
| 58 | Actin, cytoplasmic 1 | ACTB | P60709 | 41737 | 5.29 | | | 378 | 14 |
| 59 | Superoxide dismutase (Cu-Zn) | SOD1 | P00441 | 15936 | 5.70 | | | 88 | 6 |
| 60 | Vimentin | VIM | P08670 | 53652 | 5.05 | | | 262 | 16 |
| 61 | Nuclear migration protein nudC | NUDC | Q9Y266 | 38243 | 5.27 | | | 232 | 14 |
| 62 | Proteasome subunit alpha type-3 | PSMA3 | P25788 | 28415 | 5.19 | | | 225 | 9 |
| 63 | Proteasome subunit beta type-7 | PSMB7 | Q99436 | 29946 | 7.58 | | | 128 | 6 |
| 64 | T-complex protein 1 subunit alpha | TCP1 | P17987 | 60306 | 5.80 | | | 190 | 8 |
| 65 | Peroxiredoxin-6 | PRDX6 | P30041 | 25035 | 6.00 | | | 261 | 9 |
| 66 | Vimentin | VIM | P08670 | 53619 | 5.05 | | | 438 | 14 |
| 67 | Hydroxymethyl glutaryl-CoA synthase, cytomplasmic | HMGCS1 | Q01581 | 57257 | 5.22 | | | 516 | 11 |
| 68 | 60 kDa heat shock protein,mitochondrial | HSPD1 | P10809 | 61016 | 5.70 | | | 600 | 19 |
| 69 | Cytoplasmic dynein 1 intermediate chain 2 | DYNC1I2 | Q13409 | 71457 | 5.08 | | | 59 | 6 |
| 70 | Peroxiredoxin-5, mitochondrial | PRDX5 | P30044 | 22026 | 8.93 | | | 140 | 8 |
| 71 | Nucleophosmin | NPM1 | P06748 | 32575 | 4.64 | 60 | 17 | | |
| 72 | Prelamin-A/C | LMNA | P02545 | 74139 | 6.57 | | | 148 | 4 |
| 73 | Annexin A5 | ANXA5 | P08758 | 35937 | 4.93 | 235 | 25 | | |
| 74 | WD repeat-containing protein 61 | WDR61 | Q9GZS3 | 33581 | 5.16 | 100 | 11 | | |
| 75 | 78 kDa glucose-regulated protein | HSPA5 | P11021 | 72333 | 5.07 | 165 | 12 | | |

| | | | | | | | | | |
|---|---|---|---|---|---|---|---|---|---|
| 76 | Actin, cytoplasmic 2 | ACTG1 | P63261 | 41793 | 5.31 | 70 | 13 | | |
| 77 | Collagen alpha-1 (I) chain | COL1A1 | P02452 | 138911 | 5.50 | | | 83 | 7 |
| 78 | Laminin subunit gamma-1 | LAMC1 | P11047 | 177603 | 5.01 | | | 61 | 4 |
| 79 | Sex hormone-binding globulin | SHBG | P04278 | 43779 | 6.22 | | | 62 | 5 |
| 80 | Cytoplasmic dynein 1 heavy chain 1 | DYNC1H1 | Q14204 | 532408 | 6.01 | | | 78 | 4 |
| 81 | Serine hydroxymethyltransferase, mitochondrial | SHMT2 | P34897 | 55993 | 8.76 | | | 164 | 12 |
| 82 | Glutamate dehydrogenase 1, mitochondrial | GLUD1 | P00367 | 61398 | 7.66 | | | 112 | 6 |
| 83 | Ezrin | EZR | P15311 | 69413 | 5.94 | | | 85 | 7 |
| 84 | Glial fibrallary acidic protein | GFAP | P14136 | 49880 | 5.42 | | | 77 | 4 |
| 85 | Elongation factor 2 | EEF2 | P13639 | 95338 | 6.41 | | | 95 | 6 |

**Table 3.1: Proteins differently expressed in the ANG II treated TK-173 cell line**

The gene name, accession number in Swiss-Prot, molecular weight (Mol. Wt.), the calculated isoelectric point (CPI), the peptide mass fingerprinting (PMF) score and sequence coverage (Seq. Cov.), MS/MS information and sequence coverage are given. The spots where MS/MS-data are missing were only identified with PMF.

| Spot Nr. | Protein Name | Gene Name | SwissProt Accession | Mol. Wt. | CPI | PMF Score | PMF Seq. Cov. | MS/MS Score | MS/MS Seq. Cov. |
|---|---|---|---|---|---|---|---|---|---|
| 1 | Actin, cytoplasmic 1 | ACTB | P60709 | 41710 | 5.29 | | | 305 | 15 |
| 2 | Actin, cytoplasmic 1 | ACTB | P60709 | 41710 | 5.29 | | | 238 | 7 |
| 3 | Elongation factor 1-delta | EEF1D | P29692 | 31103 | 4.9 | | | 388 | 8 |
| 4 | Chromobox protein homolog 5 | CBX5 | P45973 | 22211 | 5.71 | | | 174 | 6 |
| 5 | Proteasome subunit alpha type-3 | PSMB3 | P49720 | 28415 | 6.13 | | | 254 | 6 |
| 6 | Tubulin beta chain | TUBB | Q9BUU9 | 49639 | 4.75 | 60 | 14 | | |
| 7 | Tubulin beta chain | TUBB | Q9BUU9 | 49639 | 4.75 | | | 88 | 8 |
| 8 | Peptidyl-prolyl cis-trans isomerase A | PPIA | P62937 | 18001 | 7.68 | 101 | 11 | | |
| 9 | Tubulin beta chain | TUBB | Q9BUU9 | 49639 | 4.75 | | | 262 | 6 |
| 10 | Adapter molecule crk | CRK | P46108 | 33810 | 5.38 | 101 | 13 | | |
| 11 | L-lactate dehydrogenase B chain | LDHB | P07195 | 36615 | 5.71 | 63 | 3 | | |
| 12 | Inorganic pyrophosphatase | PPA1 | Q15181 | 32639 | 5.54 | 65 | 3 | | |
| 13 | Heat shock protein 90-beta | HSP90AB1 | P08238 | 83212 | 4.96 | 65 | 2 | | |
| 14 | Heat shock 70 kDa protein 4 | HSPA4 | P34932 | 94271 | 5.10 | 91 | 4 | | |
| 15 | Heat shock 70 kDa protein 4 | HSPA4 | P34932 | 94271 | 5.10 | 84 | 4 | | |
| 16 | Heat shock 70 kDa protein 4 | HSPA4 | P34932 | 94271 | 5.10 | 79 | 3 | | |
| 17 | Hypoxia up-regulated protein 1 | HYOU1 | Q9Y4L1 | 111266 | 5.16 | | | 133 | 26 |
| 18 | Hypoxia up-regulated protein 1 | HYOU1 | Q9Y4L1 | 111266 | 5.16 | | | 110 | 22 |
| 19 | Caprin-1 | CAPRIN1 | Q14444 | 78318 | 5.14 | 114 | 5 | | |
| 20 | Heat shock 70 kDa protein 4 | HSPA4 | P34932 | 94271 | 5.10 | | | 292 | 10 |
| 21 | Transitional endoplasmic reticulum ATPase | VCP | P55072 | 89266 | 5.14 | 90 | 20 | | |
| 22 | Transitional endoplasmic reticulum ATPase | VCP | P55072 | 89266 | 5.14 | 71 | 16 | | |
| 23 | Thioredoxin | TXN | P10599 | 11730 | 4.82 | 77 | 8 | | |
| 24 | Coactosin-like protein | COTL1 | Q14019 | 15935 | 5.50 | 83 | 11 | | |
| 25 | Actin, cytoplasmic 1 | ACTB | P60709 | 41710 | 5.29 | | | 210 | 9 |
| 26 | Actin, cytoplasmic 1 | ACTB | P60709 | 41710 | 5.29 | | | 217 | 9 |
| 27 | Peroxiredoxin-1 | PRDX1 | Q06830 | 22096 | 8.27 | | | 174 | 8 |
| 28 | Annexin A2 | ANXA2 | P07355 | 38580 | 7.57 | | | 547 | 16 |
| 29 | Prohibitin | PHB | P35232 | 29786 | 5.57 | | | 266 | 7 |
| 30 | Tubulin beta-4B chain | TBB4B | P68371 | 49799 | 4.79 | | | 424 | 18 |
| 31 | Nucleoside diphosphate kinase A | NME1 | P15531 | 17138 | 5.81 | | | 243 | 9 |

| | | | | | | | | | |
|---|---|---|---|---|---|---|---|---|---|
| 32 | Protein DJ-1 | PARK7 | Q99497 | 19878 | 6.32 | | | 115 | 7 |
| 33 | Cofilin-1 | CFL1 | P10668 | 18491 | 8.16 | | | 117 | 6 |
| 34 | Superoxide dismutase [Mn], mitochondrial | SOD2 | P04179 | 24707 | 8.35 | 90 | 10 | | |
| 35 | GTP-binding nuclear protein Ran | RAN | P62826 | 24408 | 7.01 | | | 193 | 5 |
| 36 | Phosphoglycerate mutase 1 | PGAM1 | P18669 | 28786 | 6.67 | | | 112 | 8 |
| 37 | Far upstream element-binding protein 2 | KHSRP | Q92945 | 73101 | 6.85 | 115 | 19 | | |
| 38 | Stress-induced-phosphoprotein 1 | STIP1 | P31948 | 62599 | 6.40 | 150 | 35 | | |
| 39 | Prelamin-A/C | LMNA | P02545 | 74095 | 6.57 | 147 | 31 | | |
| 40 | Prelamin-A/C | LMNA | P02545 | 74095 | 6.57 | | | 44 | 3 |
| 41 | Prelamin-A/C | LMNA | P02545 | 74095 | 6.57 | 169 | 19 | | |
| 42 | Prelamin-A/C | LMNA | P02545 | 74095 | 6.57 | | | 71 | 20 |
| 43 | Heat shock protein HSP 90-beta | HSP90AB1 | P08238 | 83212 | 4.96 | | | 454 | 12 |
| 44 | Nucleolin | NCL | P19338 | 76568 | 4.60 | | | 305 | 13 |
| 45 | Nucleolin | NCL | P19338 | 76568 | 4.60 | | | 219 | 9 |
| 46 | Heat shock protein HSP 90-beta | HSP90AB1 | P08238 | 83212 | 4.96 | | | 502 | 15 |
| 47 | Spectrin alpha chain, brain | SPTAN1 | Q13813 | 284364 | 5.22 | | | 340 | 19 |
| 48 | Pyruvate kinase isozymes M1/M2 | PKM2 | P14618 | 57900 | 7.96 | 159 | 20 | | |
| 49 | Pyruvate kinase isozymes M1/M2 | PKM2 | P14618 | 57900 | 7.96 | 180 | 23 | | |
| 50 | Pyruvate kinase isozymes M1/M2 | PKM2 | P14618 | 57900 | 7.96 | 130 | 20 | | |
| 51 | Heterogeneous nuclear ribonuleoprotein K | HNRNPK | P61978 | 50944 | 5.39 | 67 | 13 | | |
| 52 | Pyruvate kinase isozymes M1/M2 | PKM2 | P14618 | 57900 | 7.96 | | | 201 | 7 |
| 53 | Pyruvate kinase isozymes M1/M2 | PKM2 | P14618 | 57900 | 7.96 | | | 113 | 25 |
| 54 | Pyruvate kinase isozymes M1/M2 | PKM2 | P14618 | 57900 | 7.96 | | | 69 | 15 |
| 55 | TAR DNA-binding protein 43 | TARDBP | Q13148 | 44711 | 5.85 | | | 166 | 6 |
| 56 | Heterogeneous nuclear ribonucleoprotein D0 | HNRNPD | Q14103 | 38410 | 7.61 | | | 98 | 4 |
| 57 | Acetyl-CoA acetyltransferase, cytosolic | ACAT2 | Q9BWD1 | 41324 | 6.46 | | | 73 | 6 |
| 58 | Crk-like protein | CRKL | P46109 | 33756 | 6.26 | | | 63 | 3 |
| 59 | Proliferation-associated protein 2G4 | PA2G4 | Q9UQ80 | 43759 | 6.13 | | | 146 | 9 |
| 60 | Vimentin | VIM | P08670 | 53619 | 5.05 | | | 274 | 38 |
| 61 | Aldose reductase | AKR1B1 | P15121 | 35830 | 6.52 | | | 193 | 4 |
| 62 | Poly (rC)-binding protein 1 | PCBP1 | Q15365 | 37474 | 6.66 | | | 104 | 6 |
| 63 | 14-3-3 protein epsilon | YWHAE | P62258 | 29155 | 4.63 | | | 95 | 3 |
| 64 | Chloride intracellular channel protein 1 | CLIC1 | O00299 | 26906 | 5.09 | | | 192 | 5 |
| 65 | Actin, cytoplasmic 1 | ACTB | P60709 | 41710 | 5.29 | | | 193 | 8 |
| 66 | Proteasome subunit alpha type-2 | PSMA2 | P25787 | 25882 | 6.91 | | | 229 | 16 |

| | | | | | | | | | |
|---|---|---|---|---|---|---|---|---|---|
| 67 | Electron transfer flavoprotein subunit alpha, mitochondrial | ETFA | P13804 | 35058 | 8.62 | | | 235 | 14 |
| 68 | Alpha-enolase | ENO1 | P06733 | 47139 | 7.01 | 142 | 22 | | |
| 69 | Heterogeneous nuclear ribonucleoprotein H | HNRNPH1 | P31943 | 49198 | 5.89 | | | 86 | 10 |
| 70 | Aldehyde dehydrogenase X, mitochondrial | ALDH1B1 | P30837 | 57202 | 6.36 | | | 218 | 18 |
| 71 | Prefoldin subunit 5 | PFDN5 | Q99471 | 17317 | 5.94 | | | 123 | 9 |
| 72 | Prefoldin subunit 2 | PFDN2 | Q9UHV9 | 16638 | 6.20 | | | 244 | 13 |
| 73 | Thioredoxin | TXN | P10599 | 11730 | 4.82 | | | 125 | 4 |
| 74 | Glutathione S-transferase P | GSTP1 | P09211 | 23341 | 5.43 | 62 | 7 | | |
| 75 | Peroxiredoxin-6 | PRDX6 | P30041 | 25035 | 6.00 | | | 211 | 12 |
| 76 | Protein disulfide-isomerase A3 | PDIA3 | P30101 | 56747 | 5.98 | 157 | 27 | | |
| 77 | Vimentin | VIM | P08670 | 53619 | 5.05 | | | 75 | 4 |
| 78 | Annexin A5 | ANXA2 | P07355 | 38580 | 7.57 | | | 105 | 6 |
| 79 | Elongation factor1-delta | EEF1D | P29692 | 31103 | 4.90 | | | 89 | 5 |
| 80 | Actin, cytoplasmic 1 | ACTB | P60709 | 41710 | 5.29 | | | 217 | 7 |
| 81 | 78-kDa glucose regulated protein | HSPA5 | P11021 | 72288 | 5.07 | | | 117 | 8 |
| 82 | Heat shock cognate 71 kDa protein | HSPA8 | P11142 | 70854 | 5.37 | 73 | 19 | | |
| 83 | Heat shock cognate 71 kDa protein | HSPA8 | P11142 | 70854 | 5.37 | 80 | 17 | | |
| 84 | Endoplasmin | HSP90B1 | P14625 | 92411 | 4.76 | | | 156 | 7 |
| 85 | 39S ribosomal protein L12, mitochondrial | MRPL12 | P52815 | 21335 | 9.05 | | | 174 | 5 |
| 86 | Glyceraldehyde-3-phosphate dehydrogenase | GAPDH | P04406 | 36030 | 8.57 | | | 165 | 5 |
| 87 | N(G),N(G)-dimethylarginine dimethylaminohydrolase 1 | DDAH1 | O94760 | 31102 | 5.53 | | | 140 | 6 |

**Table 3.2: Proteins differently expressed in the PDGF treated TK-173 cell line**

The gene name, accession number in Swiss-Prot, molecular weight (Mol. Wt.), the calculated isoelectric point (CPI), the peptide mass fingerprinting (PMF) score and sequence coverage (Seq. Cov.), MS/MS information and sequence coverage are given. The spots where MS/MS-data are missing were only identified with PMF.

| Spot Nr. | Protein Name | Gene Name | SwissProt Accession | Mol. Wt. | CPI | PMF Score | PMF Seq. Cov. | MS/MS Score | MS/MS Seq. Cov. |
|---|---|---|---|---|---|---|---|---|---|
| 1 | Serine/arginine-rich splicing factor 1 | SFRS1 | Q07955 | 27728 | 10.37 | 80 | 12 | 198 | 13 |
| 2 | Serine/arginine-rich splicing factor 1 | SFRS1 | Q07955 | 27728 | 10.37 | 91 | 9 | | |
| 3 | Glutathione S-transferase omega-1 | GSTO 1 | P78417 | 27548 | 6.24 | 68 | 11 | 112 | 5 |
| 4 | Cathepsin D | CTSD | P07339 | 44524 | 6.10 | 60 | 11 | | |
| 5 | Pyridoxal kinase | PDXK | O00764 | 35080 | 5.75 | | | 122 | 6 |
| 6 | Heat shock protein beta-1 | HSPB1 | P04792 | 22768 | 5.98 | 109 | 8 | 161 | 13 |
| 7 | GTP-binding nuclear protein Ran | RAN | P62826 | 24408 | 7.01 | | | 164 | 14 |
| 8 | Proteasome subunit beta type-2 | PSMB2 | P49721 | 22822 | 6.52 | | | 135 | 8 |
| 9 | 5'(3')-deoxyribonucleotidase, cytosolic type | NT5C | Q8TCD5 | 23368 | 6.18 | | | 156 | 8 |
| 10 | Proteasome subunit alpha type-6 | PSMA6 | P60900 | 27382 | 6.34 | | | 200 | 13 |
| 11 | S-formylglutathione hydrolase | ESD | P10768 | 31442 | 6.54 | 65 | 10 | 68 | 5 |
| 12 | Protein DJ-1 | PARK7 | Q99497 | 19878 | 6.32 | | | 179 | 9 |
| 13 | Peroxiredoxin-6 | PRDX6 | P30041 | 25035 | 6.00 | | | 148 | 7 |
| 14 | Far upstream element-binding protein 2 | KHSRP | Q92945 | 73101 | 6.85 | | | 159 | 14 |
| 15 | Far upstream element-binding protein 1 | FUBP1 | Q96AE4 | 67518 | 7.18 | 113 | 13 | 111 | 5 |
| 16 | C-1-tetrahydrofolate synthase, cytoplasmic | MTHFD1 | P11586 | 101495 | 6.89 | | | 64 | 13 |
| 17 | Elongation factor 2 | EEF2 | P13639 | 95277 | 6.41 | | | 137 | 6 |
| 18 | Glutamate dehydrogenase 1, mitochondrial | GLUD1 | P00367 | 61359 | 7.66 | | | 132 | 7 |
| 19 | Vinculin | VCL | P18206 | 123722 | 5.50 | | | 68 | 16 |
| 20 | Spectrin alpha chain, brain | SPTAN1 | Q13813 | 284364 | 5.22 | 93 | 40 | | |
| 21 | Spectrin alpha chain, brain | SPTAN1 | Q13813 | 284364 | 5.22 | | | 122 | 12 |
| 22 | Spectrin alpha chain, brain | SPTAN1 | Q13813 | 284364 | 5.22 | 103 | 34 | 139 | 21 |
| 23 | Endoplasmin | HSP90B1 | P14625 | 92411 | 4.76 | | | 447 | 23 |
| 24 | Major vault protein | MVP | Q14764 | 99266 | 5.34 | | | 95 | 8 |
| 25 | Endoplasmin | HSP90B1 | P14625 | 92411 | 4.76 | | | 178 | 12 |
| 26 | Endoplasmin | HSP90B1 | P14625 | 92411 | 4.76 | 166 | 13 | | |
| 27 | Heat shock 70 kDa protein 4 | HSPA4 | P34932 | 94331 | 5.10 | | | 180 | 12 |
| 28 | Heat shock 70 kDa protein 4 | HSPA4 | P34932 | 94331 | 5.10 | 78 | 11 | | |
| 29 | Endoplasmin | HSP90B1 | P14625 | 92411 | 4.76 | | | 131 | 7 |
| 30 | Fascin | FSCN1 | Q16658 | 54496 | 6.84 | 142 | 20 | | |
| 31 | Heterogeneous nuclear ribonucleoprotein L | HNRNPL | P14866 | 64092 | 8.46 | 115 | 18 | 70 | 6 |
| 32 | Bifunctional purine biosynthesis protein PURH | ATIC | P31939 | 64575 | 6.27 | 127 | 21 | | |
| 33 | Prelamin-A/C | LMNA | P02545 | 74095 | 6.57 | | | 141 | 13 |
| 34 | Prelamin-A/C | LMNA | P02545 | 74095 | 6.57 | 98 | 11 | 153 | 14 |
| 35 | Prelamin-A/C | LMNA | P02545 | 74095 | 6.57 | | | 145 | 14 |
| 36 | Pre-mRNA-processing factor 19 | PRPF19 | Q9UMS4 | 55146 | 6.14 | | | 146 | 9 |

| | | | | | | | | | |
|---|---|---|---|---|---|---|---|---|---|
| 37 | T- complex protein 1 subunit gamma | CCT3 | P49368 | 60495 | 6.10 | | | 253 | 7 |
| 38 | T-complex protein 1 subunit beta | CCT2 | P78371 | 57452 | 6.01 | 145 | 19 | | |
| 39 | Sorting nexin-6 | SNX6 | Q9UNH7 | 46620 | 5.81 | | | 155 | 12 |
| 40 | Aflatoxin B1 aldehyde reductase member 2 | AKR7A2 | O43488 | 39564 | 6.70 | | | 249 | 17 |
| 41 | Sialic acid synthase | NANS | Q9NR45 | 40281 | 6.29 | | | 255 | 12 |
| 42 | Lipocalin-1 | LCN1 | P31025 | 19238 | 5.38 | 76 | 6 | 132 | 7 |
| 43 | Stress-70 protein | HSPA9 | P38646 | 73635 | 5.87 | 66 | 13 | 117 | 8 |
| 44 | Proliferation-associated protein 2G4 | PA2G4 | Q9UQ80 | 43759 | 6.13 | 92 | 16 | 158 | 11 |
| 45 | 28S ribosomal protein S22, mitochondrial | MRPS22 | P82650 | 41254 | 7.70 | 111 | 15 | 135 | 9 |
| 46 | Short-chain specific acyl-CoA dehydrogenase, mitochondrial | ACADS | P16219 | 44269 | 8.13 | 61 | 9 | 126 | 7 |
| 47 | Heterogeneous nuclear ribonucleoproteins C1/C2 | HNRNPC | P07910 | 33650 | 4.94 | | | 82 | 4 |
| 48 | Ribose- phosphate pyrophosphokinase 1 | PRPS1 | P60891 | 34812 | 6.51 | 67 | 7 | 112 | 5 |
| 49 | Annexin A1 | ANXA1 | P04083 | 38690 | 6.57 | 92 | 15 | | |
| 50 | RNA - binding protein 4 | RBM4 | Q9BWF3 | 40289 | 6.61 | | | 279 | 8 |
| 51 | RNA - binding protein 4B | RBM4B | Q9BQ04 | 40124 | 6.28 | | | 253 | 9 |
| 52 | 78 kDa glucose-regulated protein | HSPA5 | P11021 | 72288 | 5.07 | 188 | 32 | | |
| 53 | Thioredoxin domain- containing protein 12 | TXNDC12 | O95881 | 19194 | 5.25 | | | 149 | 10 |
| 54 | Actin, cytoplasmic 1 | ACTB | P60709 | 41710 | 5.29 | | | 106 | 14 |
| 55 | Proteasome subunit beta type-4 | PSMB4 | P28070 | 29185 | 5.70 | | | 113 | 13 |
| 56 | Thioredoxin-dependent peroxide reductase, mitochondrial | PRDX3 | P30048 | 27675 | 7.68 | 185 | 23 | 133 | 14 |
| 57 | Actin, cytoplasmic 1 | ACTB | P60709 | 41710 | 5.29 | | | 105 | 7 |
| 58 | Tubulin beta chain | TUBB | P07437 | 49639 | 4.78 | 75 | 15 | 198 | 13 |
| 59 | Heterogeneous nuclear ribonucleoproteins C1/C2 | HNRNPC | P07910 | 33650 | 4.94 | | | 178 | 9 |
| 60 | Aldose reductase | AKR1B1 | P15121 | 35830 | 6.52 | 60 | 14 | 88 | 6 |
| 61 | Endoplasmin | HSP90B1 | P14625 | 92411 | 4.76 | 87 | 20 | 67 | 4 |
| 62 | Nucleoprotein TPR | TPR | P12270 | 267131 | 4.97 | | | 133 | 7 |
| 63 | Stress-70 protein, mitochondrial | HSPA9 | P38646 | 73635 | 5.87 | | | 154 | 11 |
| 64 | Lamin- B1 | LMNB1 | P20700 | 66368 | 5.11 | 71 | 15 | 139 | 7 |
| 65 | Peptidyl-prolyl cis-trans isomerase FKBP10 | FKBP10 | Q96AY3 | 64204 | 5.36 | | | 251 | 12 |
| 66 | 26S protease regulatory subunit 7 | PSMC2 | P35998 | 48603 | 5.71 | 127 | 23 | | |
| 67 | Eukaryotic translation initiation factor 3 subunit G | EIF3G | O75821 | 35589 | 5.87 | | | 110 | 5 |
| 68 | Cytochrome b-c1 complex subunit Rieske, mitochondrial | UQCRFS1 | P47985 | 29649 | 8.55 | | | 122 | 5 |
| 69 | Omega-amidase NIT2 | NIT2 | Q9NQR4 | 30589 | 6.83 | 169 | 19 | 295 | 10 |
| 70 | Heterogeneous nuclear ribonuclear protein L | HNRNPL | P14866 | 64092 | 8.46 | | | 249 | 18 |
| 71 | Alpha-enolase | ENO1 | P06733 | 47139 | 7.01 | 157 | 19 | | |
| 72 | Histone H4 | HIST1H4A | P62805 | 11360 | 11.36 | 158 | 18 | 413 | 32 |
| 73 | Heterogeneous nuclear ribonucleoprotein K | HNRNPK | P61978 | 50944 | 5.39 | 118 | 29 | 305 | 18 |
| 74 | 60 kDa shock protein, mitochondrial | HSPD1 | P10809 | 61016 | 5.70 | | | 501 | 17 |

| | | | | | | | | |
|---|---|---|---|---|---|---|---|---|
| 75 | Cytochrome c oxidase subunit 6B1 | COX6B1 | P14854 | 10186 | 6.54 | | 103 | 8 |

**Table 3.3: Proteins differently expressed in the ANG II treated HK-2 cell line**

The gene name, accession number in Swiss-Prot, molecular weight (Mol. Wt.), the calculated isoelectric point (CPI), the peptide mass fingerprinting (PMF) score and sequence coverage (Seq. Cov.), MS/MS information and sequence coverage are given. The spots where MS/MS-data are missing were only identified with PMF.

| Spot Nr. | Protein Name | Gene Name | SwissProt Accession | Mol. Wt. | CPI | PMF Score | PMF Seq. Cov. | MS/MS Score | MS/MS Seq. Cov. |
|---|---|---|---|---|---|---|---|---|---|
| 1 | Small ubiquitin-related modifier 2 | SUMO2 | P61956 | 10864 | 5.32 | | | 92 | 6 |
| 2 | Coactosin-like protein | COTL1 | Q14019 | 15935 | 5.50 | | | 274 | 11 |
| 3 | 78 kDa glucose-regulated protein | HSPA5 | P11021 | 72288 | 5.07 | | | 218 | 15 |
| 4 | Sorcin | SRI | P30626 | 21662 | 5.32 | | | 191 | 9 |
| 5 | Chloride intracellular channel protein 1 | CLIC1 | O00299 | 26906 | 5.09 | 151 | 18 | | |
| 6 | Protein DJ-1 | PARK7 | Q99497 | 19878 | 6.32 | 132 | 18 | | |
| 7 | Annexin A5 | ANXA5 | P08758 | 35914 | 4.93 | 95 | 9 | 128 | 10 |
| 8 | Tubulin-folding cofactor B | TBCB | Q99426 | 27308 | 5.06 | 78 | 10 | 127 | 4 |
| 9 | Annexin A5 | ANXA5 | P08758 | 35914 | 4.93 | 194 | 24 | | |
| 10 | Elongation factor 1-delta | EEF1D | P29692 | 31103 | 4.90 | | | 204 | 8 |
| 11 | Peroxiredoxin 1 | PRDX1 | Q06830 | 22096 | 8.27 | 98 | 18 | 156 | 14 |
| 12 | Serine/arginine-rich splicing factor 7 | SFRS7 | Q16629 | 27350 | 9.64 | | | 186 | 15 |
| 13 | Nucleophosmin | NPM1 | P06748 | 32555 | 4.64 | 150 | 19 | | |
| 14 | Nucleophosmin | NPM1 | P06748 | 32555 | 4.64 | 153 | 17 | | |
| 15 | Nucleophosmin | NPM1 | P06748 | 32555 | 4.64 | | | 191 | 8 |
| 16 | Nucleophosmin | NPM1 | P06748 | 32555 | 4.64 | | | 155 | 4 |
| 17 | Heterogeneous nuclear ribonucleoprotein C1/C2 | HNRNPC | P07910 | 33650 | 4.94 | | | 258 | 9 |
| 18 | Heterogeneous nuclear ribonucleoprotein C1/C2 | HNRNPC | P07910 | 33650 | 4.94 | 112 | 12 | 72 | 7 |
| 19 | Serine-threonine kinase receptor associated protein | STRAP | Q9Y3F4 | 38414 | 4.98 | 120 | 16 | | |
| 20 | Heterogenous nuclear ribonucleoprotein C1/C2 | HNRNPC | P07910 | 33650 | 4.94 | | | 159 | 6 |
| 21 | Histidine triad nucleotide-binding protein 2, mitochondrial | HINT2 | Q9BX68 | 17151 | 9.20 | | | 253 | 18 |
| 22 | 40S ribosomal protein S12 | RPS12 | P25398 | 14505 | 6.81 | | | 82 | 9 |
| 23 | Cytochrome c oxidase subunit 5B, mitochondrial | COX5B | P10606 | 13687 | 9.07 | | | 237 | 16 |
| 24 | Eukaryotic translation initiation factor 1 | EIF1 | P41567 | 12725 | 6.90 | | | 169 | 6 |
| 25 | Cystatin-B | CSTB | P04080 | 11133 | 6.96 | | | 195 | 8 |
| 26 | Prefoldin subunit 2 | PFDN2 | Q9UHV9 | 16638 | 6.20 | | | 164 | 6 |
| 27 | Alpha-crystallin B chain | CRYAB | P02511 | 20146 | 6.76 | | | 140 | 7 |
| 28 | Proteasome subunit alpha type 2 | PSMA2 | P25787 | 25882 | 6.91 | 142 | 15 | 115 | 5 |

| | | | | | | | | | |
|---|---|---|---|---|---|---|---|---|---|
| 29 | Chloride intracellular channel protein 4 | CLIC4 | Q9Y696 | 28754 | 5.45 | 72 | 10 | 84 | 5 |
| 30 | Glutathione S-transferase omega-1 | GSTO1 | P78417 | 27548 | 6.24 | | | 128 | 7 |
| 31 | UMP-CMP kinase | CMPK1 | P30085 | 22208 | 5.44 | 65 | 8 | 132 | 6 |
| 32 | Heme-binding protein 1 | HEBP1 | Q9NRV9 | 21084 | 5.71 | 189 | 17 | 164 | 6 |
| 33 | Calponin-3 | CNN3 | Q15417 | 36391 | 5.69 | | | 92 | 6 |
| 34 | Ubiquitin-fold modifier-conjugating enzyme 1 | UFC1 | Q9Y3C8 | 19446 | 6.91 | | | 152 | 8 |
| 35 | Superoxide dismutase [Mn], mitochondrial | SOD2 | P04179 | 24707 | 8.35 | 69 | 9 | 114 | 7 |
| 36 | Superoxide dismutase [Mn], mitochondrial | SOD2 | P04179 | 24707 | 8.35 | | | 118 | 7 |
| 37 | Delta(3,5)-Delta(2,4)-dienoyl-CoA isomerase, mitochondrial | ECH1 | Q13011 | 35793 | 8.16 | | | 288 | 18 |
| 38 | Vimentin | VIM | P08670 | 53619 | 5.05 | 137 | 33 | | |
| 39 | Tubulin beta -4 chain | TUBB4 | P04350 | 49554 | 4.78 | 163 | 22 | | |
| 40 | Tubulin beta chain | TUBB | P07437 | 49639 | 4.78 | 71 | 10 | 154 | 9 |
| 41 | Gamma-enolase | ENO2 | P09104 | 47239 | 4.91 | | | 175 | 7 |
| 42 | Vimentin | VIM | P08670 | 53619 | 5.05 | 174 | 35 | | |
| 43 | Galactokinase | GALK1 | P51570 | 42246 | 6.04 | | | 136 | 8 |
| 44 | Alpha-enolase | ENO1 | P06733 | 47139 | 7.01 | 98 | 12 | 197 | 12 |
| 45 | Proliferation-associated protein 2G4 | PA2G4 | Q9UQ80 | 43759 | 6.13 | | | 132 | 13 |
| 46 | Heterogeneous nuclear ribonucleoprotein H3 | HNRNPH3 | P31942 | 36903 | 6.37 | | | 117 | 7 |
| 47 | Eukaryotic translation initiation factor 3 subunit G | EIF3G | O75821 | 35589 | 5.87 | 88 | 11 | 129 | 5 |
| 48 | Heterogeneous nuclear ribonucleoprotein D-like | HNRPDL | O14979 | 46409 | 9.59 | | | 175 | 8 |
| 49 | Poly(rC)-binding protein 1 | PCBP1 | Q15365 | 37474 | 6.66 | | | 211 | 10 |
| 50 | Heterogeneous nuclear ribonucleoprotein D0 | HNRNPD | Q14103 | 38410 | 7.61 | | | 162 | 6 |
| 51 | Medium- chain specific acyl-CoA dehydrogenase, mitochondrial | ACADM | P11310 | 46559 | 8.61 | 79 | 12 | 203 | 13 |
| 52 | Mannose-1-phosphate guanyltransferase alpha | GMPPA | Q96IJ6 | 46262 | 6.73 | | | 140 | 5 |
| 53 | Fascin | FSCN1 | Q16658 | 54496 | 6.84 | 78 | 14 | 212 | 12 |
| 54 | LIM and SH3 domain protein 1 | LASP1 | Q14847 | 29698 | 6.61 | 115 | 16 | 146 | 12 |
| 55 | PDZ and LIM domain protein 1 | PDLIM1 | O00151 | 36049 | 6.56 | | | 252 | 12 |
| 56 | Mitotic checkpoint protein BUB3 | BUB3 | O43684 | 37131 | 6.36 | | | 122 | 7 |
| 57 | Isocitrate dehydrogenase [NADP], cytoplasmic | IDH1 | O75874 | 46630 | 6.53 | | | 247 | 11 |
| 58 | Actin, cytoplasmic 1 | ACTB | P60709 | 41710 | 5.29 | 158 | 13 | | |

| | | | | | | | | | |
|---|---|---|---|---|---|---|---|---|---|
| 59 | Actin, cytoplasmic 1 | ACTB | P60709 | 41710 | 5.29 | 162 | 33 | | |
| 60 | Thioredoxin | TXN | P10599 | 11730 | 4.82 | 143 | 17 | 152 | 8 |
| 61 | Protein S100-A6 | S100A6 | P06703 | 10173 | 5.32 | 82 | 8 | 107 | 4 |
| 62 | Protein S100-A11 | S100A11 | P31949 | 11733 | 6.56 | 159 | 11 | 69 | 4 |
| 63 | Endoplasmic reticulum resident protein 29 | ERP29 | P30040 | 28975 | 6.77 | 118 | 18 | | |
| 64 | 26S proteasome non-ATPase regulatory subunit 10 | PSMD10 | O75832 | 24412 | 5.71 | 150 | 16 | | |
| 65 | Peroxiredoxin-4 | PRDX4 | Q13162 | 30521 | 5.86 | 79 | 13 | 111 | 7 |
| 66 | Src substrate cortactin | CTTN | Q14247 | 61549 | 5.24 | 101 | 22 | 153 | 8 |
| 67 | Heat shock cognate 71 kDa protein | HSPA8 | P11142 | 70854 | 5.37 | 96 | 18 | | |
| 68 | Macrophage-capping protein | CAPG | P40121 | 38494 | 5.82 | 176 | 24 | | |
| 69 | Galactokinase | GALK1 | P51570 | 42246 | 6.04 | 113 | 27 | 76 | 4 |
| 70 | Sialic acid synthase | NANS | Q9NR45 | 40281 | 6.29 | 95 | 16 | 110 | 4 |
| 71 | Thioredoxin-dependent peroxide reductase, mitochondrial | PRDX3 | P30048 | 27675 | 7.68 | 145 | 18 | | |
| 72 | 78 kDa glucose-regulated protein | HSPA5 | P11021 | 72288 | 5.07 | 222 | 30 | | |
| 74 | Lamin-B1 | LMNB1 | P20700 | 66368 | 5.11 | 112 | 26 | | |
| 75 | Transitional endoplasmic reticulum ATPase | VCP | P55072 | 89266 | 5.14 | 197 | 37 | | |
| 76 | Protein disulfide-isomerase A3 | PDIA3 | P30101 | 56747 | 5.98 | 131 | 22 | | |
| 77 | Isocitrate dehydrogenase [NADP], cytoplasmic | IDH1 | O75874 | 46630 | 6.53 | 97 | 19 | 143 | 8 |
| 78 | Aldose reductase | AKR1B1 | P15121 | 35830 | 6.52 | 120 | 12 | 176 | 8 |
| 79 | Prelamin-A/C | LMNA | P02545 | 74095 | 6.57 | 74 | 26 | 198 | 10 |
| 80 | Endoplasmin | HSP90B1 | P14625 | 92411 | 4.76 | 82 | 22 | | |
| 81 | Endoplasmin | HSP90B1 | P14625 | 92411 | 4.76 | | | 152 | 14 |
| 82 | 60 kDa heat shock protein, mitochondrial | HSPD1 | P10809 | 61016 | 5.70 | 80 | 20 | | |
| 83 | Tubulin beta chain | TUBB | P07437 | 49639 | 4.78 | 110 | 18 | | |
| 84 | Actin, cytoplasmic 1 | ACTB | P60709 | 41710 | 5.29 | 104 | 18 | | |
| 85 | Vimentin | VIM | P08670 | 53619 | 5.05 | 149 | 27 | | |
| 86 | Heterogeneous nuclear ribonucleoproteins C1/C2 | HNRNPC | P07910 | 33650 | 4.95 | 68 | 14 | 75 | 6 |
| 87 | Annexin A3 | ANXA3 | P12429 | 36353 | 5.62 | 77 | 17 | 193 | 11 |

**Table 3.4: Proteins differently expressed in the PDGF treated HK-2 cell line**

The gene name, accession number in Swiss-Prot, molecular weight (Mol. Wt.), the calculated isoelectric point (CPI), the peptide mass fingerprinting (PMF) score and sequence coverage (Seq. Cov.), MS/MS information and sequence coverage are given. The spots where MS/MS-data are missing were only identified with PMF.

### 3.4.3 Ontogenic classification of the proteins involved in cell response to profibrotic cytokine treatment

To gain more information on the biological mechanisms of the identified proteins, which are associated with cytokine treatment we used DAVID bioinformatics ***(http://david.abcc.ncifcrf.gov/).*** Each identified protein was assigned to cellular components, functional categories and biological process based on the Gene Ontology (GO) annotation system. Under all experimental conditions, the highest percentage of the identified proteins was found located in the intracellular part of the cell (Fig. 3.3A, B). Interestingly, GO assignment to molecular function illustrated that a large part of the regulated proteins were involved in stress response (Fig. 4A, B). Moreover the percent of stress responsive proteins in TK-173 cells was 35.9% for ANG II treated cells and 34.5% for PDGF treated cells. However, a lower percentage was obtained in HK-2 cells: 26.4% in cells exposed to ANG II and 26.5% in cells subjected to PDGF treatment (Fig. 4C). Our findings indicate that although the number of the differently regulated identified proteins was almost equal in TK-173 and HK-2 cell samples (Tables 3.1-3.4), the percent of stress responsive proteins was higher in the fibroblastic TK-173 cells compared to the epithelial HK-2 cells under both cytokine treatments.

**(A)**

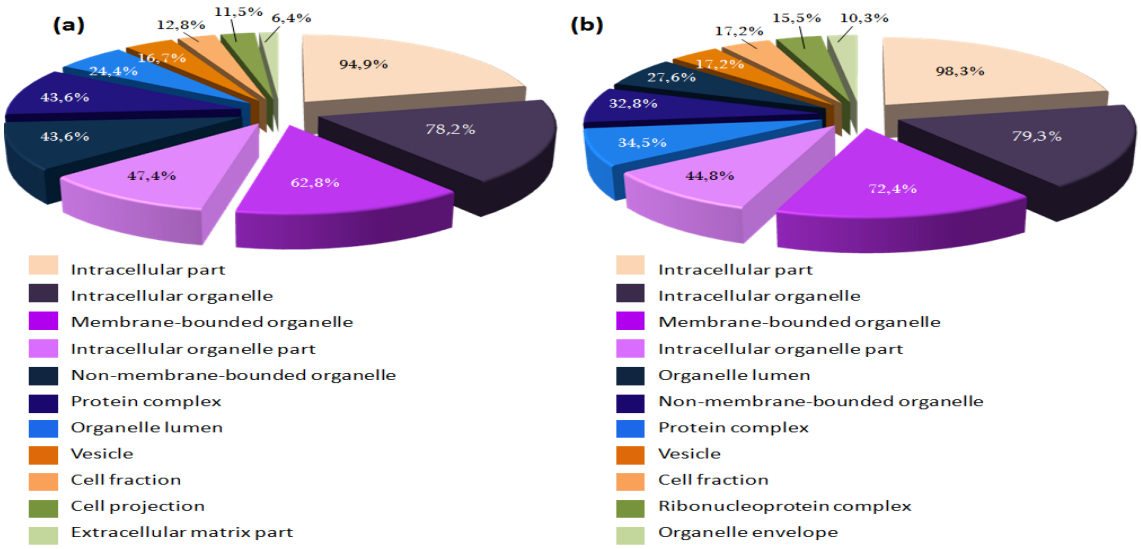


**Figure 3.3B continued**

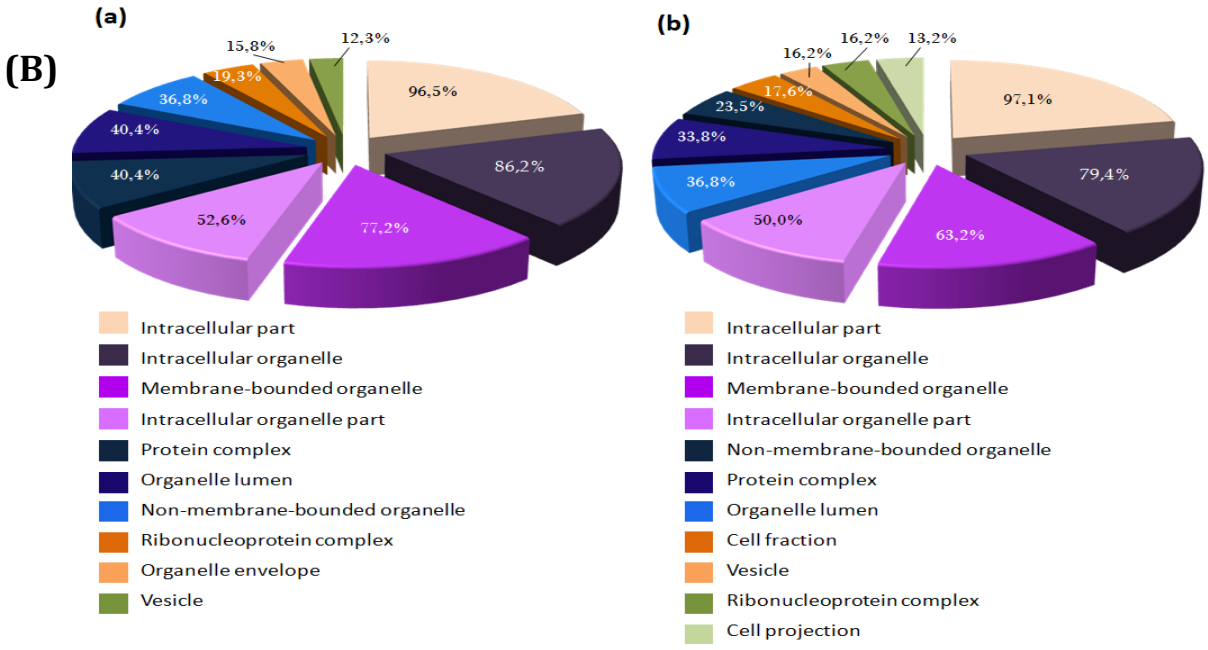


**Figure 3.3: Gene Ontology (GO) classification of differently regulated proteins in TK-173 and HK-2 cell lines by DAVID bioinformatics**

The list of genes to be analysed was uploaded into Gene list Manager window and *Homo sapiens* was chosen as background. The gene list was then submitted to DAVID conversion tool. Based on the corresponding DAVID gene IDs and threshold adjustment (Max-Prob≤0.1 and Min Count≥2) in Chart Option section, functional annotations associated with each gene were displayed in a chart. GO analyses of **subcellular location** are represented as pie charts showing the different categories.Values in figures presented the ratio distribution of proteins found in that respective category. **(A):** TK-173 cells and **(B):** HK-2 cells. **(a):** ANG II treated cells and **(b):** PDGF treated cells.

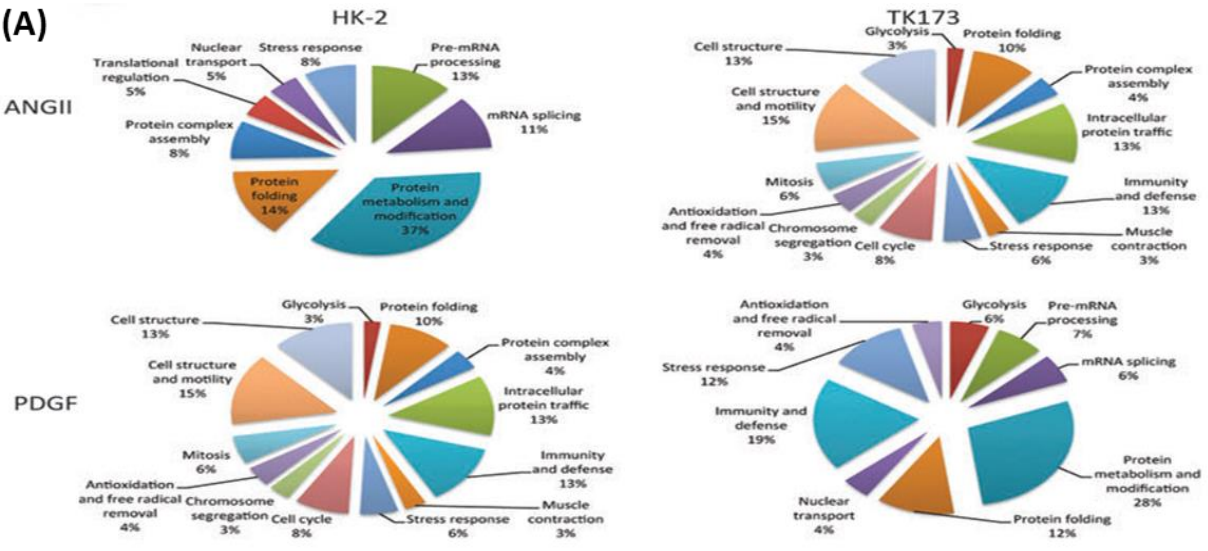


**Figure 3.4B, C continued**

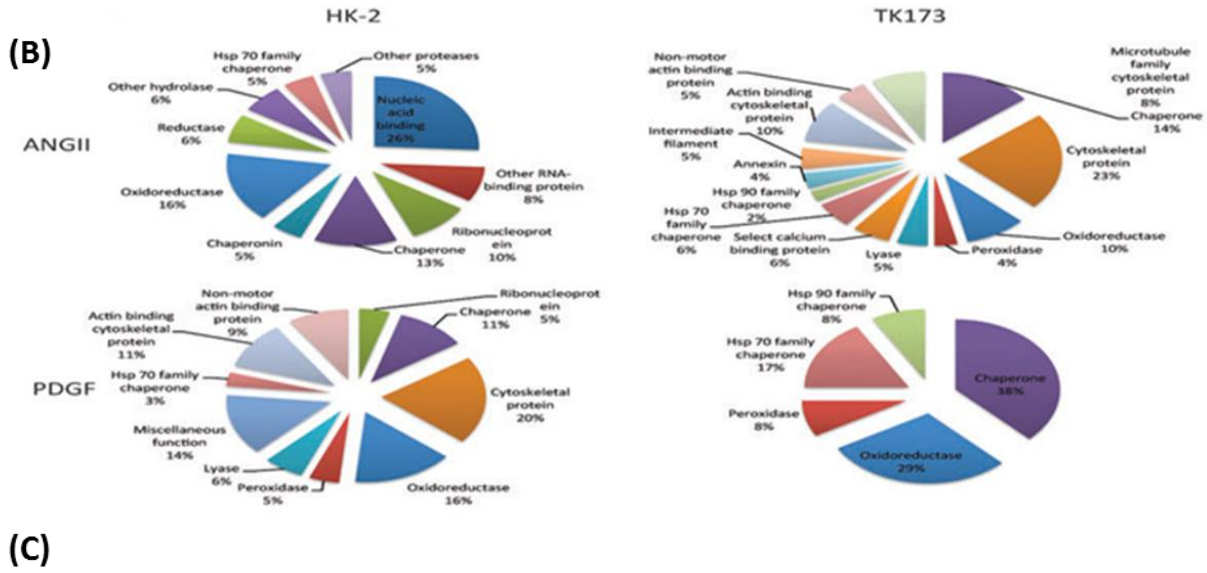


(C)

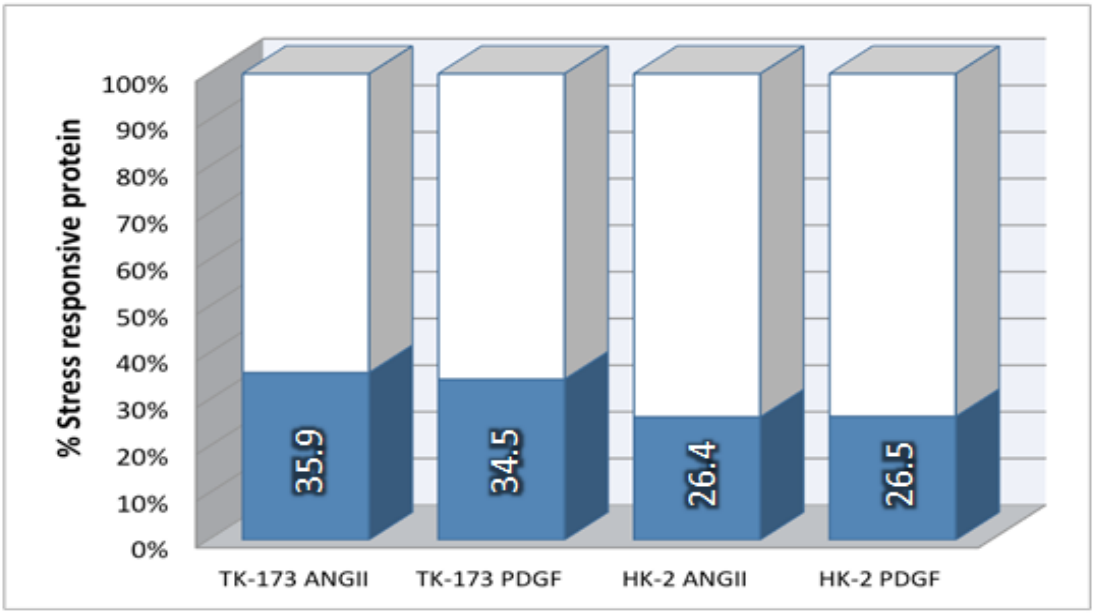


**Figure 3.4: GO annotations for biological processes and molecular function**

Assignment of identified proteins into groups using DAVID bioinformatics database resource. The list of genes to be analysed was uploaded into Gene list Manager window and *Homo sapiens* was chosen as background. The gene list was then submitted to DAVID conversion tool. Based on the corresponding DAVID gene IDs and threshold adjustment (Max-Prob≤0.1 and Min Count≥2) in Chart Option section, functional annotations associated with each gene were displayed in a chart. GO analysis of molecular function was chosen. **(A):** Pie charts of the **biological processes** in which the identified proteins from both treatments and in both cell types are involved. Most of the proteins are involved in metabolic and cellular processes. A large part of the identified proteins were found to be involved in immunity defense and stress response. **(B):** Pie charts of the classification

of the **molecular function** of the identified proteins. The classification revealed an activation of OS response pathways and alteration in the expression of proteins involved in anti-oxidative response. Moreover stress proteins, e.g. heat shock proteins and cytoskeletal proteins, were also regulated. **(C):** Percent stress responsive protein under each treatment is represented as a bar chart.

Among the stress proteins which were regulated as response to ANG II or PDGF treatment in both cells, protein DJ-1 was significantly upregulated in both cell types and under both treatments. In our former study, we established protein DJ-1 as OS responsive protein in renal cells (128). The present study confirmed the role of DJ-1 as a pivotal protein in the OS response in kidney cells. DJ-1 is a molecule that occupies an important role in cellular biology and is reported to be involved in diverse cellular processes. The fact that DJ-1 promotes cell survival by protecting neural cells (121, 129), and recently renal cells (128) from OS; and that knockout of the DJ-1 gene enhances cytotoxicity mediated by $H_2O_2$ (128, 184) had enthused our group to further explore the potential role of DJ-1 in kidney fibrosis. Interestingly, the 2-DE experimental results clearly implicate protein DJ-1 as an OS marker protein in renal cells. Figure 3.2 depicts the over expression of DJ-1 in fibroblastic (Fig. 3.2A) as well as epithelial cells (Fig. 3.2B) agonizing OS triggered through treatment with profibrotic cytokines (ANG II and PDGF). However, no shift in the protein *pI* value that resulted in the formation of a more acidic isoform was observed as a result of stress induced by the profibrotic agents as we previously demonstrated in similar cells subjected to the OS inducer $H_2O_2$ (128) or in human endothelial cells exposed to paraquat ($PQ2^{+}$), which generates ROS within cells (135) thereby suggesting different pathways for DJ-1 action in restraint to the stress stimulating agent.

### 3.4.4 Immunoblotting validation of protein expression alteration

To validate the data obtained from 2-DE experiments, we confirmed using WB, the involvement of DJ-1 in renal response to cytokine triggered OS. In addition, other first line defense key proteins against OS namely PRDX6, SOD1, and PRDX1 could also be confirmed. Overall results represented in Figure 3.5 show apparent marked increase in all OS marker proteins tested after 72 h of cell culture with PDGF, ANG II, or TGFß1. Statistical evaluation of the experimental results obtained in Figure 3.5A elucidates high significance reaching (P<0.001) under most conditions in particular for DJ-1 protein (Fig. 3.5B).

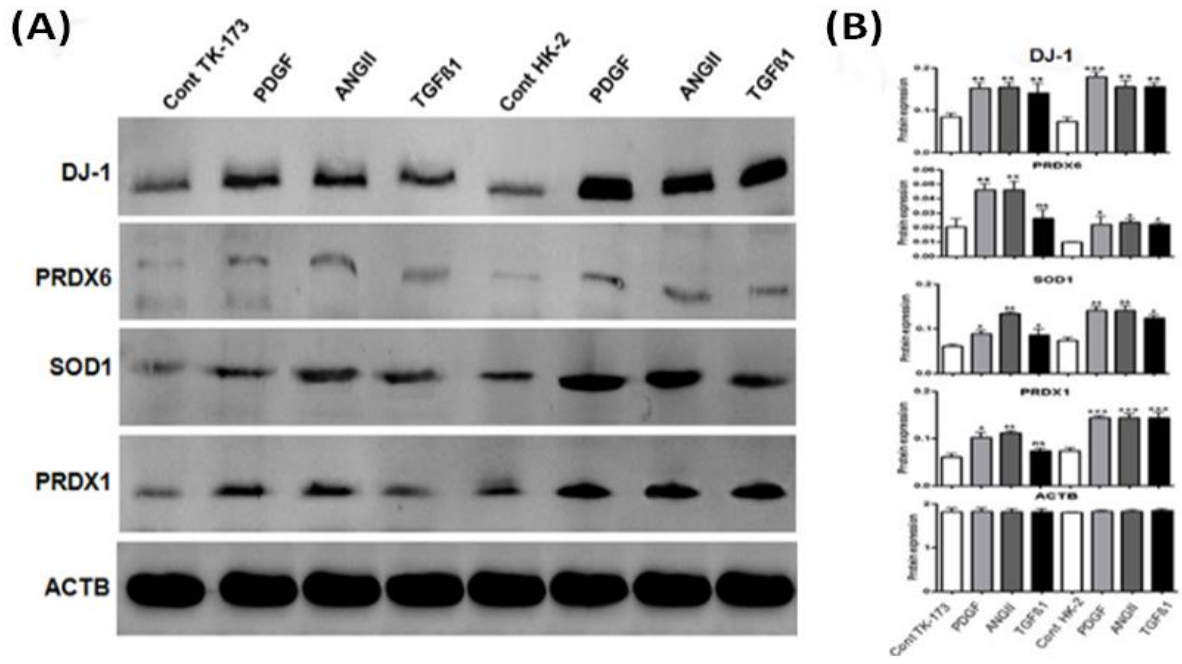


**Figure 3.5: Western blot analysis of expression changes of OS marker proteins under OS induced by the different cytokines (PDGF, ANG II and TGFß1)**

The cell extracts from TK-173 and HK-2 (Control, PDGF, ANG II and TGFß1 72 h treated cells) were used. **(A):** Blots were probed with antibodies against the appropriate protein. ACTB was kept as control. **(B):** Bar charts representing the quantification of the blots. Results are given as the means ±SD from three independent experiments. *P<0.05, **P<0.01, ***P<0.001with respect to their corresponding control.

### 3.4.5 Analysis of OS protein expression alteration in animal model of fibrosis: Involvement of DJ-1 in renal fibrosis

We further attempted to investigate the role of DJ-1 in renal fibrosis. For this purpose, we utilized the *Col4a3* knock-out mice tissue as a fibrosis animal model ***(www.jax.org)*** predisposed to develop CKD. The *Col4a3* deficient mice have a normal phenotype until 4 weeks of age. Abnormal renal glomerulus basement membrane morphology and irregular thickening and splitting of the glomerular basement membrane can be seen only by electron microscopy at 4 weeks of age (185). Occasionally minor glomerular lesions can be observed at 6 weeks of age by light microscopy. At 10 weeks of age, mice demonstrate glomerulosclerosis associated with inflammatory cell infiltration, interstitial fibrosis, and tubular atrophy (185).

In the present work, we applied whole kidney lysate of wild type (WT) animals and that of different stages of *Col4a3* knock-out mice for WB analysis. Figure 3.6A demonstrates blots reflecting and comparing the response of OS markers (DJ-1, PRDX6, SOD1, and PRDX1), fibrosis markers (FN1, and VCL), and the ER-stress marker protein GRP78 at the distinct stages. Bar diagrams representing the quantification of the blots (Fig. 3.6B) apparently illustrate a parallel increase in response of OS markers with the increase of the fibrotic stage. However, significance was only attained at the 7.5 week except for SOD1 where 6.5 week showed $P<0.05$ significance. Fibrosis marker proteins and ER-stress marker protein displayed no discrepancy from their corresponding control WT during the primary stages. At 7.5 week an abrupt raise that sustained in the 9.5 week was evinced (Fig. 3.6B).

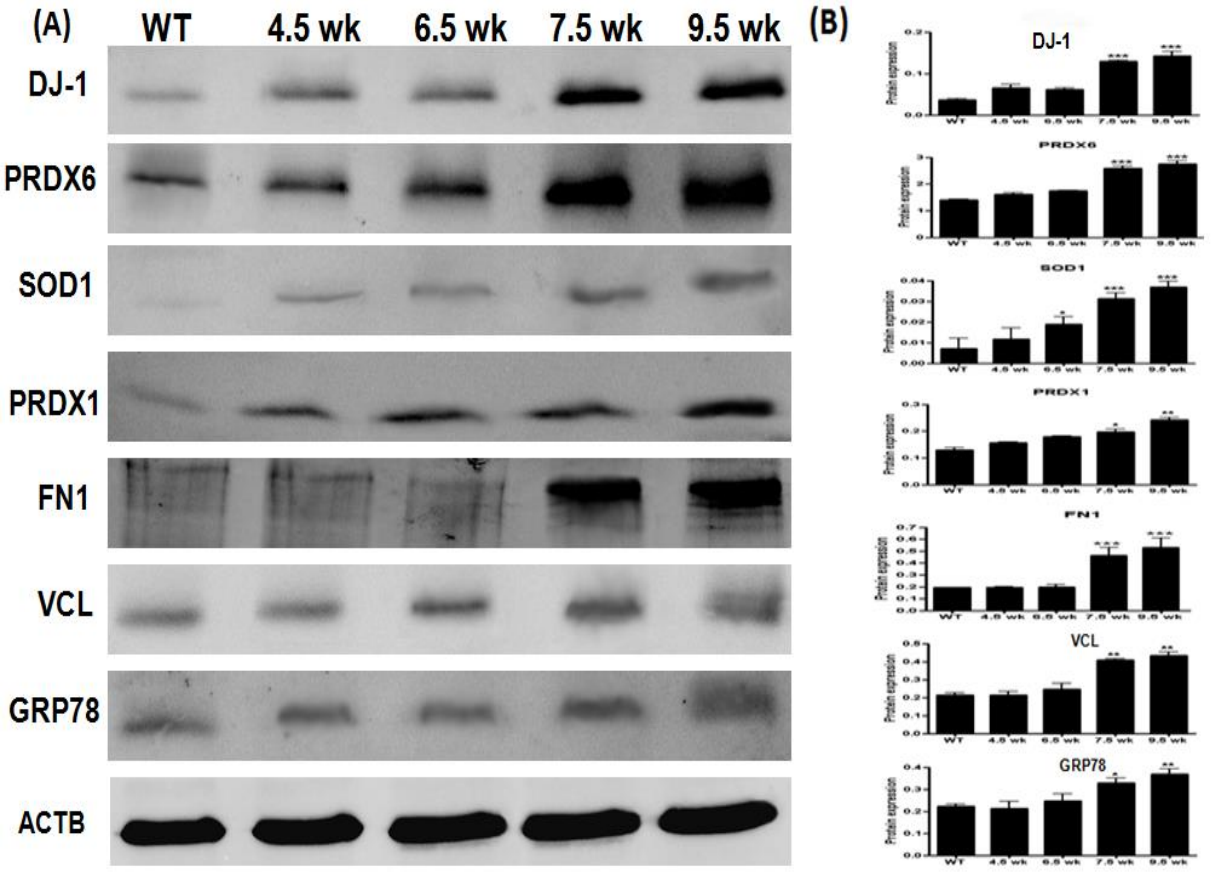


**Figure 3.6: Western blot analysis of OS and fibrotic markers in whole kidney lysates of WT and different stages of *Col4a3* knockout mice as a fibrosis model**

**(A):** Blots were probed with antibodies against the appropriate proteins. ACTB was kept as control. **(B):** Bar diagrams representing the quantification of the blot. Results are given as the means ±SD from three independent experiments. *P<0.05, **P<0.01, ***P<0.001 with respect to the WT. wk: week.

### 3.4.6 Immunohistochemical and immunofluorescence staining

To further validate and characterize DJ-1 role in renal OS and subsequent fibrosis, we sought to determine the expression status of the protein in different parts of the *Col4a3* knock-out mice kidneys using immunohistochemical and immunofluorescence staining. Figure 3.7 (A, B) shows immunohistochemical staining images of the glomerular and tubulointerstitial areas from WT and representative sections from each group (4.5 wk, 6.5 wk, 7.5 wk, and 9.5 wk) respectively stained with DJ-1 (upper panel) and PRDX6 (lower panel). PRDX6 staining was employed for resembling aspects to that of DJ-1. The images reveal progressive increase in

both DJ-1 and PRDX6 expression concomitant with the progression of renal fibrosis as evidenced by HE stained tissue from the same used animals (Fig. 3.7C). In parallel to interstitial fibrosis at 9.5 week, apparent expression of both proteins was noted (Fig. 7B).

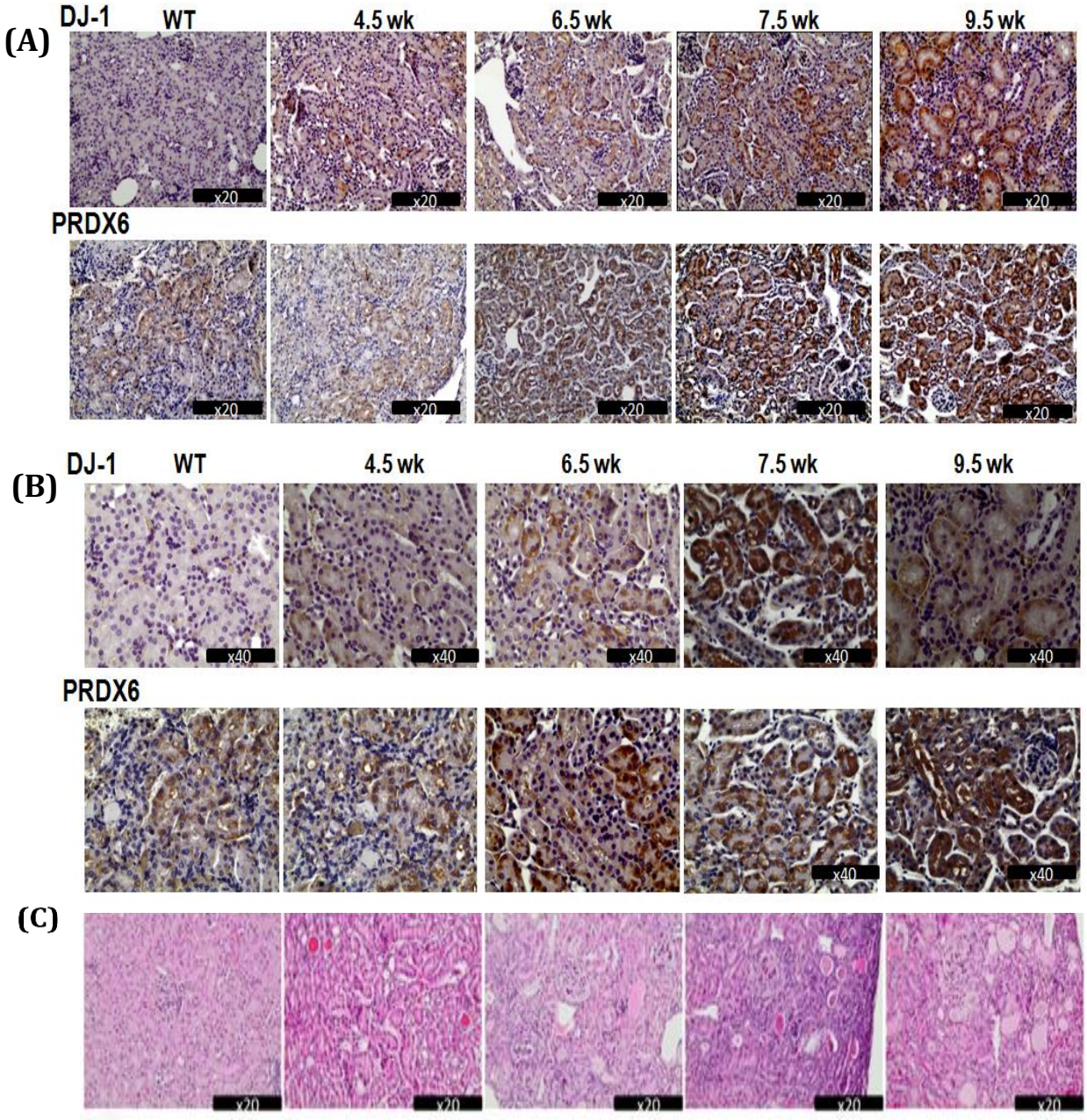


**Figure 3.7: Immunohistochemical staining of DJ-1 and PRDX6 as OS markers**

**(A):** Representative images of glomerular and tubulointerstitial areas from WT and different stages of *Col4a3* knockout mice kidneys stained with DJ-1 (upper panel) and PRDX6 (lower panel). Magnification (x20). The

immunohistochemical staining of the kidney tissue from these stages showed clear expression of DJ-1 in proximal tubule of the *Col4A3* mice compared to WT. The DJ-1 expression became more prominent at 7.5 wk and 9.5 wk especially in the proximal tubule. At 9.5 wk the DJ-1 expression showed even interstitial staining indicating an increase in the number of interstitial fibroblasts. A similar staining behavior was observed for PRDX6. **(B):** Higher magnification of the previous images (A) showing the localization of proteins (Magnification x40). **(C):** HE staining of kidney from *Col4a3* mice presenting the different stages of fibrosis. The tissue show a normal kidney structure without any sign of injury at the 4.5 wk of age, the tubulointerstitium shows intact structure with no pathological manifestation. At 7.5 wk the first signs of tubulointerstitial fibrosis emerged and became more prominent in tissue from animals at the 9.5 wk.

In concert with the immunohistochemical staining results, immunofluorescence staining of the analogous tissues using similar antibodies for DJ-1 and PRDX6 localization detection, exhibited a comparable staining pattern with strong expression of the proteins in tubular part especially in proximal tubule and less in the glomerulus (Fig. 3.8). A gradual rise in protein expression was concurrent with OS augmentation. At 9.5 wk the DJ-1 expression became more prominent and showed even interstitial staining indicating an increase in the number of interstitial fibroblasts.

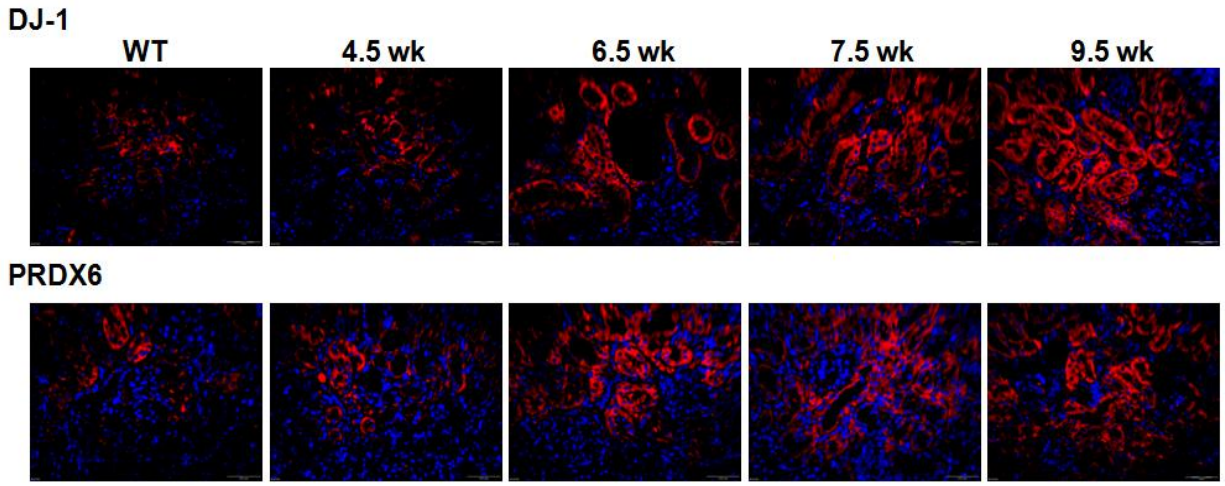


**Figure 3.8: Immunofluorescence staining of DJ-1 and PRDX6 as OS markers**

Representative images of glomerular and tubulointerstitial areas from WT and different stages of *Col4a3* knockout mice kidneys stained with DJ-1 (upper panel) and PRDX6 (lower panel). Magnification (x20). Marked increase in the expression of both proteins was observed with the increase of the fibrotic stage.

Thus, tissue staining confirmed WB results and reinforced the crucial role of DJ-1 in OS and its prominence as an endogenous antioxidant defense protein in the kidney.

For figuring, strewing, and supporting purposes, other OS marker and fibrotic marker proteins were examined in parallel to protein DJ-1 in the various experiments.

### 3.4.7 Over expression of DJ-1 and its mutant forms and their effect on renal cell viability

In light of the imminent importance to understand the role of DJ-1 and elucidate its high expression as an endogenous antioxidant defense protein in renal cells during OS; we transfected our experimental cell models (TK-173 and HK-2) with WT-DJ-1 and mutant vectors (pGW1-Myc-DJ-1-WT, pDEST40-DJ-1-E18Q, and pDEST40-DJ-1-E18D) in a series of separate experiments. Transfected cells were then subjected for MTT test to investigate the impact of transfection on cell survival under untreated and treated ($H_2O_2$, ANG II, or PDGF) conditions.

DJ-1 in humans is a homodimeric protein of 189 amino acids. Crystallization structural analysis of the purified protein DJ-1 has led to the identification of three cysteine residues at amino acids numbers 46, 53, and 106 (Cys46, Cys53, and Cys106) and the first speculation that Cys106 is the most sensitive one to OS (148). The conserved Cys106 is both functionally essential and target of oxidation. Consequently, the oxidative modification of Cys106 has been proposed to allow DJ-1 to act as a sensor of cellular redox homeostasis and to participate in signaling cytoprotective pathways in the cell (126). Furthermore, atomic resolution X-ray crystallography and UV spectroscopy showed that C106 thiolate accepts a hydrogen bond

from a protonated glutamic acid sidechain (E18) that is required to maximally stabilize the C106 thiolate (156). Hence, we investigated the impact of E18 mutation on oxidative behavior of DJ-1 by utilizing DJ-1 mutants: E18Q possessing a glutamine side chain substitution and E18D having an aspartic acid substitution. Cells (TK-173 and HK-2) were transfected with plasmids expressing E18-C106 (WT), E18Q-C106 (mutant 1), and E18D-C106 (mutant 2) separately. Over-expression was confirmed by immunoblotting. Figure 3.9 (A) reveals the efficiency of the DJ-1 transfection analyzed by immunoblotting. Quantification of blots indicated significant increase in DJ-1 expression in all transfected cells compared to non-transfected control (Fig. 3.9B).

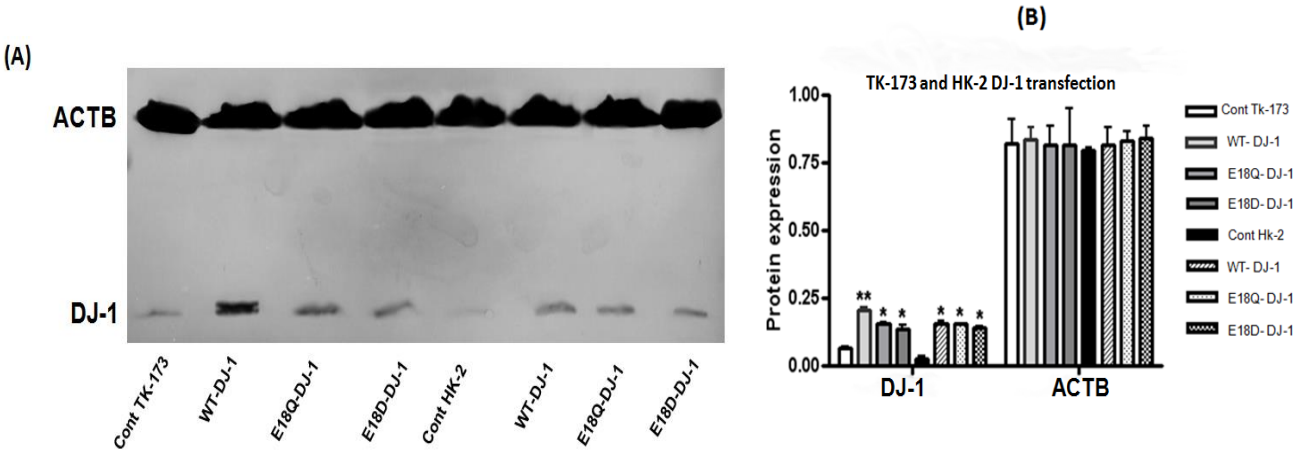


**Figure 3.9: Western blot analysis of DJ-1 for TK-173 and HK-2 cells before and after transfection**

**(A):** Western blot analysis of TK-173 and HK-2 cell lysates before and after transfection with wild type WT-DJ-1, and mutants E18Q-DJ-1 and E18D-DJ-1 plasmids. Over expression of DJ-1 antibody compared to control cells indicates successful transfection. ACTB antibody was loaded as control. **(B):** Bar charts representing the quantification of the blots. Results are given as the means ±SD from three independent experiments. *P<0.05, **P<0.01 with respect to their corresponding control.

To assess whether the over expression of DJ-1 affects the cell survival under OS conditions, the cell viability assay was carried out with cells transfected with plasmids coding for WT and

mutants. The OS conditions were generated by treating the cells as described in material and methods section. Interestingly, over expressing the DJ-1 mutant E18D-DJ-1 markedly suppressed the growth in both used cell lines. The effect was more pronounced in case of the fibroblasts cell line TK-173 cells (Fig. 3.10A, B). Subsequent treatment with $H_2O_2$, ANG II, or PDGF did not add significant changes to the effect of the E18D-DJ-1 plasmid transfection. Significant ($P<0.05$) additional suppression was attained only in HK-2 cells under $H_2O_2$ treatment (Fig. 3.10B). In contrast, the viability of the cells transfected with either WT-DJ-1 or E18Q-DJ-1 was not significantly altered compared to the control cells in both cell lines (Fig. 3.10A, B) indicating that under normal cell conditions, DJ-1 augmentation is dispensable for cell survival. In case of ANG II and PDGF treatment the overexpression of WT-DJ-1 or E18Q-DJ-1 did not affect significantly the cell reaction to cytokines application (Fig. 3.10A, B). One explanation of this unexpected result could be that ROS in low level stimulated the cell proliferation but were dispensable for maintaining this impact. Accordingly, the scavenging effect that might had resulted from the overexpression of DJ-1 did not affect the cells' proliferation. The negative effect of $H_2O_2$ on cell proliferation could be slightly restored through overexpression of WT-DJ-1 or E18Q-DJ-1 (Fig. 3.1, Fig. 3.10 A, B). It seems that the overexpression level of the proteins was not sufficient enough to scavenge the produced ROS.

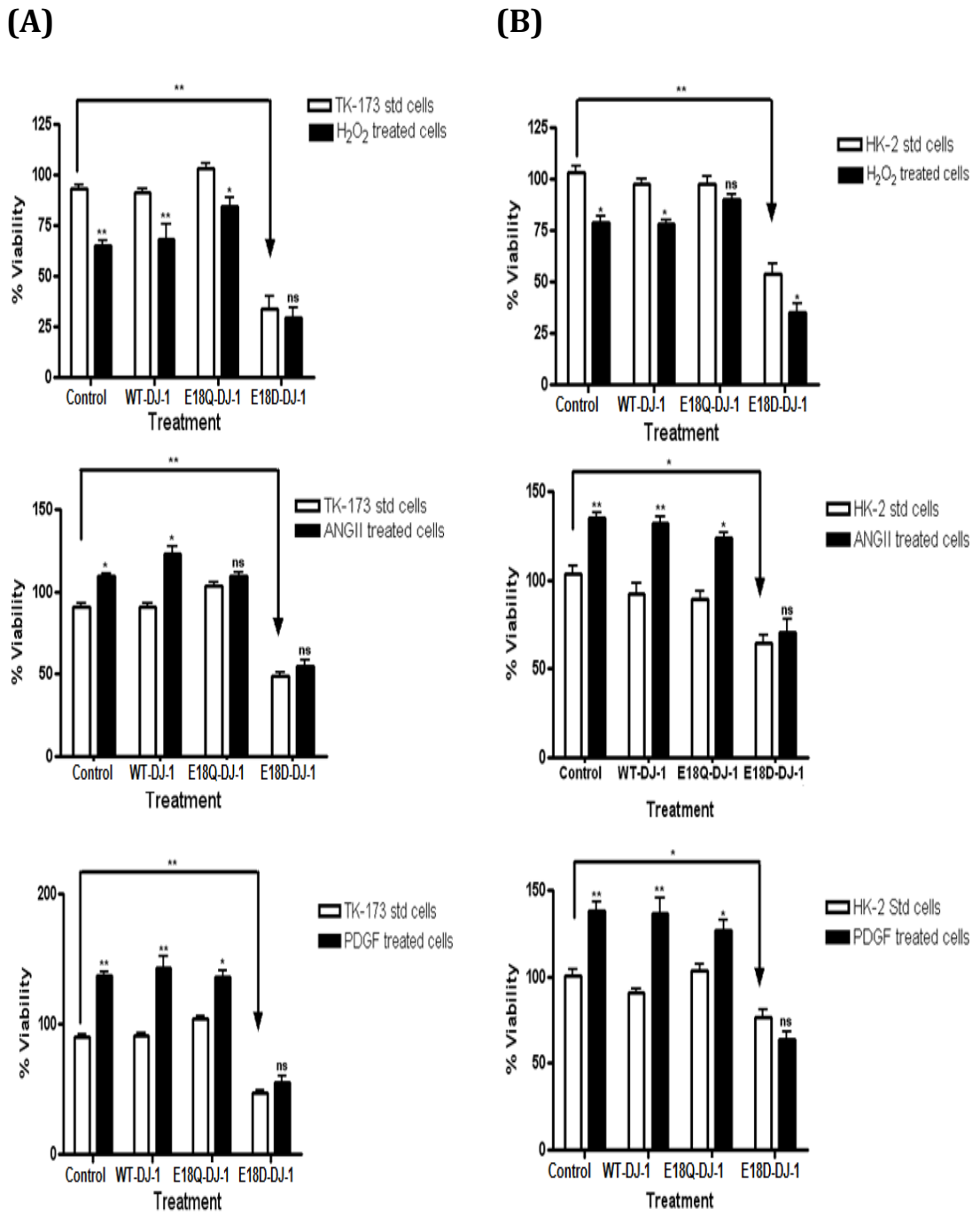


**Figure 3.10: Cell Viability test for transfected TK-173 and HK-2 cells and after transfection combined with $H_2O_2$, ANG II or PDGF treatment**

Cells were transfected with the required plasmid according to manufacturer's standard protocol then moved into the 96 well tissue culture plates. 5000 control (untransfected) or transfected (WT-DJ-1, E18Q-DJ-1, or E18D-DJ-1) TK-173 or HK-2 cells/well were cultured in 96 well cell culture plates. Groups of each experimental

cellular status were then incubated with $H_2O_2$ (200 µM), ANG II (0.5 µM) or PDGF (10 nM) for 72 h. For ANG II and PDGF treated cells, cells were deprived from FCS in the medium 24 h before treatment. The cell viability was measured and plotted in the form of bar diagrams with the cell treatment on x-axis and cell viability on y-axis. **(A):** TK-173 cells and **(B):** HK-2 cells. Results are represented as a mean of 12 readings ±SD. Statistical analysis was performed using Graphpad Prism 4 software and the paired t-test for comparison between two measures in the same group and the unpaired t-test for comparing two groups. Statistical significance was assumed for p-values <0.05. *P<0.05, **P<0.01. Significance shown by an arrow indicates the comparison between the control untransfected cells (TK-173 or HK-2) and the untreated E18D-DJ-1 TK-173 or HK-2. Otherwise significance was calculated for each separate untreated and treated condition.

### 3.4.8 Immunoprecipitation and identification of the DJ-1 interaction partners

To identify potential interaction partners of DJ-1 and to shed light on its mechanism of action in renal cells, immunoprecipitation and mass spectrometry analyses were combined. For this purpose, cell lysates from TK-173 or HK-2 cells expressing an empty vector (control), a Myc tag WT or a 6xHis-tagged mutant (E18Q or E18D) were used to overexpress the target forms of DJ-1(Figure 3.11A). The proteins and their potential interaction partners were then purified either with protein G agarose for the WT DJ-1 or with Ni-NTA metal-affinity chromatography for the His-tagged proteins following the protocol described in material and methods section. After repeated PBS wash and protein elution, the proteins were precipitated and resolved on SDS-PAGE gels. The potential interaction partners in all three cases were identified by mass spectrometry and illustrated on Figure 3.11A, B and Tables (3.5-3.7).

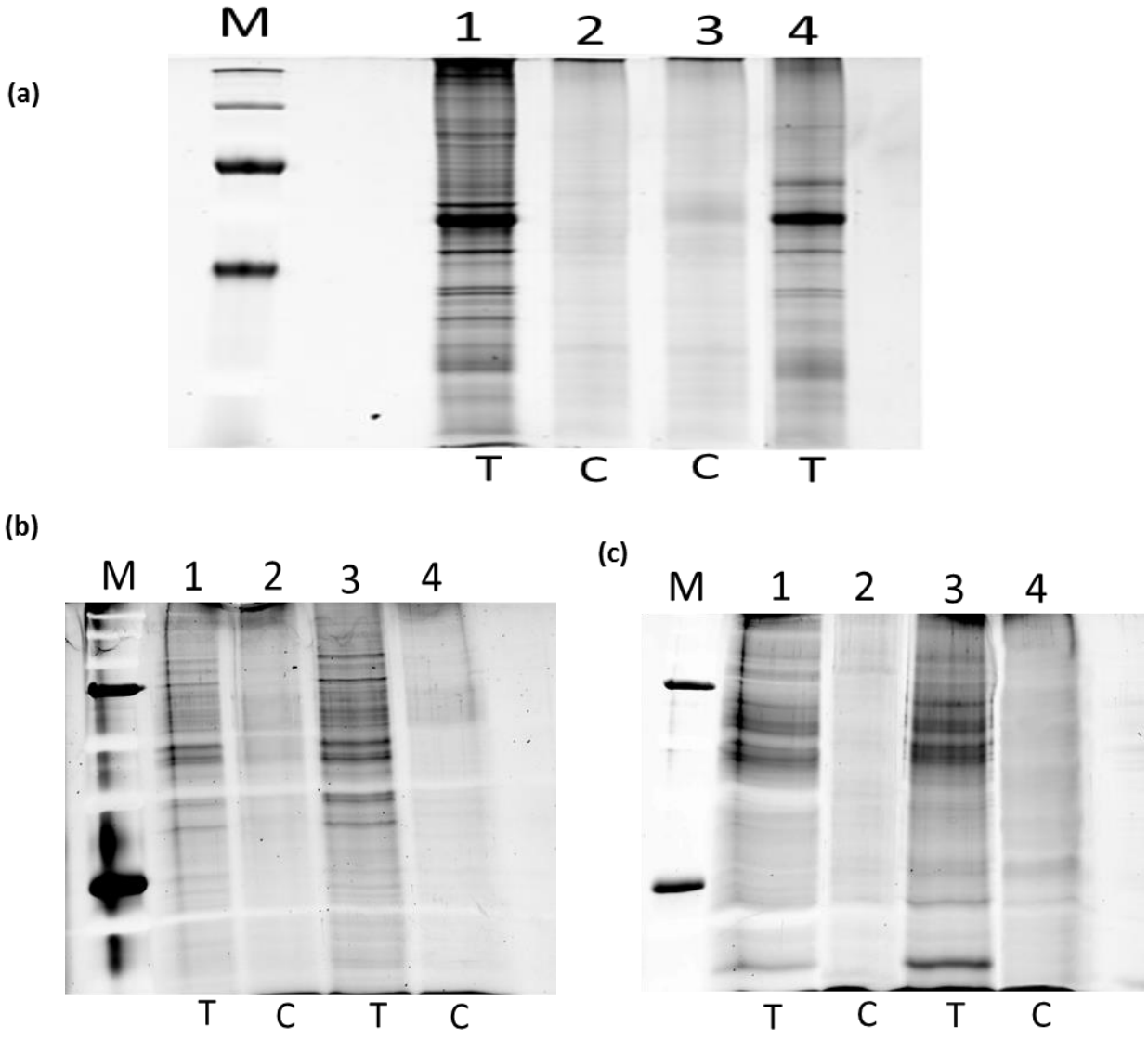


**Figure 3.11: Immunoprecipitation (IP) and protein identification in transfected TK-173 and HK-2 cells**

**(A): IP and protein identification in control (empty vector) and transfected TK-173 and HK-2 cells.** Protein-protein interaction for **(a):** WT-DJ-1 using G-protein agarose matrix and antibody against DJ-1, **(b):** Protein-protein interaction for mutant E18Q-DJ-1, and **(c):** mutant E18D-DJ-1 E18D-DJ-1 (6xHis tag proteins) using QIA express Ni-NTA Fast Start assay. DJ-1 was immunoprecipitated with its interaction partners. The resulting proteins were separated using SDS-PAGE and identified using tryptic digestion and mass spectrometry. M= marker, 1 and 2= TK-173 cells, 3 and 4= HK-2 cells. T= transfected, C= control empty vector.

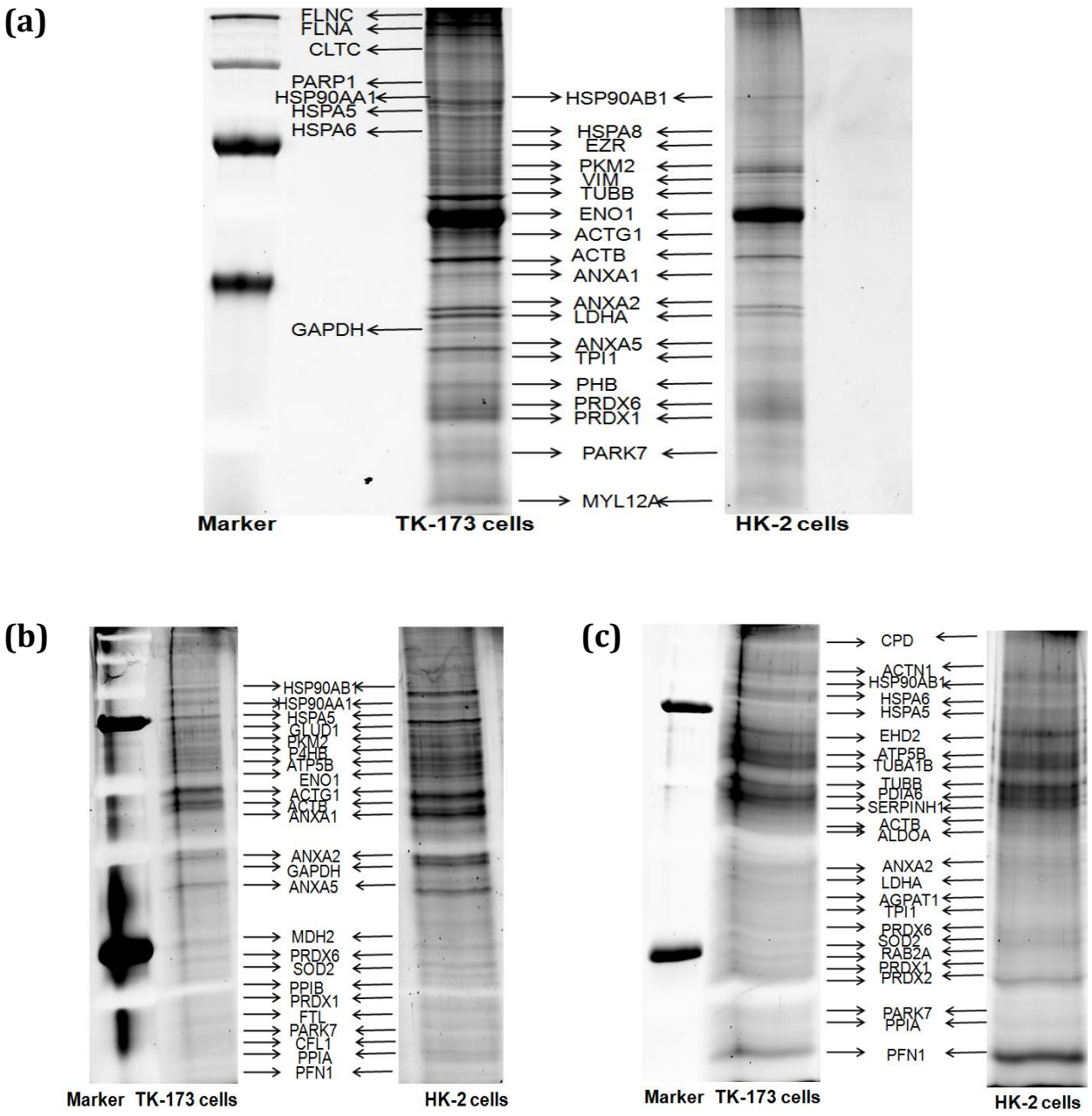


**(B): IP and protein identification in transfected TK-173 and HK-2 cells (a):** Protein-protein interaction for WT-DJ-1 **(b):** mutant E18Q-DJ-1, and **(c):** mutant E18D-DJ- The empmty control was skipped. Under each case, DJ-1 was immunoprecipitated with its interaction partners. The resulting proteins were separated using SDS-PAGE and identified using tryptic digestion and mass spectrometry. All identified proteins are listed in Tables (3.5-3.7).

| Spot Nr. | Protein Name | Gene Name | SwissProt Accession | Mol. Wt. | CPI | MS/MS Score | MS/MS Seq. Cov. |
|---|---|---|---|---|---|---|---|
| 1 | Myosin regulatory light chain 12A | MYL12A | P19105 | 19781 | 4.65 | 139 | 4 |
| 2 | Protein DJ-1 | PARK7 | Q99497 | 19878 | 6.32 | 118 | 6 |
| 3 | Peroxiredoxin-1 | PRDX1 | Q06830 | 22096 | 8.27 | 108 | 5 |
| 4 | Peroxiredoxin-6 | PRDX6 | P30041 | 25035 | 6.00 | 88 | 4 |
| 5 | Prohibitin | PHB | P35232 | 29786 | 5.57 | 99 | 8 |
| 6 | ADP/ATP translocase 2 | SLC25A5 | P05141 | 32831 | 9.71 | 126 | 6 |
| 7 | Annexin A5 | ANXA5 | P08758 | 35914 | 4.93 | 167 | 8 |
| 8 | Glyceraldehyde-3-phosphate dehydrogenase | GAPDH | P04406 | 36030 | 8.57 | 335 | 10 |
| 9 | L-lactate dehydrogenase A chain | LDHA | P00338 | 36665 | 8.44 | 100 | 5 |
| 10 | Annexin A2 | ANXA2 | P07355 | 38580 | 7.57 | 580 | 12 |
| 11 | Annexin A1 | ANXA1 | P04083 | 38690 | 6.57 | 304 | 11 |
| 12 | Actin, cytoplasmic 1 | ACTB | P60709 | 41710 | 5.29 | 258 | 9 |
| 13 | Actin, cytoplasmic 2 | ACTG1 | P63261 | 41766 | 5.31 | 140 | 6 |
| 14 | Alpha-enolase | ENO1 | P06733 | 47139 | 7.01 | 390 | 11 |
| 15 | Tubulin beta chain | TUBB | P07437 | 49639 | 4.78 | 259 | 13 |
| 16 | Vimentin | VIM | P08670 | 53619 | 5.05 | 574 | 21 |
| 17 | Pyruvate kinase isozymes M1/M2 | PKM | P14618 | 57900 | 7.96 | 179 | 6 |
| 18 | Heterogeneous nuclear ribonucleoprotein L | HNRNPL | P14866 | 64092 | 8.46 | 98 | 4 |
| 19 | Ezrin | EZR | P15311 | 69370 | 5.94 | 149 | 7 |
| 20 | Heat shock cognate 71 kDa protein | HSPA8 | P11142 | 70854 | 5.37 | 372 | 9 |
| 21 | Heat shock 70 kDa protein 6 | HSPA6 | P17066 | 70984 | 5.81 | 153 | 6 |
| 22 | 78 kDa glucose-regulated protein | HSPA5 | P11021 | 72288 | 5.07 | 347 | 8 |
| 23 | Heat shock protein HSP 90-beta | HSP90AB1 | P08238 | 83212 | 4.96 | 522 | 14 |
| 24 | Elongation factor 2 | EEF2 | P13639 | 95277 | 6.41 | 110 | 5 |
| 25 | Poly [ADP-ribose] polymerase 1 | PARP1 | P09874 | 113012 | 8.99 | 148 | 5 |
| 26 | Clathrin heavy chain 1 | CLTC | Q00610 | 191493 | 5.48 | 190 | 6 |
| 27 | Filamin-A | FLNA | P21333 | 280564 | 5.70 | 776 | 20 |
| 28 | Filamin-C | FLNC | Q14315 | 290841 | 5.65 | 420 | 16 |

**Table 3.5: Immunoprecipitation of the WT-DJ-1 transfected cell lysates.**

Immunoprecipitated proteins with WT-DJ-1 transfected TK-173 and HK-2 cells using anti-DJ-1 antibody and G-protein agarose matrix. The gene name, accession number in Swiss-Prot, protein mass (Mol. Wt.), the calculated isoelectric point (CPI), and MS/MS information are given.

| Spot Nr. | Protein Name | Gene Name | SwissProt Accession | Mol. Wt. | CPI | MS/MS Score | MS/MS Seq. Cov. |
|---|---|---|---|---|---|---|---|
| 1 | 60S ribosomal protein L31 | RPL31 | P62899 | 14454 | 10.54 | 59 | 4 |
| 2 | Peptidyl-prolyl cis-trans isomerase A | PPIA | P62937 | 18001 | 7.68 | 59 | 5 |
| 3 | Cofilin-1 | CFL1 | P23528 | 18491 | 8.22 | 44 | 4 |
| 4 | Protein DJ-1 | PARK7 | Q99497 | 19878 | 6.32 | 52 | 6 |
| 5 | Ferritin light chain | FTL | P02792 | 20007 | 5.50 | 46 | 4 |
| 6 | Peroxiredoxin-1 | PRDX1 | Q06830 | 22096 | 8.27 | 43 | 4 |
| 7 | Peptidyl-prolyl cis-trans isomerase B | PPIB | P23284 | 23728 | 9.42 | 104 | 8 |
| 8 | Ras-related protein Rab-11A | RAB11A | P62491 | 24378 | 6.12 | 67 | 6 |
| 9 | Superoxide dismutase [Mn], mitochondrial | SOD2 | P04179 | 24707 | 8.35 | 68 | 7 |
| 10 | Malate dehydrogenase, mitochondrial | MDH2 | P40926 | 35481 | 8.92 | 76 | 4 |
| 11 | Annexin A5 | ANXA5 | P08758 | 35914 | 4.93 | 334 | 10 |
| 12 | Glyceraldehyde-3-phosphate dehydrogenase | GAPDH | P04406 | 36030 | 8.57 | 197 | 4 |
| 13 | Annexin A2 | ANXA2 | P07355 | 38580 | 7.57 | 289 | 12 |
| 14 | Annexin A1 | ANXA1 | P04083 | 38690 | 6.57 | 141 | 5 |
| 15 | Actin, cytoplasmic 1 | ACTB | P60709 | 41710 | 5.29 | 202 | 6 |
| 16 | Actin, cytoplasmic 2 | ACTG1 | P63261 | 41766 | 5.31 | 191 | 12 |
| 17 | Alpha-enolase | ENO1 | P06733 | 47139 | 7.01 | 68 | 7 |
| 18 | Serine hydroxymethyltransferase, mitochondrial | SHMT2 | P34897 | 55958 | 8.76 | 92 | 9 |
| 19 | Protein disulfide-isomerase | P4HB | P07237 | 57081 | 4.76 | 72 | 5 |
| 20 | Pyruvate kinase isozymes M1/M2 | PKM2 | P14618 | 57900 | 7.96 | 206 | 15 |
| 21 | Glutamate dehydrogenase 1, mitochondrial | GLUD1 | P00367 | 61359 | 7.66 | 69 | 5 |
| 22 | 78 kDa glucose-regulated protein | HSPA5 | P11021 | 72288 | 5.07 | 131 | 7 |
| 23 | Heat shock protein HSP 90-alpha | HSP90AA1 | P07900 | 84607 | 4.94 | 99 | 6 |
| 24 | Endoplasmin | HSP90B1 | P14625 | 92411 | 4.76 | 130 | 7 |

**Table 3.6: Immunoprecipitation of the mutant E18Q-DJ-1 transfected cell lysates.**

Immunoprecipitated proteins with E18Q-DJ-1 transfected TK-173 and HK-2 cells using the QIA express Ni-NTA Fast Start assay. The gene name, accession number in Swiss-Prot, protein mass (Mol. Wt.), the calculated isoelectric point (CPI), and MS/MS information are given.

| Spot Nr. | Protein Name | Gene Name | SwissProt Accession | Mol. Wt. | CPI | MS/MS Score | MS/MS Seq. Cov. |
|---|---|---|---|---|---|---|---|
| 1 | Profilin-1 | PFN1 | P07737 | 15045 | 8.44 | 40 | 3 |
| 2 | Peptidyl-prolyl cis-trans isomerase A | PPIA | P62937 | 18001 | 7.68 | 53 | 4 |
| 3 | Lipocalin-1 | LCN1 | P31025 | 19238 | 5.38 | 98 | 3 |
| 4 | Peroxiredoxin-2 | PRDX2 | P32119 | 21878 | 5.66 | 147 | 12 |
| 5 | Peroxiredoxin-1 | PRDX1 | Q06830 | 22096 | 8.27 | 89 | 5 |
| 6 | Ras-related protein Rab-2A | RAB2A | P61019 | 23531 | 6.08 | 54 | 6 |
| 7 | Superoxide dismutase [Mn], mitochondrial | SOD2 | P04179 | 24707 | 8.35 | 64 | 4 |
| 8 | Peroxiredoxin-6 | PRDX6 | P30041 | 25035 | 6.00 | 83 | 9 |
| 9 | Triosephosphate isomerase | TPI1 | P60174 | 30772 | 5.65 | 55 | 4 |
| 10 | 1-acyl-sn-glycerol-3-phosphate acyltransferase alpha | AGPAT1 | Q99943 | 31696 | 9.48 | 68 | 6 |
| 11 | Enoyl-CoA delta isomerase 1, mitochondrial | ECI1 | P42126 | 32795 | 8.80 | 88 | 7 |
| 12 | Annexin A2 | ANXA2 | P07355 | 38580 | 7.57 | 319 | 8 |
| 13 | Fructose-bisphosphate aldolase A | ALDOA | P04075 | 39395 | 8.30 | 44 | 7 |
| 14 | Actin, cytoplasmic 1 | ACTB | P60709 | 41710 | 5.29 | 65 | 10 |
| 15 | Serpin H1 | SERPINH1 | P50454 | 46411 | 8.75 | 212 | 7 |
| 16 | Protein disulfide-isomerase A6 | PDIA6 | Q15084 | 48091 | 4.95 | 87 | 4 |
| 17 | Acyl-coenzyme A thioesterase 9, mitochondrial | ACOT9 | Q9Y305 | 49870 | 8.81 | 137 | 10 |
| 18 | Tubulin alpha-1B chain | TUBA1B | P68363 | 50120 | 4.94 | 166 | 5 |
| 19 | ATP synthase subunit beta, mitochondrial | ATP5B | P06576 | 56525 | 5.26 | 205 | 5 |
| 20 | EH domain-containing protein 2 | EHD2 | Q9NZN4 | 61123 | 6.02 | 99 | 3 |
| 21 | 78 kDa glucose-regulated protein | HSPA5 | P11021 | 72288 | 5.07 | 235 | 18 |
| 22 | Stress-70 protein, mitochondrial | HSPA6 | P38646 | 73635 | 5.87 | 62 | 3 |
| 23 | Endoplasmin | HSP90B1 | P14625 | 92411 | 4.76 | 120 | 9 |
| 24 | Alpha-actinin-1 | ACTN1 | P12814 | 102993 | 5.25 | 64 | 4 |
| 25 | Carboxypeptidase D | CPD | O75976 | 152835 | 5.68 | 61 | 3 |

**Table 3.7: Immunoprecipitation of the mutant E18D-DJ-1 transfected cell lysates.**

Immunoprecipitated proteins with E18D-DJ-1 transfected TK-173 and HK-2 cells using the QIA express Ni-NTA Fast Start assay. The gene name, accession number in Swiss-Prot, protein mass (Mol. Wt.), the calculated isoelectric point (CPI), and MS/MS information are given.

To investigate the impact of alteration of C106 thiolate stability on interaction partners of DJ-1, comparative analyses were performed with the immunoprecipitated proteins from the three cases (WT, E18Q, E18D) (Fig. 3.12). A coordinated proteomic cascade that has fundamental physiological and pathological properties was detected to cooperate with protein DJ-1. Six prime proteins, namely PRDX1, PRDX6, ANXA2, ACTB, HSPA5, and HSP90B1 were identified in all transfected cell groups. Peroxiredoxins (PRDX) are a ubiquitous family of antioxidant enzymes that are involved in redox regulation of the cell as well as in the protection against oxidative injury (82, 186). Regarding annexins (ANXA), several subfamilies have been identified based on structural and functional differences (187). ANXA2 being a pleiotropic protein is generally implicated in diverse processes, depending on its cellular localization. It plays a main role in the regulation of cellular growth and signal transduction pathways (188). Recently, ANXA2 has been identified as novel cellular redox regulatory protein (189). Heat shock proteins (HSP) are a class of proteins entangled in the folding and unfolding of other proteins. Production of high levels of HSP is triggered by exposure to various kinds of environmental stress conditions (190). Their up regulation is described as part of the stress response. Actins (ACTB) are highly conserved proteins that are concerned in cell motility, structure, and integrity (191). Moreover, GAPDH, ENO1, and PKM2 proteins were also noticed to be shared between WT-DJ-1 and E18Q-DJ-1 transfected cells. It is noteworthy mentioning, that GAPDH beside its classical glycolytic function and its involvement in many metabolic functions, has been implicated in a diverse non-metabolic processes including transcription activation and initiation of apoptosis (192-194). Fukuhara *et al.*, 2001 (194), stated that GAPDH acts as a reversible metabolic switch under OS. In case of ENO1 protein, is generally known to play a part in growth control and hypoxia tolerance (195). PKM2 is a glycolytic enzyme involved in a variety of pathways and protein-protein

interactions (196). The precipitation of more annexins namely ANXA1 and ANXA5 and the heat shock protein HSP90AA1 may provide an additional clue to the cellular recovery response to stress under both transfection states.

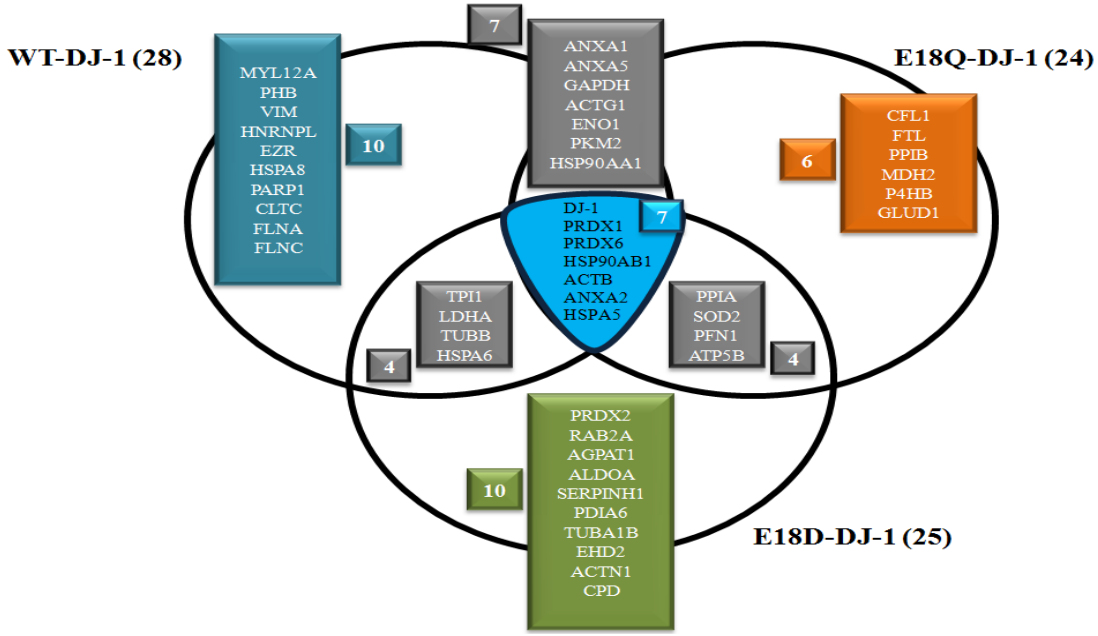


**Figure 3.12: Comparison between immunoprecipitated proteins as potential interaction partners of different forms of DJ-1**

Diagrammatic presentation showing the number of immunoprecipitated proteins in each experimental set and the proteins shared between the different sets.

Finally, despite more OS marker proteins (PRDX2 and SOD2) were identified as interacting partners for E18D-DJ-1 variant (Figs. 3.11C and 3.12), yet transfecting cells with this mutant showed severe apoptosis (Fig. 3.10 A,B) indicating that in case of the DJ-1 the amino acid E18 and not its negative charge is that important for cell survival under stress conditions. Moreover, comparing the number of the supplemental precipitated proteins in cells transfected with DJ-1 mutants (Fig. 3.12) reveals that more proteins were co-precipitated with DJ-1 protein under E18D-DJ-1 transfection outlining the enhancement of additional cellular pathways in response to severe stress condition.

The present data provide a framework linking DJ-1 to OS and afford insight into the interaction between complex mechanisms and multistep pathway by which DJ-1 exerts its action. In fact, functional and association networks analyses of the immunoprecipitated proteins using STRING: 9.05 ***(http://string-db.org/),*** revealed a strong networking of the identified proteins, suggesting a functional link between these proteins and their importance in the mechanism of action of DJ-1 (Fig. 3.13). STRING quantitatively integrates interaction data from four sources: Genomic context, high-throughput experiments, conserved co-expression, and previous knowledge.

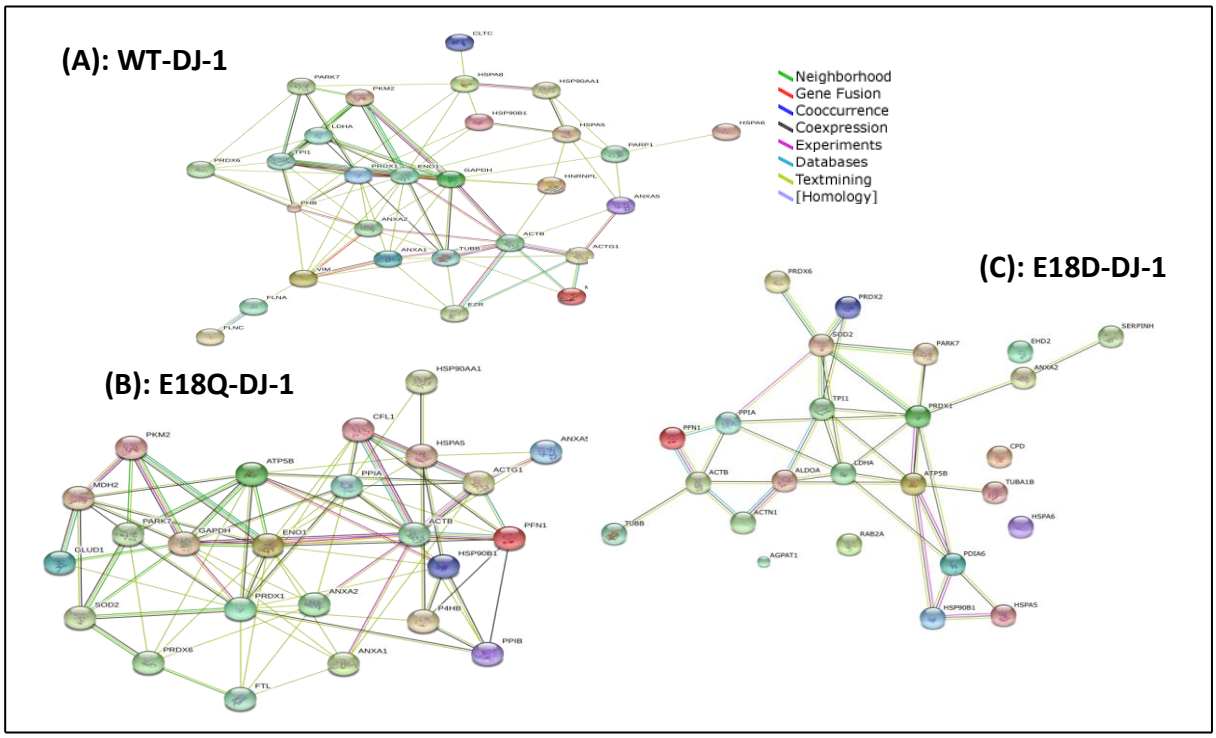


**Figure 3.13: STRING 9.05: Functional protein association networks**

Database of known and predicted protein-protein interactions. The interactions include direct (physical) and indirect (functional) associations; they are derived from four sources: Genomic context, high-throughput experiments, conserved co-expression and previous knowledge. STRING quantitatively integrates interaction data from these sources. The evidence view for the immunoprecipitation experimental results suggesting the different functional links of **(A):** WT-DJ-1, **(B):** E18Q-DJ-1, and **(C):** E18D-DJ-1. Different line colors represent the types of evidence for the association. Medium confidence (0.400).

## 3.5 Discussion

A number of kidney diseases and their progression to end-stage renal disease are driven, in part, by the effects of ANG II. Increasing levels of ANG II may, in turn, up regulate the expression of a large number of growth factors including PDGF. Most of these compounds promote cell growth and fibrosis (62, 197). Well-documented growth-promoting effect of angiotensins in various tissues has been reported (198-203). The ANG II-stimulated blood vessel growth has been previously demonstrated in some experimental models (204-206). In addition, results of many studies have reported that peptides from the angiotensin family are involved in the regulation of cell growth, proliferation, migration, apoptosis, differentiation and inflammation (207-209) of many types of cells, including fibroblasts (210), cardiomyocytes (211), and renal proximal tubular cells (212).

Similar to ANG II, PDGF isoforms were also observed to stimulate the replication and migration of myofibroblasts in fibrotic processes, including renal fibrosis (213), whereas antagonism of PDGF-D isoform prevented renal fibrosis in an experimental model of glomerulonephritis (214, 215), and treatment with anti PDGF-C antibody induced fibrosis in obstructive nephropathy (216).

Our results are consistent with and advance the results from Piastowska-Ciesielska *et al.*, 2013 (217), by demonstrating that ANG II had a significant effect on viability of renal cells (TK-173 and HK-2) in a dose and time-dependent manner. A statistically significant difference between the control and treated cells with maximal survival response was achieved at a concentration 0.5 µM ANG II which was then chosen for further experiments.

The prevailing interpretations existing for cell proliferation under ANG II treatment are either, via mitochondrial metabolic activity (217), through signaling pathways mediated by

the AT1 receptor (218, 218), or are often the consequence of ANG II-induced activation of many cytoplasmic tyrosine kinase and transactivation of membrane associated growth factor receptor kinases (220-222). In mammalian cells, ANG II mediates biological effects through binding to two classical angiotensin receptors. Interestingly, ANG II induced cell proliferation by activating $AT_1$-receptors, while stimulation of the $AT_2$-receptor inhibited cell growth in different cell types (223-225). The effect of ANG II on prostate cancer cells (LNCaP) viability was generally similar to the control (226). The lack of ANG II effect in the later study (226) was, in part, due to the short incubation time with ANG II (24 h) compared to other published studies demonstrating proliferation stimulation of the similar cell type cultured in presence of ANG II for 3 days (227) and for 5 days (222).

Our proteomic analysis of renal cells' response to ANG II and PDGF treatment helmed to the identification of a vast number of proteins, which may be directly or indirectly involved in cytokines regulated events. The expressions of proteins involved in the metabolic, cytoskeletal, inflammatory, biological, cellular homeostasis, and cell proliferation processes were significantly altered. Some of the proteins that were positively identified in our study were previously shown to be regulated directly or indirectly by growth factors. Disulfide isomerase and lactate dehydrogenase have been shown to be up-regulated in vascular smooth muscle cells (228, 229) and primary fibroblasts (230) upon exposure to PDGF. PHB, AHSA1, and PAK2 were also quantitatively altered in the later study (230). In respect to the abundant proinflammatory proteins identified in our study (heat shock proteins, annexins, tubulins, redoxins and collagens), previous work also reported that ANG II up-regulated the expression of some proinflammatory genes (connective tissue growth factor, collagen and fibronectin) through the activation of several intracellular signaling systems (231-233). The elucidation of the exact role of each specified protein is of dignified prominence and claims further

investigation for inspecting their relevance to renal fibrosis. However, the activation of the endogenous antioxidant defense mechanism that was marked by the concomitant up-regulation of stress responsive proteins was of our central interest.

Multiple stimuli and agonists, including ANG II and PDGF have been shown to ultimately induce OS (61, 234) and increase ROS production (56). ANG II-induced OS and ROS are pivotal in several signal transduction pathways and redox-sensitive transcriptional factors involved in renal pathphysiology (22,165). Schieffer *et al.*, 2000 (235), demonstrated that ANG II played an important role in modulating the expression of the proinflammatory molecule (IL-6) through a mechanism that required the production of ROS. In year 2004 and later in 2006 a regulatory role of ROS in PDGF and ANG II induced signal transduction was further documented (236, 237). Acute ANG II infusion experiments into naïve rats in the presence or absence of various free radical scavengers showed that scavengers partly inhibited cellular damage (238, 239). ANG II-mediated ROS formation is thus substantial for renal growth processes that are part of an adaptive process of surviving nephrons during chronic renal injury (240).

Our prior study (128) has focused on providing evidence for the critical role of protein DJ-1 during OS acquired by $H_2O_2$ in cultured human renal fibroblasts and epithelial cells. In an attempt to reveal the effect of profibrotic cytokines on DJ-1 expression in the similar cell lines, the present survey additionally displayed that the fibrosis triggering cytokines (ANG II and PDGF) treatment, resulted in cellular DJ-1 up-regulation in both tested cell lines despite no change in the protein *pI* value was observed compared to the formerly detected shift under $H_2O_2$ treated cells, suggesting a crucial biological *in vivo* significance of DJ-1 as a modulator of OS and/or fibrosis possessing discipline functions during renal injury. Moreover, our

investigation of DJ-1 expression in renal tissue of mice model for renal fibrosis (*Col4a3* knock-out mice) confirmed the augmentation of the protein with the progression of fibrosis.

It is worthwhile mentioning that the incubation of the prostatic benign cells (exhibiting low basal level of DJ-1 expression) with TNF-related-apoptosis-inducing-ligand/Apo-2L (TRAIL) had led to the enhancement of DJ-1 expression associated with the induction of apoptosis. While in cancer cell lines expressing relatively high DJ-1 level, rendered cells resistant to TRAIL with no further modulation of the polypeptide level, proposing that DJ-1 played a differential role between cells expressing a low but inducible level of DJ-1 and those expressing a high but constitutive level (241). Similarly, Zhang *et al.*, 2008 (242), also found that the basal level of DJ-1 appeared to be inversely correlated with TRAIL-induced apoptosis in the investigated thyroid cancer lines. However, no isoelectric focusing phoresis was represented in both studies. In 2009, Waak and coworkers (243) demonstrated that after activation with the endotoxin lipopolysaccharide (LPS), DJ-1 deficient mouse astrocytes showed dramatic overproduction of the inflammatory mediator nitric oxide (NO), proposing that loss of DJ-1 may selectively derepress an LPS-activated TLR4-ASK1-p38MAPK pathway, leading to an overshoot of iNOS induction and consequently excessive NO production. This may contribute significantly to secondary neurodegeneration. Recently, it was also demonstrated that Toll-like receptor 4 (TLR4), the main receptor for endotoxin (LPS), mutant mice developed less interstititial fibrosis in comparison to WT mice and were protected from progressive CKD in a low-dose ANG II infusion +5/6 nephrectomy model, suggesting that TLR4 may play an important role in kidney scarring and fibrosis and contribute to CKD progression (244). Linking these observations to our cytokine (ANG II and PDGF) treated renal cell models and the observed protective role of DJ-1 an exact molecular mechanism by which DJ-1 may regulate proinflammatory signaling via TLR4 pathway in

renal cells remains to be rigorously proven. To present the precise impact of DJ-1 in renal fibrosis remains entirely ambiguous. To our knowledge, our previously published work (128) is the sole attempt that has been as yet executed. However, several pieces of information are available in literature, which provide clues to possible pathways and allow hypotheses linking DJ-1 to renal fibrosis thereby assisting, in collaboration to our results, to accentuate the multiple effects of DJ-1.

It has been reported that DJ-1 functions in multiple pathways that promote cell survival. Enormous studies indicated that DJ-1 is an antioxidant that can quench ROS by self-oxidation (121, 129, 151). Consistent with this observation, our previous notification that gene deletion or down regulation of DJ-1 by small interfering RNA (siRNA) sensitize renal cells to OS (128), similarly neuronal cells (245), and to ER stress (245) and enhances cytotoxicity mediated by MPTP (184).

DJ-1 has been modified under OS both *in vitro* and *in vivo* by oxidation of the Cys106 residue to form cysteine sulfinic acid (Cys106-$SO_2^-$) (109, 126, 146, 154, 245). The formation of Cys106-$SO_2^-$ has been identified as a key modification required for DJ-1 to exert its protective function (101, 129, 133, 141, 148, 153-155, 245). Altering the oxidative propensity of Cys106 caused the protein to lose its normal protective activity against oxidative stressors in a number of systems (100, 142, 246). The substitution of M261 and over-oxidation with $H_2O_2$ showed an increased propensity to aggregate and decreased secondary structure (142). Likewise, loss of protein function caused by the Parkinson's-associated mutation L166P was interpreted due to disruption of the C-terminal region and dimerization of the protein (100, 246). Moreover, X-ray crystallography analysis suggested that the carboxylic acid sidechain E18 residue forms a hydrogen bond with Cys106-$SO_2^-$, which is important for the stabilization of the modified residue (101, 126, 129, 156, 247).

Like WT protein (101), mutant E18Q-DJ-1 allowed Cys106 to be oxidized to Cys106-$SO_2^-$. In contrast, E18D-DJ-1 mutant was oxidized to the easily reduced cysteine sulfenic acid (Cys106-$SO^-$) resulting in oxidation impairment of Cys106 (101). Mitochondrial fission assay in the later study (101), demonstrated that E18Q could partially substitute for WT-DJ-1, while the oxidatively impaired E18D behaved as an inactive mutant and failed to protect cells from OS. Examining the role that the specific formation of Cys106-$SO_2^-$ has on cellular protective function of DJ-1 by mutating E18, our transfection viability assay results clearly emphasizes that the oxidative modification of Cys106 to Cys106-$SO_2^-$ is a critical determinant for DJ-1 to protect renal cells against loss of viability due to $H_2O_2$ and cytokines exposure.

Interestingly, despite E18D was proved to have identical p*Ka* value to E18N (126, 156), different oxidative and *in vivo* protective capabilities were later demonstrated for the two mutants (101), denoting that it is the oxidative propensity rather than the nucleophilicity or general reactivity of Cys106 that is required for DJ-1 protective activity.

Based on the viability assay results for transfected cells presented herein and data reported by Blackinton *et al*., 2009 (101), we would suggest that E18D substitution has led to the tremendous disruptive effect as a result of the formation of a functionally compromised DJ-1.

Mutation of Cys106 to alanine, serine or aspartic acid eliminated the ability of DJ-1 to protect against OS in several model systems including various types of cultured mammalian cells (101, 129, 141, 152). Similarly, L166P mutant abrogated DJ-1 function by destabilizing the native homodimer (88, 248, 249), and M261 mutant exhibited reduced protective activity as a result of decreased ability to undergo oxidation to the functionally important "2O" form (93, 101, 110, 126, 129, 142, 250) with deleterious effects on DJ-1 function.

Interestingly, knockdown of DJ-1 in the corneal endothelial cells (CEC) resulted in decreased translocation of Nrf2 to the nucleus and significant down-regulation of Heme oxygenase 1 (HO-1). These *in vitro* data corroborated findings detected in Fuchs endothelial corneal dystrophy (FECD) tissue samples where DJ-1 down-regulation was accompanied by diminished Nrf2-regulated antioxidant defense (251). Since FECD has been shown to be an OS disorder (252) possessing an oxidative modification at Cys106 of DJ-1 occurring during OS and rendering DJ-1 inactive (251), authors speculated that the oxidant-antioxidant imbalance seen in FECD had led to irreversible oxidative modifications of DJ-1 and its rapid degradation, which in turn affected the cytoplasmic stability of Nrf2 and impaired its nuclear translocation. DJ-1 down-regulation resulting in attenuated gene expression of Nrf2 and its target gene HO-1 leading to increased oxidative damage has been then repeatedly cited in CEC (253), in mouse kidneys and proximal tubule cells (254), and in rat heart-derived H9c2 cells (255). Similarly Sun *et al.*, (256) suggested that the activation of DJ-1/Nrf2 pathway was involved in the pathogenesis of diabetic nephropathy in rats.

Targeting the DJ-1/Nrf2 axis may provide a potential mechanism by which DJ-1 can mediate the delayed protection and enhance its antioxidant defense under OS in our renal cell model.

Given the established apparent oxidation of Cys106, can DJ-1 function be regulated in terms of intracellular redox state thus believed as a typical peroxiredoxin-like protein? Published data are conflicting. Several studies indicated that Cys106 residue of DJ-1 can undergo reversible oxidation in response to OS although the mechanism(s) involved in regenerating the non-oxidized isoforms and controlling Cys modification in DJ-1 have yet to be established (129, 148, 151). Others illustrated that DJ-1 is a new type of scavenger protein (101, 121). Wilson, 2011 (126) invoked that DJ-1 oxidized at Cys106 is not reverted to the thiol and accumulates as the oxidized isoforms. Turnover of the oxidized isoforms and new synthesis of

the reduced protein would be, therefore, required for the clearance of the oxidized DJ-1 (110). However, this is a convincing observation clarifying the provided evidence that DJ-1 functions as a cytoplasmic redox-molecular chaperone of alpha-synuclein (109, 110, 119, 257). The oxidation of Cys106 was obviously critical for the ability of DJ-1 to translocate to the mitochondria (129), inhibit mitochondrial fragmentation (101, 258, 259) or suppress alpha-synuclein fibrillation (110). Consequently, DJ-1 is not a ROS detoxifying enzyme like the peroxiredoxins, glutaredoxins or catalase, the true catalysts competent of multiple turnovers and massive ROS detoxification. Yet DJ-1 was observed to elevate glutathione levels (119, 257) by increasing the transcription and enzymatic activity of glutamate cysteine ligase, the rate limiting enzyme of glutathione synthesis (119).

Our immunoprecipitation data provide further clues for DJ-1 suggested chaperone activity and its cytosolic RNA-binding activity. Under all experimental conditions, proteomic approach targeting DJ-1 interacting partner proteins, revealed the co-precipitation of heat shock proteins HSPA5 and HSP90AB1, additionally HSP90AA1 in WT and E18Q experiments, the premium chaperones assisting to refold misfolded proteins and suppress their aggregation in the presence of OS and other stress conditions. Consistent with our observation, previous reports manifested that OS enhanced the interaction between DJ-1 and the heat shock protein 70 (Hsp70) (260). DJ-1 was also shown to be protective in cooperation with Hsp70 against alpha-synuclein toxicity in cultured human and rat cell models (120, 257), and to act in an Hsp70-dependent manner in cultured human dopaminergic cells (119).

In light of the earlier report characterizing DJ-1 as a regulatory subunit of a 400 kDa RNA-binding protein complex (173), coupled with the co-purification of glyceraldehyde 3-phosphate dehydrogenase (GAPDH), possessing functional links to apoptosis (192-194), with

these complexes, together with the co-precipitation of GAPDH with DJ-1 in WT and E18Q but not E18D in the current work immunoprecipitation experiments, provide insight and distinctly expand DJ-1 function at the transcriptional level by influencing stress response gene expression. This observation may also explain and clarify the drastic negative effect of E18D substitution on cell viability. Interestingly, the yeast genes encoding DJ-1 and GAPDH homologs were induced during cell stress together with chaperones, antioxidants and other stress response proteins (261).

An explicit role of annexins in DJ-1 multiple pathways, to our knowledge, has never as yet been explored. However, extracellular annexins have been linked to inflammation and apoptosis (262). Generally, annexins function as scaffolding proteins to anchor other proteins to the cell membrane (263). ANXA1 has been implicated in apoptotic mechanisms by promoting the removal of cells that have undergone apoptosis (188, 264). Recently, ANXA2 has been identified as a novel cellular redox regulatory protein that played a significant role in cells undergoing OS induced by $H_2O_2$ via the reaction of its cysteine residue with $H_2O_2$ resulting in the oxidation of this residue and the conversion of $H_2O_2$ to $H_2O$ (189). Over expression of ANXA2 as an OS sensitive protein in cells treated with $H_2O_2$ in our previous work (128), and in fibroblastic cells treated with OS prompting factors ANG II and PDGF in the present study, supports the later observation. Further, the co-expression of ANXA2 as a partner protein to the WT-DJ-1 and both mutants emphasizes that ANXA2 is unique among the annexins that possesses redox sensitive cysteine as previously stated (189). Yet the possible interacting mechanism with DJ-1 warrants extra investigations.

Referring and counseling to the functional protein association networks procured via STRING database, a variety of predicted protein-protein interactions through disparate enzymatic pathways could be speculated.

Moreover, the remarkable and apparent precipitation of key players OS marker proteins (PRDX2 and SOD1) with DJ-1 in experiments for E18D mutant, clearly interprets the extreme stress condition challenged by cells as a result of E18D substitution.

Our data strengthens previous determinations for DJ-1 diverse pathways and indicate that DJ-1 is part of a concerted and complex cellular response to OS. Although much work remains to be done to clarify the relationship between DJ-1 and renal dysfunction, yet results reported here lay the ground work relevant to develop better strategies for defining the precise activity of DJ-1 that is responsible for cellular protection against OS in renal cells.

Dividing the cellular response to stress inducing agents into three major steps, a protective response, a repair response, and a signaling and activation response, a spectacular switching action for the 20 kDa multifunctional protein DJ-1 according to the exact need of the cell, could be estimated. A dual function may also be proposed.

# 4. GENERAL DISCUSSION

Oxidative stress (OS) has been implicated in human disease by a growing body of facts. The kidney is a highly vulnerable organ to damage caused by OS and large number of literature has been concerned with the link between OS and renal diseases. OS is known to desperately affect the survival and proliferation of renal cells through biomolecular pathways resulting in impairment of kidney function and final progression of renal tubulointerstitial fibrosis. Hence, renal fibrosis is a state of chronic deterioration of oxidative mechanism due to enhanced reactive oxygen species (ROS) release. Over production of ROS has been implicated as a driving force, which evokes a cascade of oxidative damage that can eventually result in renal failure. To understand the molecular basis in renal fibrosis with respect to regulation and expression of stress responsive proteins, we aimed to explore the effect of $H_2O_2$, and the profibrotic cytokines (ANG II and PDGF) as promoters of OS. In our study, human renal fibroblasts (TK-173) were used as they are believed to be the primary effector cells with respect to renal fibrogenesis process responsible for the synthesis and deposition of ECM components. Human renal epithelial cells (HK-2) were additionally investigated for comparison purposes. Our proteomic approach; 2-DE combined with mass spectrometry analysis has made possible the identification of OS associated proteins, among these, markers of the OS pathway were highly regulated in treated cells. DAVID database resource for assignment of the proteins according to their molecular function, showed that the percent stress responsive proteins was more in the fibroblastic TK-173 compared to the epithelial HK-2 cells under treatments. The up-regulation of the over viewed proteins could be interpreted as one of the major cellular recovery response after oxidative damage. The information obtained, in the present study, has far revealed relatively comprehensive view in protein expression, facilitating the determination of novel OS biomarkers for early disease detection and new targets for therapeutic intervention. Among the regulated proteins of the OS pathway, protein

DJ-1 (PARK7) was found to acquire a *pI* shift in addition to its high expression under $H_2O_2$ treatment. An important clue to a possible role in OS, as relevant from accumulating studies strongly suggesting the expression of PARK7 in cellular defensive response to OS and has been repeatedly cited to possess a *pI* shift in neurodegenerative diseases linked to OS. However, it is worthwhile mentioning that the absence of PARK7 *pI* shift under fibrosis triggering cytokines (ANG II or PDGF) treatment, surmise a crucial biological *in vivo* significance of PARK7 as a modulator of OS and/or fibrosis possessing discipline functions during renal injury. Knockdown of PARK7 using siRNA led to significant reduction in renal cell viability that was further enhanced under $H_2O_2$ treatment. MTT cell viability assay together with microscopic morphological investigation elucidated that suppression of endogenous PARK7 protein simultaneously with OS induction resulted in massive cell death and increase in apoptosis compared to controls. Therefore, we have put forward, for the first time, a specific and novel hypothesis for the vital role of PARK7 in OS resistance in renal cells, a protein originally discovered as an oncogene, and was later found to be responsible for the early onset of Parkinson's disease. Based on this finding we sought to intensively investigate the expression and the role of PARK7 in balancing OS in renal fibrosis. Western blot (WB) analysis for lysates of $H_2O_2$ or cytokine treated cells showed the upregulation of all stress and fibrotic marker proteins tested including PARK7. Moreover, investigation of PARK7 in *Col4a3* knockout mice, as a fibrosis animal model, revealed the parallel increase of PARK7 with the progression of fibrosis as evident by WB analysis for tissue lysate samples and documented by immunofluorescence and immunohistochemical staining of the tissues at successive stages of fibrosis. Consequently, PARK7 (DJ-1) confers protection against OS and enhances cell survival when challenged with OS and/or pro-apoptotic stimuli. Although the mechanisms by which DJ-1 accomplishes this are not fully understood, a promising

observation that may connect the established role for DJ-1 in OS response to possible biochemical functions of the protein is that a conserved cysteine residue (Cys106) is both critical for DJ-1 function and very sensitive to oxidative modification. WT-DJ-1 is modified under OS both *in vitro* and *in vivo* by oxidation of Cys106 to form a Cys-$SO_2^-$. Cys106 interacts with a neighboring protonated E18 residue, required for stabilizing the Cys106-$SO_2^-$ form of DJ-1. To study this important post translational modification, we have tested this approach by characterizing the effect of E18 mutations on the cytoprotective activity of Cys106 using designed E18 mutations (E18Q and E18D). Comparing cell viability for both cell line models of transfected WT-DJ-1(E18) to either DJ-1 mutation forms (E18Q or E18D) under naïve or OS condition, our results emphasized and provided additional evidence that the formation of Cys106-$SO_2^-$ is advantageous for optimal DJ-1 protective function.

In an effort to characterize DJ-1 mechanism(s) of action, our immunoprecipitation data identified possible interacting protein partners supporting and strengthening pre-existing postulated determinations for DJ-1 potential pathways (summarized in Fig. 4.1). Summing up, beyond DJ-1 role as an oxidative sensor or ROS scavenger by self-oxidation, the co-precipitation of heat shock proteins, the premium chaperones assisting to refold misfolded proteins and suppress their aggregation in the presence of OS, provides clues for DJ-1 suggested chaperone activity. Moreover, the co-purification of GAPDH, possessing functional links to apoptosis, with DJ-1 in WT and E18Q but not E18D insights into DJ-1 function at the transcriptional level and its cystolic RNA-binding activity and elucidates the drastic negative effect of E18D substitution on cell viability.

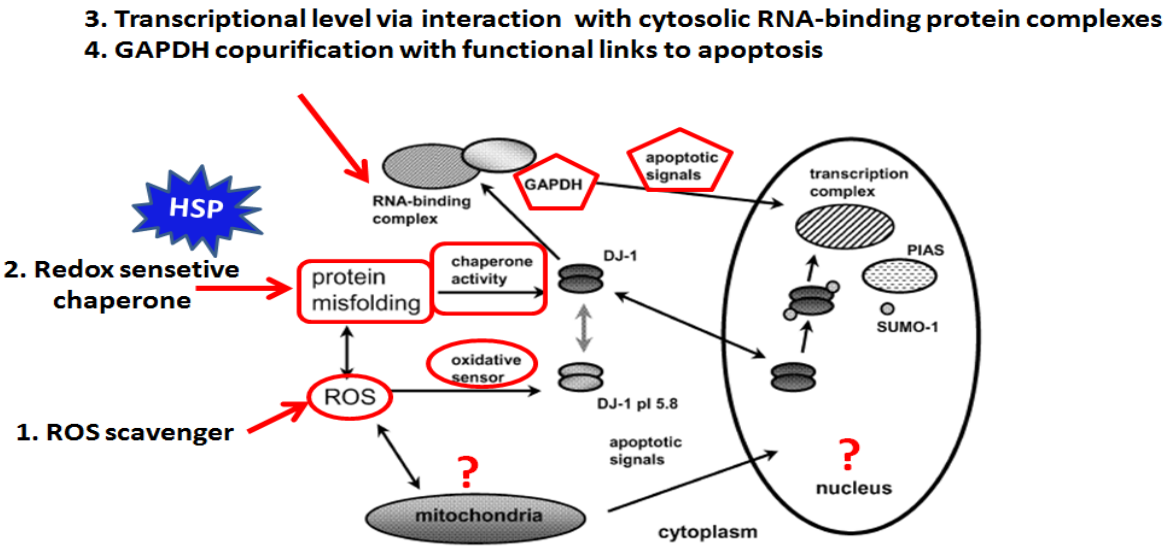


**Figure 4.1: Simplified schematic diagram for protein DJ-1 pathways**

**1:** DJ-1 itself senses oxidative signals (ROS) via oxidation of the Cys106 residue into sulfinic acid (self-oxidation). **2:** DJ-1 has a chaperone activity by interacting with heat shock proteins (HSP) which helps refolding misfolded proteins induced by oxidative and other cell-stress conditions. **3:** DJ-1 influences the expression of genes for the stress response at transcriptional and post-transcriptional levels by interacting with cytosolic RNA-binding protein complexes. **4:** The latter complexes may also be associated with GAPDH, a protein with functional links to apoptosis. *Modified from reference 87.*

Yet, it is tempting to speculate and investigate the apparent role of annexins in co-operation with DJ-1, being linked to inflammation and involved in apoptotic mechanisms; the over expression of ANXA2, in particular, as an OS sensitive protein in the diverse OS experiments, its purification as a DJ-1 partner protein, in addition to the recently published finding (189) establishing ANXA2 as a novel cellular redox regulatory protein emphasize that ANXA2 is unique among other annexins as a redox sensitive protein, a function unmasked in the context of OS. On the other hand, answers to the copious debates concerning DJ-1's multiple roles at the nuclear and mitochondrial levels (Fig. 4.1) necessitate supplementary efforts to provide conceptual support for determining the contribution of protein DJ-1 in renal dysfunction that

may yield therapeutic profile and efficacy. The aforementioned points are designed for our future work extending our OS project. However, the present data provide a framework linking DJ-1 biological actions and generating new sights into the interaction between the complex mechanisms of oxidative damage in renal fibrosis. Moreover, implicate a multistep pathway for protein DJ-1 each afforded according to the cellular requirement.

It is worth mentioning that the cellular redox system is complex with significant cross talk between various proteins and often several proteins compensate for each other's function in a relatively efficient way under various pathological conditions.

# 5. SUMMARY

It is well established that oxidative stress (OS) is an important cause of cell damage associated with the initiation and progression of many diseases including renal diseases. Consequently, all living organisms have developed efficient antioxidant defense systems to cope with these oxidative conditions and limit OS by detoxifying reactive oxygen species (ROS) in aerobic metabolism under normal physiological conditions. These systems are composed of antioxidant enzymes and repair proteins. An excess production of ROS may overwhelm the antioxidant defense system and cause oxidative damage to various cellular constituents including DNA, RNA, proteins, and lipids. A functional proteomics approach used at a wide scale in the present study has explored global changes and provided new molecular targets linking profibrotic cytokines (ANG II and PDGF) and $H_2O_2$-induced OS to cellular dysfunction by recognizing changes of protein expression profiles. A number of OS protein biomarkers have been compiled from our *in vitro* study using human renal cell cultures (TK173 and HK-2). The regulation of the identified proteins has been interpreted as one of the major cellular recovery responses after oxidative damage. The mass spectrometry results were documented by Western Blot (WB) analysis of treated cell lysates for a number of OS biomarkers.

With a shift in the *pI* value in addition to its over expression as a result of oxidation, I provided the first evidence for the incorporation of protein DJ-1 (PARK7) as an endogenous antioxidant defense protein in renal cells. The knock down of PARK7 in renal cells using siRNA dramatically inhibited cell viability as manifested by the morphological changes and MTT viability assay and showed high cellular apoptosis after OS induction. Further, WB analysis for whole kidney lysates of wild type (WT) and different stages of fibrosis from *Col4a3* knockout mice as a fibrosis model revealed a parallel increase in response of PARK7 with the increase of the fibrotic stage. Moreover, immunohistochemical staining and

immunofluorescence staining images of the glomerular and tubulointerstitial areas from similar fibrosis successive stages of *Col4a3* knockout mice kidneys stained with PARK7 further documented WB results.

How may have PARK7 (DJ-1) a benefit in ameliorating the progression of renal fibrosis? I aimed to elucidate the molecular mechanisms of PARK7 action to define the role of PARK7 in balancing OS in renal fibrosis by transfecting cells with plasmids of the WT-DJ-1 and 2 different mutants. I then identified DJ-1 interaction partners in the different transfected cell lysates using affinity purification combined with mass spectrometry. Mutants were chosen according to crystallization structural analysis of the purified protein DJ-1 consolidating cysteine residue (Cys106) to be the most sensitive to OS and the key modification required for DJ-1 to exert its protective function by acting as a sensor of cellular redox homeostasis. Results obtained strengthened and emphasized previous reports by displaying that the oxidative modification of Cys106 to Cys106-$SO_2^-$ is a critical determinant for DJ-1 to protect cells against loss of viability. Besides DJ-1 function as ROS scavenger by self-oxidation, my immunoprecipitation data provided the following clues: i) DJ-1 seems to have a role at the transcriptional and post-transcriptional levels via interacting with cystolic RNA-binding protein complexes and, ii) DJ-1 might have a chaperone activity assisting to refold misfolded proteins induced by oxidative and other cell-stress conditions. Finally, the strong networking of the identified proteins that were detected to cooperate with protein DJ-1 using STRING functional protein association networks analysis manifested DJ-1 as a multifunctional protein and a vital candidate of a concerted and complex cellular response to OS.

# Bibliography

1. Small DM, Coombes JS, Bennett N, Johnson DW, Gobe GC (2012) Oxidative stress, anti-oxidant therapies and chronic kidney disease. ***Nephrology (Carlton)*** 17(4):311-21.

2. Sud M, Tangri N, Pintilie M, Levey AS, Naimark D(2014) Risk of end-stage renal disease and death after cardiovascular events in chronic kidney disease. ***Circulation*** 130(6):458-65.

3. Abboud H, Henrich WL (2010) Clinical practice. Stage IV chronic kidney disease. ***N Engl J Med*** 362(1):56-65.

4. National Kidney Foundation (2002) K/DOQI clinical practice guidlines for chronic kidney disease: Evaluation, classification, and stratification. Part IV: Definition and classification of stages of chronic kidney disease. ***Am J Kidney Dis*** 39:S46-S75.

5. Go AS, Chertow GM, Fan D, McCulloch CE, Hsu CY (2004) Chronic kidney disease and the risks of death, cardiovascular events, and hospitalization. ***N Engl J Med*** 351(13):1296-305.

6. Oberg BP, McMenamin E, Lucas FL, McMonagle E, Morrow J, Ikizler TA, Himmelfarb J (2004) Increased prevalence of oxidant stress and inflammation in patients with moderate to severe chronic kidney disease. ***Kidney Int*** 65(3):1009-16.

7. Keith DS, Nichols GA, Gullion CM, Brown JB, Smith DH (2004) Longitudinal follow-up and outcomes among a population with chronic kidney disease in a large managed care organization. ***Arch Intern Med*** 164(6):659-63.

8. Percy CJ, Brown L, Power DA, Johnson DW, Gobe GC (2009) Obesity and hypertension have differing oxidant handling molecular pathways in age-related chronic kidney disease. ***Mech Ageing Dev*** 130(3):129-38.

9. Chadban SJ, Briganti EM, Kerr PG, Dunstan DW, Welborn TA, Zimmet PZ, Atkins RC (2003) Prevalence of kidney damage in Australian adults: The Aus Diab kidney study. ***J Am Soc Nephrol*** 7(2):S131-8.

10. Wijetunge S, Ratnatunga NV, Abeysekera DT, Wazil AW, Selvarajah M, Ratnatunga CN (2013) Retrospective analysis of renal histology in asymptomatic patients with probable chronic kidney disease of unknown aetiology in Sri Lanka. ***Ceylon Med J*** 58(4):142-7.

11. Campanholle G, Ligresti G, Gharib SA, Duffield JS (2013) Cellular mechanisms of tissue fibrosis. 3. Novel mechanisms of kidney fibrosis. ***Am J Physiol Cell Physiol***304(7):C591-603.

12. Small DM, Bennett NC, Roy S, Gabrielli BG, Johnson DW, Gobe GC (2012) Oxidative stress and cell senescence combine to cause maximal renal tubular

epithelial cell dysfunction and loss in an *in vitro* model of kidney disease. ***Nephron Exp Nephrol*** 122(3-4):123-30.

13. Ozbek E (2012) Induction of Oxidative Stress in Kidney. ***Int J Nephrol*** 2012:1-9.

14. Corda S, Laplace C, Vicaut E, Duranteau J (2001) Rapid reactive oxygen species production by mitochondria in endothelial cells exposed to tumor necrosis factor-alpha is mediated by ceramide. ***Am J Resp Cell Mol Biol*** 24(6):762-8.

15. Haynes CM, Titus EA, Cooper AA (2004) Degradation of misfolded proteins prevents ER-derived oxidative stress and cell death. ***Mol Cell*** 15(5):767-76.

16. He YY, Hader DP (2002) UV-B-induced formation of reactive oxygen species and oxidative damage of the *Cyanobacterium anabaena sp*.: protective effects of ascorbic acid and N-acetyl-L-cysteine. ***J Photochem Photobiol*** 66(2):115-24.

17. Gomez-Mendikute A, Cajaraville MP (2003) Comparative effects of cadmium, copper, paraquat and benzo[a]pyrene on the actin cytoskeleton and production of reactive oxygen species (ROS) in mussel haemocytes. ***Toxicol in Vitro*** 17(5-6):539-46.

18. Sundaresan M, Yu ZX, Ferrans VJ, Irani K, Finkel T (1995) Requirement for generation of $H_2O_2$ for platelet-derived growth factor signal transduction. ***Science*** 270 (5234):296-9.

19. Kanda M, Ihara Y, Murata H, Urata Y, Kono T, Yodoi J, Seto S, Yano K, Kondo T(2006) Glutaredoxin modulates platelet derived growth factor-dependent cell signaling by regulating the redox status of low molecular weight protein-tyrosine phosphatase. ***J Biol Chem*** 281(39):28518-28.

20. Jensen SJK (2003) Oxidative stress and free radicals. ***J Mol Structure: THEOCHEM*** 666-667: 387-92.

21. Yousefipour Z, Oyekan A, Newaz M (2010) Interaction of oxidative stress, nitric oxide and peroxisome proliferator activated receptor gamma in acute renal failure. ***Pharmacol Ther*** 125(3):436-45.

22. Shah SV, Baliga R, Rajapurkar M, Fonseca VA (2007) Oxidants in chronic kidney disease. ***J Am Soc Nephrol*** 18(1):16-28.

23. Vaziri ND (2004) Roles of oxidative stress and antioxidant therapy in chronic kidney disease and hypertension. ***Curr Opin Nephrol Hypertens*** 13(1):93-9.

24. Himmelfarb J, Hakim RM (2003) Oxidative stress in uremia. ***Curr Opin Nephrol Hypertens*** 12(6):593-8.

25. Himmelfarb J, Stenvinkel P, Ikizler TA, Hakim RM (2002) The elephant in uremia: oxidant stress as a unifying concept of cardiovascular disease in uremia. ***Kidney Int*** 62(5):1524-38.

26. Anzalone R, La Rocca G, Di Stefano A, Magno F, Corrao S, Carbone M, Loria T, Lo Iacono M, Eleuteri E, Colombo M, Cappello F, Farina F, Zummo G, Giannuzzi P (2009) Role of endothelial cell stress in the pathogenesis of chronic heart failure. ***Front Biosci (Landmark Ed)*** 14:2238-47.

27. Zheng L, Kern TS (2009) Role of nitric oxide, superoxide, peroxynitrite and PARP in diabetic retinopathy. ***Front Biosci (Landmark Ed)*** 14:3974-87.

28. Xiao H, Li Y, Qi J, Wang H, Liu K (2009) Peroxynitrite plays a key role in glomerular lesions in diabetic rats. ***J Nephrol*** 22(6):800-8.

29. Wakamatsu TH, Dogru M, Tsubota K (2008) Tearful relations: oxidative stress, inflammation and eye diseases. ***Arq Bras Oftalmol*** 71(6):72-9.

30. Bondi CD, Manickam N, Lee DY, Block K, Gorin Y, Abboud HE, Barnes JL (2010) NAD(P)H oxidase mediates TGF-beta1-induced activation of kidney myofibroblasts. ***J Am Soc Nephrol*** 21(1):93-102.

31. Gorin Y, Block K, Hernandez J, Bhandari B, Wagner B, Barnes JL, Abboud HE (2005) Nox4 NAD(P)H oxidase mediates hypertrophy and fibronectin expression in the diabetic kidney. ***J Biol Chem*** 280(47):39616-26.

32. Lassègue B, Clempus RE (2003) Vascular NAD(P)H oxidases: specific features, expression, and regulation. ***Am J Physiol Regul Integr Comp Physiol*** 285(2):R277-97.

33. Haurani MJ, Pagano PJ (2007) Adventitial fibroblast reactive oxygen species as autacrine and paracrine mediators of remodeling: bellwether for vascular disease? ***Cardiovasc Res*** 75(4):679-89.

34. Sachse A, Wolf G (2007) Angiotensin II-induced reactive oxygen species and the kidney. ***J Am Soc Nephrol*** 18(9):2439-46.

35. Bandy B, Davison AJ (1990) Mitochondrial mutations may increase oxidative stress: implications for carcinogenesis and aging? ***Free Radic Biol Med*** 8(6):523-39.

36. Beckman KB, Ames BN (1998) The free radical theory of aging matures. ***Physiol Rev*** 78(2):547-81.

37. Haugen E, Nath KA (1999) The involvement of oxidative stress in the progression of renal injury. ***Blood Purif*** 17(2-3):58-65.

38. Cottone S, Lorito MC, Riccobene R, Nardi E, Mulè G, Buscemi S, Geraci C, Guarneri M, Arsena R, Cerasola G(2008) Oxidative stress, inflammation and cardiovascular disease in chronic renal failure. ***J Nephrol*** 21(2):175-9.

39. Barrera-Chimal J, Pérez-Villalva R, Rodríguez-Romo R, Reyna J, Uribe N, Gamba G, Bobadilla NA (2013) Spironolactone prevents chronic kidney disease caused by ischemic acute kidney injury. ***Kidney Int*** 83(1):93-103.

40. Schleicher E, Friess U (2007) Oxidative stress, AGE, and atherosclerosis. ***Kidney Int Suppl*** 106:S17-26.

41. Geiszt M, Leto TL (2004) The Nox family of NAD(P)H oxidases: host defense and beyond. ***J Biol Chem*** 279(50):51715-8.

42. Liu RM, Liu Y, Forman HJ, Olman M, Tarpey MM (2004) Glutathione regulates transforming growth factor-beta-stimulated collagen production in fibroblasts. ***Am J Physiol Lung Cell Mol Physiol*** 286(1):L121-8.

43. Salahudeen AK (1995) Role of lipid peroxidation in $H_2O_2$-induced renal epithelial (LLC-PK1) cell injury. ***Am J Physiol*** 268(1 Pt 2):F30-8.

44. Sheridan AM, Fitzpatrick S, Wang C, Wheeler DC, Lieberthal W (1996) Lipid peroxidation contributes to hydrogen peroxide induced cytotoxicity in renal epithelial cells. ***Kidney Int*** 49(1):88-93.

45. Veal EA, Day AM, Morgan BA (2007) Hydrogen peroxide sensing and signaling. ***Mol Cell*** 26(1):1-14.

46. Giacchetti G, Opocher G, Sarzani R, Rappelli A, Mantero F (1996) Angiotensin II and the adrenal. ***Clin Exp Pharmacol PhysiolSuppl*** 3:S119-24.

47. Nakayama T, Izumi Y, Soma M, Kanmatsuse K (1998) Adrenal renin-angiotensin-aldosterone system in streptozotocin-diabetic rats. ***Horm Metab Res*** 30(1):12-5.

48. Suzuki Y, Ruiz-Ortega M, Lorenzo O, Ruperez M, Esteban V, Egido J (2003) Inflammation and angiotensin II. ***Int J Biochem Cell Biol*** 35(6):881-900.

49. Xia Y, Jin X, Yan J, Entman ML, Wang Y (2014) CXCR6 plays a critical role in angiotensin II-induced renal injury and fibrosis. ***Arterioscler Thromb Vasc Biol*** 34(7):1422-8.

50. Zhong J, Guo D, Chen CB, Wang W, Schuster M, Loibner H, Penninger JM, Scholey JW, Kassiri Z, Oudit GY (2011) Prevention of angiotensin II-mediated renal oxidative stress, inflammation, and fibrosis by angiotensin-converting enzyme 2. ***Hypertension*** 57(2):314-22.

51. Wolf G (2008) Novel aspects of the renin-angiotensin-aldosterone-system. ***Front Biosci*** 13:4993-5005.

52. Wolf G, Butzmann U, Wenzel UO (2003) The renin-angiotensin system and progression of renal disease: from hemodynamics to cell biology. ***Nephron Physiol*** 93(1):P3-13.

53. Mezzano SA, Ruiz-Ortega M, Egido J (2001) Angiotensin II and renal fibrosis. ***Hypertension*** 38(3 Pt 2):635-8.

54. Macconi D (2010) Targeting the renin angiotensin system for remission/regression of chronic kidney disease. ***Histol Histopathol*** 25(5):655-68.

55. Wolf G (1998) Link between angiotensin II and TGF-beta in the kidney. ***Miner Electrolyte Metab*** 24(2-3):174-80.

56. Nie J, Hou FF (2012) Role of reactive oxygen species in the renal fibrosis. ***Chin Med J (Engl)*** 125(14):2598-602.

57. Kim SM, Kim YG, Jeong KH, Lee SH, Lee TW, Ihm CG, Moon JY (2012) Angiotensin II-induced mitochondrial Nox4 is a major endogenous source of oxidative stress in kidney tubular cells. ***PLoS One*** 7(7):e39739.

58. Palm F, Nordquist L (2011) Renal oxidative stress, oxygenation, and hypertension. ***Am J Physiol Regul Integr Comp Physiol*** 301(5):R1229-41.

59. Gill PS, Wilcox CS (2006) NADPH oxidases in the kidney. ***Antioxid Redox Signal*** 8(9-10):1597-607.

60. Mori T, Cowley AW Jr, Ito S (2006) Molecular mechanisms and therapeutic strategies of chronic renal injury: physiological role of angiotensin II-induced oxidative stress in renal medulla. ***J Pharmacol Sci*** 100(1):2-8.

61. Akishita M, Nagai K, Xi H, Yu W, Sudoh N, Watanabe T, Ohara-Imaizumi M, Nagamatsu S, Kozaki K, Horiuchi M, Toba K (2005) Renin-angiotensin system modulates oxidative stress-induced endothelial cell apoptosis in rats. ***Hypertension*** 45(6):1188-93.

62. Klahr S, Morrissey JJ (2000) The role of vasoactive compounds, growth factors and cytokines in the progression of renal disease. ***Kidney Int Suppl*** 75:S7-14.

63. Schmitz U, Berk BC (1997) Angiotensin II signal transduction: Stimulation of multiple mitogen-activated protein kinase pathways. ***Trends Endocrinol Metab*** 8(7):261-6.

64. de Queiroz TM, Monteiro MM, Braga VA (2013) Angiotensin-II-derived reactive oxygen species on baroreflex sensitivity during hypertension: new perspectives. ***Front Physiol*** 4:105.

65. Brasier AR, Li J (1996) Mechanisms for inducible control of angiotensinogen gene transcription. ***Hypertension*** 27(3 Pt 2):465-75.

66. Li J, Brasier AR (1996) Angiotensinogen gene activation by angiotensin II is mediated by the rel A (nuclear factor-kappaB p65) transcription factor: one mechanism for the renin angiotensin system positive feedback loop in hepatocytes. ***Mol Endocrinol*** 10(3):252-64.

67. Brasier AR, Li J, Wimbish KA (1996) Tumor necrosis factor activates angiotensinogen gene expression by the Rel A transactivator. ***Hypertension*** 27(4):1009-17.

68. Morrissey JJ, Klahr S (1997) Rapid communication. Enalapril decreases nuclear factor kappa B activation in the kidney with ureteral obstruction. ***Kidney Int*** 52(4):926-33.

69. Klahr S, Morrissey J (1998) Angiotensin II and gene expression in the kidney. ***Am J Kidney Dis*** 31:171-6.

70. Egido J, Gómez-Chiarri M, Ortíz A, Bustos C, Alonso J, Gómez-Guerrero C, Gómez-Garre D, López-Armada MJ, Plaza J, Gonzalez E (1993) Role of tumor necrosis factor-alpha in the pathogenesis of glomerular diseases. ***Kidney Int Suppl*** 39:S59-64.

71. Baud L, Fouqueray B, Philippe C, Amrani A (1992) Tumor necrosis factor alpha and mesangial cells. ***Kidney Int*** 41(3):600-3.

72. Ortiz A, Bustos C, Alonso J, Alcázar R, López-Armada MJ, Plaza JJ, González E, Egido J (1995) Involvement of tumor necrosis factor-alphain the pathogenesis of experimental and human glomerulonephritis. ***Adv Nephrol Necker Hosp*** 24:53-77.

73. Wolf G, Aberle S, Thaiss F, Nelson PJ, Krensky AM, Neilson EG, Stahl RA (1993) TNF alpha induces expression of the chemo attract antcytokine RANTES in cultured mouse mesangial cells. ***Kidney Int*** 44(4):795-804.

74. Border WA, Ruoslahti E (1992) Transforming growth factor-beta in disease: the dark side of tissue repair. ***J Clin Invest*** 90(1):1-7.

75. Wolf G, Neilson EG (1991) Molecular mechanisms of tubulointerstitial hypertrophy and hyperplasia. ***Kidney Int*** 39(3):401-20.

76. Eddy AA (1996) Molecular insights into renal interstitialfibrosis. ***J Am Soc Nephrol*** 7(12):2495-508.

77. Fogo A, Ichikawa I (1989) Evidence for the central role of glomerular growth promoters in the development of sclerosis. ***Semin Nephrol*** 9(4):329-42.

78. Gongora MC, Qin Z, Laude K, Kim HW, McCann L, Folz JR, Dikalov S, Fukai T, Harrison DG (2006) Role of extracellular superoxide dismutase in hypertension. ***Hypertension*** 48(3):473-81.

79. Sindhu RK, Ehdaie A, Farmand F, Dhaliwal KK, Nguyen T, Zhan CD, Roberts CK, Vaziri ND (2005) Expression of catalase and glutathione peroxidase in renal insufficiency. ***Biochim Biophys Acta*** 1743(1-2):86-92.

80. Paravicini TM, Touyz RM (2008) NADPH oxidases, reactive oxygen species, and hypertension: clinical implications and therapeutic possibilities. ***Diabetes Care*** 31(2):S170-80.

81. Finkel T, Holbrook NJ (2000) Oxidants, oxidative stress and the biology of ageing. ***Nature*** 408(6809):239-47.

82. Wood ZA, Schröder E, Robin Harris J, Poole LB (2003) Structure, mechanism and regulation of peroxiredoxins. ***Trends Biochem Sci*** 28(1):32-40.

83. Finkel T (2003) Oxidant signals and oxidative stress. ***Curr Opin Cell Biol*** 15(2):247-54.

84. Abdullah R, Basak I, Patil KS, Alves G, Larsen JP, Møller SG (2014) Parkinson's disease and age: The obvious but largely unexplored link. ***Exp Gerontol*** [Epub ahead of print].

85. Yang X, Xu Y (2014) Mutations in the ATP13A2 gene and Parkinsonism: a preliminary review. ***Biomed Res Int*** [Epub ahead of print].

86. Abdel-Salam OE (2014) The Paths to Neurodegeneration in Genetic Parkinson's Disease. ***CNS Neurol Disord Drug Targets*** [Epub ahead of print].

87. Bonifati V, Rizzu P, van Baren MJ, Schaap O, Breedveld GJ, Krieger E, Dekker MC, Squitieri F, Ibanez P, Joosse M, van Dongen JW, Vanacore N, van Swieten JC, Brice A, Meco G, van Duijn CM, Oostra BA, Heutink P (2003) Mutations in the DJ-1 gene associated with autosomal recessive early-onset parkinsonism. ***Science*** 299(5604):256-9.

88. Olzmann JA, Brown K, Wilkinson KD, Rees HD, Huai Q, Ke H, Levey AI, Li L, Chin LS (2004) Familial Parkinson's disease-associated L166P mutation disrupts DJ-1 protein folding and function. ***J Biol Chem*** 279(9):8506-15.

89. Monroy-Jaramillo N, Guerrero-Camacho JL, Rodríguez-Violante M, Boll-Woehrlen MC, Yescas-Gómez P, Alonso-Vilatela ME, López-López M (2014) Genetic mutations in early-onset Parkinson's disease Mexican patients: molecular testing implications. ***Am J Med Genet B Neuropsychiatr Genet*** 165B(3):235-44.

90. Koziorowski D, Hoffman-Zacharska D, Sławek J, Jamrozik Z, Janik P, Potulska-Chromik A, Roszmann A, Tataj R, Bal J, Friedman A (2013) Incidence of mutations in the PARK2, PINK1, PARK7 genes in Polish early-onset Parkinson disease patients. ***Neurol Neurochir Pol*** 47(4):319-24.

91. Lai HJ, Lin CH, Wu RM (2012) Early-onset autosomal-recessive parkinsonian-pyramidal syndrome. ***Acta Neurol Taiwan*** 21(3):99-107.

92. Martin I, Dawson VL, Dawson TM (2011) Recent advances in the genetics of Parkinson's disease. ***Annu Rev Genomics Hum Genet*** 12:301-25.

93. Malgieri G, Eliezer D (2008) Structural effects of Parkinson's disease linked DJ-1 mutations. ***Protein Sci*** 17(5):855-68.

94. Healy DG, Abou-Sleiman PM, Valente EM, Gilks WP, Bhatia K, Quinn N, Lees AJ, Wood NW (2004) DJ-1 mutations in Parkinson's disease. ***J Neurol Neurosurg Psychiatry*** 75(1):144-5.

95. Chakraborty S, Bornhorst J, Nguyen TT, Aschner M (2013) Oxidative stress mechanisms underlying Parkinson's disease-associated neurodegeneration in *C. elegans*. ***Int J Mol Sci*** 14(11):23103-28.

96. Dias V, Junn E, Mouradian MM (2013) The role of oxidative stress in Parkinson's disease. ***J Parkinsons Dis*** 3(4):461-91.

97. Ariga H, Takahashi-Niki K, Kato I, Maita H, Niki T, Iguchi-Ariga SM (2013) Neuroprotective function of DJ-1 in Parkinson's disease. ***Oxid Med Cell Longev*** 2013:683920.

98. Janda E, Isidoro C, Carresi C, Mollace V (2012) Defective autophagy in Parkinson's disease: role of oxidative stress. ***Mol Neurobiol*** 46(3):639-61.

99. Lin TK, Liou CW, Chen SD, Chuang YC, Tiao MM, Wang PW, Chen JB, Chuang JH (2009) Mitochondrial dysfunction and biogenesis in the pathogenesis of Parkinson's disease. ***Chang Gung Med J*** 32(6):589-99.

100. Tao X, Tong L (2003) Crystal structure of human DJ-1, a protein associated with early onset Parkinson's disease. ***J Biol Chem*** 278(33):31372-9.

101. Blackinton J, Lakshminarasimhan M, Thomas KJ, Ahmad R, Greggio E, Raza AS, Cookson MR, Wilson MA (2009) Formation of a stabilized cysteine sulfinic acid is critical for the mitochondrial function of the parkinsonism protein DJ-1. ***J Biol Chem*** 284(10):6476-85.

102. Clements CM, McNally RS, Conti BJ, Mak TW, Ting JP (2006) DJ-1, a cancer- and Parkinson's disease-associated protein, stabilizes the antioxidant transcriptional master regulator Nrf2. ***Proc Natl Acad Sci USA*** 103(41):15091-6.

103. Nagakubo D, Taira T, Kitaura H, Ikeda M, Tamai K, Iguchi-Ariga SM, Ariga H (1997) DJ-1, a novel oncogene which transforms mouse NIH3T3 cells in cooperation with ras. ***Biochem Biophys Res Commun*** 231(2):509-13.

104. Kotaja N, Karvonen U, Jänne OA, Palvimo JJ (2002) PIAS proteins modulate transcription factors by functioning as SUMO-1 ligases. ***Mol Cell Biol*** 22(14):5222-34.

105. Jeong H, Kim MS, Kwon J, Kim KS, Seol W (2006) Regulation of the transcriptional activity of the tyrosine hydroxylase gene by androgen receptor. ***Neurosci Lett*** 396(1):57-61.

106. Taira T, Iguchi-Ariga SM, Ariga H (2004) Co-localization with DJ-1 is essential for the androgen receptor to exert its transcription activity that has been impaired by androgen antagonists. ***Biol Pharm Bull*** 27(4):574-7.

107. Honbou K, Suzuki NN, Horiuchi M, Niki T, Taira T, Ariga H, Inagaki F (2003) The crystal structure of DJ-1, a protein related to male fertility and Parkinson's disease. ***J Biol Chem*** 278(33):31380-4.

108. Honbou K, Suzuki NN, Horiuchi M, Taira T, Niki T, Ariga H, Inagaki F (2003) Crystallization and preliminary crystallographic analysis of DJ-1, a protein associated with male fertility and parkinsonism. ***Acta Crystallogr D Biol Crystallogr*** 59(8):1502-3.

109. Shendelman S, Jonason A, Martinat C, Leete T, Abeliovich A (2004) DJ-1 is a redox dependent molecular chaperone that inhibits alpha-synuclein aggregate formation. ***PLoS Biol*** 2(11):e362.

110. Zhou W, Zhu M, Wilson MA, Petsko GA, Fink AL (2006) The oxidation state of DJ-1regulates its chaperone activity toward alpha-synuclein. ***J Mol Biol*** 356(4):1036-48.

111. Koide-Yoshida S, Niki T, Ueda M, Himeno S, Taira T, Iguchi-Ariga SM, Ando Y, Ariga H (2007) DJ-1 degrades transthyretin and an inactive form of DJ-1 is secreted in familial amyloidotic polyneuropathy. ***Int J Mol Med*** 19(6):885-93.

112. Büeler H (2009) Impaired mitochondrial dynamics and function in the pathogenesis of Parkinson's disease. ***Exp Neurol*** 218(2):235-46.

113. Junn E, Jang WH, Zhao X, Jeong BS, Mouradian MM (2009) Mitochondrial localization of DJ-1 leads to enhanced neuroprotection. ***J Neurosci Res*** 87(1):123-9.

114. Trancikova A, Tsika E, Moore DJ (2012) Mitochondrial dysfunction in genetic animal models of Parkinson's disease. ***Antioxid Redox Signal*** 16(9):896-919.

115. Krebiehl G, Ruckerbauer S, Burbulla LF, Kieper N, Maurer B, Waak J, Wolburg H, Gizatullina Z, Gellerich FN, Woitalla D, Riess O, Kahle PJ, Proikas-Cezanne T, Krüger R (2010) Reduced basal autophagy and impaired mitochondrial dynamics due to loss of Parkinson's disease-associated protein DJ-1. ***PLoS One*** 5(2):e9367.

116. Goldberg MS, Pisani A, Haburcak M, Vortherms TA, Kitada T, Costa C, Tong Y, Martella G, Tscherter A, Martins A, Bernardi G, Roth BL, Pothos EN, Calabresi P, Shen J (2005) Nigrostriatal dopaminergic deficits and hypokinesia caused by inactivation of the familial Parkinsonism-linked gene DJ-1. ***Neuron*** 45(4):489-96.

117. Sekito A, Koide-Yoshida S, Niki T, Taira T, Iguchi-Ariga SM, Ariga H (2006) DJ-1 interacts with HIPK1 and affects $H_2O_2$-induced cell death. ***Free Radic Res*** 40(2):155-65.

118. Junn E, Taniguchi H, Jeong BS, Zhao X, Ichijo H, Mouradian MM (2005) Interaction of DJ-1 with Daxx inhibits apoptosis signal-regulating kinase 1 activity and cell death. ***Proc Natl Acad Sci USA*** 102(27):9691-6.

119. Zhou W, Freed CR (2005) DJ-1 up-regulates glutathione synthesis during oxidative stress and inhibits A53T alpha-synuclein toxicity. ***J Biol Chem*** 280(52):43150-8.

120. Batelli S, Albani D, Rametta R, Polito L, Prato F, Pesaresi M, Negro A, Forloni G (2008) DJ-1 modulates alpha-synuclein aggregation state in a cellular model of oxidative stress: relevance for Parkinson's disease and involvement of HSP70. ***PLoS One*** 3(4):e1884.

121. Taira T, Saito Y, Niki T, Iguchi-Ariga SM, Takahashi K, Ariga H (2004) DJ-1 has a role in antioxidative stress to prevent cell death. ***EMBO Rep*** 5(2):213-8.

122. Kahle PJ, Waak J, Gasser T (2009) DJ-1 and prevention of oxidative stress in Parkinson's disease and other age-related disorders. ***Free Radic Biol Med*** 47(10):1354-61.

123. Yanagida T, Kitamura Y, Yamane K, Takahashi K, Takata K, Yanagisawa D, Yasui H, Taniguchi T, Taira T, Honda T, Ariga H (2009) Protection against oxidative stress-induced neurodegeneration by a modulator for DJ-1, the wild-type of familial Parkinson's disease-linked PARK7. ***J Pharmacol Sci*** 109(3):463-8.

124. Lev N, Ickowicz D, Melamed E, Offen D (2008) Oxidative insults induce DJ-1upregulation and redistribution: implications for neuroprotection. ***Neurotoxicology*** 29(3):397-405.

125. Duan X, Kelsen SG, Merali S (2008) Proteomic analysis of oxidative stress-responsive proteins in human pneumocytes: insight into the regulation of DJ-1 expression. ***J Proteome Res*** 7(11):4955-61.

126. Wilson MA (2011) The role of cysteine oxidation in DJ-1 function and dysfunction. ***Antioxid Redox Signal*** 15(1):111-22.

127. Baulac S, Lu H, Strahle J, Yang T, Goldberg MS, Shen J, Schlossmacher MG, Lemere CA, Lu Q, Xia W (2009) Increased DJ-1 expression under oxidative stress and in Alzheimer's disease brains. ***Mol Neurodegener*** 4:12.

128. Eltoweissy M, Müller GA, Bibi A, Nguye PV, Dihazi GH, Müller CA, Dihazi H (2011) Proteomics analysis identifies PARK7 as an important player for renal cell resistance and survival under oxidative stress. ***Mol Biosyst*** 7(4):1277-88.

129. Canet-Avilés RM, Wilson MA, Miller DW, Ahmad R, McLendon C, Bandyopadhyay S, Baptista MJ, Ringe D, Petsko GA, Cookson MR (2004) The Parkinson's disease protein DJ-1 is neuroprotective due to cysteine-sulfinic acid-driven mitochondrial localization. ***Proc Natl Acad Sci USA*** 101(24):9103-8.

130. Parsanejad M, Bourquard N, Qu D, Zhang Y, Huang E, Rousseaux MW, Aleyasin H, Irrcher I, Callaghan S, Vaillant DC, Kim RH, Slack RS, Mak TW, Reddy ST, Figeys D, Park DS (2014) DJ-1 Interacts with and Regulates Paraoxonase-2, an Enzyme Critical for Neuronal Survival in Response to Oxidative Stress. ***PLoS One*** 9(9):e106601.

131. Lavara-Culebras E, Paricio N (2007) Drosophila DJ-1 mutants are sensitive to oxidative stress and show reduced lifespan and motor deficits. ***Gene*** 400(1-2):158-65.

132. Park J, Kim SY, Cha GH, Lee SB, Kim S, Chung J (2005) Drosophila DJ-1mutants show oxidative stress-sensitive locomotive dysfunction. ***Gene*** 361:133-9.

133. Aleyasin H, Rousseaux MW, Phillips M, Kim RH, Bland RJ, Callaghan S, Slack RS, During MJ, Mak TW, Park DS (2007) The Parkinson's disease gene DJ-1 is also a key regulator of stroke-induced damage. ***Proc Natl Acad Sci USA*** 104(47):18748-53.

134. Aleyasin H, Rousseaux MW, Marcogliese PC, Hewitt SJ, Irrcher I, Joselin AP, Parsanejad M, Kim RH, Rizzu P, Callaghan SM, Slack RS, Mak TW, Park DS

(2010) DJ-1 protects the nigrostriatal axis from the neurotoxin MPTP by modulation of the AKT pathway. ***Proc Natl Acad Sci USA*** 107(7):3186-91.

135. Mitsumoto A, Nakagawa Y, Takeuchi A, Okawa K, Iwamatsu A, Takanezawa Y (2001) Oxidized forms of peroxiredoxins and DJ-1 on two-dimensional gels increased in response to sublethal levels of paraquat. ***Free Radic Res*** 35(3):301-10.

136. Mitsumoto A, Nakagawa Y (2001) DJ-1 is an indicator for endogenous reactive oxygen species elicited by endotoxin. ***Free Radic Res*** 35(6):885-93.

137. Woo HA, Chae HZ, Hwang SC, Yang KS, Kang SW, Kim K, Rhee SG (2003) Reversing the inactivation of peroxiredoxins caused by cysteine sulfinic acid formation. ***Science*** 300(5619):653-6.

138. Woo HA, Kang SW, Kim HK, Yang KS, Chae HZ, Rhee SG (2003) Reversible oxidation of the active site cysteine of peroxiredoxins to cysteine sulfinic acid. Immunoblot detection with antibodies specific for the hyper oxidized cysteine-containing sequence. ***J Biol Chem*** 278(48):47361-4.

139. Chevallet M, Wagner E, Luche S, van Dorsselaer A, Leize-Wagner E, Rabilloud T (2003) Regeneration of peroxiredoxins during recovery after oxidative stress: only some overoxidized peroxiredoxins can be reduced during recovery after oxidative stress. ***J Biol Chem*** 278(39):37146-53.

140. Biteau B, Labarre J, Toledano MB (2003) ATP-dependent reduction of cysteine-sulphinic acid by *S. cerevisiae* sulphiredoxin. ***Nature*** 425(6961):980-4.

141. Waak J, Weber SS, Görner K, Schall C, Ichijo H, Stehle T, Kahle PJ (2009) Oxidizable residues mediating protein stability and cytoprotective interaction of DJ-1 with apoptosis signal-regulating kinase 1. ***J Biol Chem*** 284(21):14245-57.

142. Hulleman JD, Mirzaei H, Guigard E, Taylor KL, Ray SS, Kay CM, Regnier FE, Rochet JC (2007) Destabilization of DJ-1 by familial substitution and oxidative modifications: implications for Parkinson's disease. ***Biochem*** 46(19):5776-89.

143. Huai Q, SunY, Wang H, Chin LS, Li L, Robinson H, Ke H (2003) Crystal structure of DJ-1/RS and implication on familial Parkinson's disease. ***FEBS Lett*** 549(1-3):171-5.

144. Lee SJ, Kim SJ, Kim IK, Ko J, Jeong CS, Kim GH, Park C, Kang SO, Suh PG, Lee HS, Cha SS (2003) Crystal structures of human DJ-1 and *Escherichia coli* Hsp31, which share an evolutionarily conserved domain. ***J Biol Chem*** 278(45):44552-9.

145. Lin J, Prahlad J, Wilson MA (2012) Conservation of oxidative protein stabilization in an insect homologue of parkinsonism-associated protein DJ-1. ***Biochem*** 51(18):3799-807.

146. Madian AG, Hindupur J, Hulleman JD, Diaz-Maldonado N, Mishra VR, Guigard E, Kay CM, Rochet JC, Regnier FE (2012) Effect of single amino acid substitution on oxidative modifications of the Parkinson's disease-related protein, DJ-1. ***Mol Cell Proteomics*** 11(2):1-15.

147. Prahlad J, Hauser DN, Milkovic NM, Cookson MR, Wilson MA (2014) Use of cysteine-reactive cross-linkers to probe conformational flexibility of human DJ-1 demonstrates that Glu18 mutations are dimers. ***J Neurochem*** 130(6):839-53.

148. Kinumi T, Kimata J, Taira T, Ariga H, Niki E (2004) Cysteine-106 of DJ-1 is the most sensitive cysteine residue to hydrogen peroxide-mediated oxidation *in vivo* in human umbilical vein endothelial cells. ***Biochem Biophys Res Commun*** 317(3):722-8.

149. Lucas JI, Marín I (2007) A new evolutionary paradigm for the Parkinson disease gene DJ-1. ***Mol Biol Evol*** 24(2):551-61.

150. Bandyopadhyay S, Cookson MR (2004) Evolutionary and functional relationships within the DJ1superfamily. ***BMC Evol Biol*** 4:6.

151. Andres-Mateos E, Perier C, Zhang L, Blanchard-Fillion B, Greco TM, Thomas B, Ko HS, Sasaki M, Ischiropoulos H, Przedborski S, Dawson TM, Dawson VL (2007) DJ-1 gene deletion reveals that DJ-1 is an atypical peroxiredoxin-like peroxidase. ***Proc Natl Acad Sci USA*** 104(37):14807-12.

152. Im JY, Lee KW, Junn E, Mouradian MM (2010) DJ-1 protects against oxidative damage by regulating the thioredoxin/ASK1complex. ***Neurosci Res*** 67(3):203-8.

153. Kim YC, Kitaura H, Taira T, Iguchi-Ariga SM, Ariga H (2009) Oxidation of DJ-1-dependent cell transformation through direct binding of DJ-1 to PTEN. ***Int J Oncol*** 35(6):1331-41.

154. Meulener MC, Xu K, Thomson L, Ischiropoulos H, Bonini NM (2006) Mutational analysis of DJ-1 in Drosophila implicates functional inactivation by oxidative damage and aging. ***Proc Natl Acad Sci USA*** 103(33):12517-22.

155. Takahashi-Niki K, Niki T, Taira T, Iguchi-Ariga SM, Ariga H (2004) Reduced anti-oxidative stress activities of DJ-1mutants found in Parkinson's disease patients. ***Biochem Biophys Res Commun*** 320(2):389-97.

156. Witt AC, Lakshminarasimhan M, Remington BC, Hasim S, Pozharski E, Wilson MA (2008) Cysteine p*Ka* depression by a protonated glutamic acid in human DJ-1. ***Biochem*** 47(28):7430-40.

157. Harris RC, Neilson EG (2006) Toward a unified theory of renal progression. ***Annu Rev Med*** 57:365-80.

158. Striker GE, Schainuck LI, Cutler RE, Benditt EP (1970) Structural-functional correlations in renal disease. I. A method for assaying and classifying histopathologic changes in renal disease. ***Hum Pathol*** 1(4):615-30.

159. Nath KA (1992) Tubulointersitial changes as a major determinant in the progression of renal damage. ***Am J Kidney Dis*** 20(1):1-17.

160. Mackensen-Haen S, Bader R, Grund KE, Bohle A (1981) Correlations between renal cortical interstitial fibrosis, atrophy of the proximal tubules and impairment of the glomerular filtration rate. ***Clin Nephrol*** 15(4):167-71.

161. Shimizu H, Maruyama S, Yuzawa Y, Kato T, Miki Y, Suzuki S, Sato W, Morita Y, Maruyama H, Egashira K, Matsuo S (2003) Anti-monocyte chemoattractant protein-1 gene therapy attenuates renal injury induced by protein-overload proteinuria. ***J Am Soc Nephrol*** 14(6):1496-505.

162. Chuang PY, Menon MC, He JC (2013) Molecular targets for treatment of kidney fibrosis. ***J Mol Med*** 91(5):549-59.

163. Zeisberg M, Duffield JS (2010) Resolved: EMT produces fibroblasts in the kidney. ***J Am Soc Nephrol*** 21(8):1247-53.

164. Strutz F, Mueller GA (2001) Mechanisms of renal fibrogenesis. In: Neilson EG, Couser WG (eds). Immunologic renal diseases, 2nd edn. Lippincott Williams & Wilkins. Philadelphia, pp 73-101.

165. Paravicini TM, Touyz RM (2006) Redox signaling in hypertension. ***Cardiovas Res*** 71(2):247-58.

166. Basile DP (2004) Rarefaction of peritubular capillaries following ischemic acute renal failure: a potential factor predisposing progressive nephropathy. ***Curr Opin Nephrol Hypertens*** 13(1):1-7.

167. Griendling KK, Sorescu D, Ushio-Fukai M (2000) NAD(P)H oxidase: role in cardiovascular biology and disease. ***Circ Res*** 86(5):494-501.

168. Rajagopalan S, Kurz S, Muenzel T, Tarpey M, Freeman BA, Griendling KK, Harrison DG (1996) Angiotensin II-mediated hypertension in the rat increases vascular superoxide production via membrane NADH/NADPH oxidase activation. Contribution to alterations of vasomotor tone. ***J Clin Invest*** 97(8):1916-23.

169. Zafari AM, Ushio-Fukai M, Akers M, Yin Q, Shah A, Harrison DG, Taylor WR, Griendling KK (1998) Role of NADH/NADPH oxidase-derived $H_2O_2$ in angiotensin II-induced vascular hypertrophy. ***Hypertension*** 32(3):488-95.

170. Hattori Y, Akimoto K, Gross SS, Hattori S, Kasai K (2005) Angiotensin II-induced oxidative stress elicites hypoadiponectinaemia in rates. ***Diabetologia*** 48(6):1066-74.

171. Zhang L, Ma Y, Zhang J, Cheng J, Du J (2005) A new cellular signaling mechanism for angiotensin II activation of NF-kappaB: an IkappaB-independent, RSK-mediated phosphorylation of p65. ***Arterioscler Thromb Vasc Biol*** 25(6):1148-53.

172. Barnes JL, Gorin Y (2011) Myofibroblast differentiation during fibrosis: role of NAD(P)H oxidases. ***Kidney Int*** 79(9):944-56.

173. Hod Y, Pentyala SN, Whyard TC, El-Maghrabi MR (1999) Identification and characterization of a novel protein that regulates RNA-protein interaction. ***J Cell Biochem*** 72(3):435-44.

174. Takahashi K, Taira T, Niki T, Seino C, Iguchi-Ariga SM, Ariga H (2001) DJ-1 positively regulates the androgen receptor by impairing the binding of PIASx alpha to the receptor. ***J Biol Chem*** 276(40):37556-63.

175. Niki T, Takahashi-Niki K, Taira T, Iguchi-Ariga SM, Ariga H (2003) DJBP: a novel DJ-1-binding protein, negatively regulates the androgen receptor by recruiting histone deacetylase complex, and DJ-1 antagonizes this inhibition by abrogation of this complex. ***Mol Cancer Res*** 1(4):247-61.

176. Bonifati V, Oostra BA, Heutink P (2004) Linking DJ-1 to neurodegeneration offers novel insights for understanding the pathogenesis of Parkinson's disease. ***J Mol Med*** 82(3):163-74.

177. Mueller GA, Frank J, Rodemann HP, Engler-Blum G (1995) Human renal fibroblast cell lines (tFKIF and tNKF) are new tools to investigate pathophysiologic mechanisms of renal interstitial fibrosis. ***Exp Nephrol*** 3(2):127-33.

178. Ryan MJ, Johnson G, Kirk J, Fuerstenberg SM, Zager RA, Torok-Storb B (1994) HK-2: an immortalized proximal tubule epithelial cell line from normal adult human kidney. ***Kidney Int*** 45(1):48-57.

179. Dihazi H, Dihazi GH, Jahn O, Meyer S, Nolte J, Asif AR, Mueller GA, Engel W (2011) Multipotent adult germline stem cells and embryonic stem cells functional proteomics revealed an important role of eukaryotic initiation factor 5A (Eif5a) in stem cell differentiation. ***J Proteome Res*** 10(4):1962-73.

180. Wessel D, Fluegge UI (1984) A method for the quantitative recovery of protein in dilute solution in the presence of detergents and lipids. ***Anal Biochem*** 138(1):141-3.

181. Bradford MM (1976) A rapid and sensitive method for the quantitation of microgram quantities of protein utilizing the principle of protein-dye binding. ***Anal Biochem*** 72:248-54.

182. Towbin H, Staehelin T, Gordon J (1989) Immunoblotting in the clinical laboratory. ***J Clin Chem Clin Biochem*** 27(8):495-501.

183. Towbin H, Staehelin T, Gordon J (1992) Electrophoretic transfer of proteins from polyacrylamide gels to nitrocellulose sheets: procedure and some applications. 1979. ***Biotechnol*** 24:145-9.

184. Kim RH, Smith PD, Aleyasin H, Hayley S, Mount MP, Pownall S, Wakeham A, You-Ten AJ, Kalia SK, Horne P, Westaway D, Lozano AM, Anisman H, Park DS, Mak TW (2005) Hypersensitivity of DJ-1-deficient mice to 1-methyl-4-phenyl-1,2,3,6-tetrahydropyrindine (MPTP) and oxidative stress. ***Proc Natl Acad Sci USA*** 102(14):5215-20.

185. Tanaka M, Asada M, Higashi AY, Nakamura J, Oguchi A, Tomita M, Yamada S, Asada N, Takase M, Okuda T, Kawachi H, Economides AN, Robertson E, Takahashi S, Sakurai T, Goldschmeding R, Muso E, Fukatsu A, Kita T, Yanagita M (2010) Loss of the BMP antagonist USAG-1 ameliorates disease in a mouse model of the progressive hereditary kidney disease Alport syndrome. ***J Clin Invest*** 120(3):768-77.

186. Lu J, Holmgren A (2014) The thioredoxin antioxidant system. ***Free Radic Biol Med*** 66:75-87.

187. Gerke V, Creutz CE, Moss SE (2005) Annexins: linking $Ca^{2+}$ signalling to membrane dynamics. ***Nat Rev Mol Cell Bio*** 6(6):449-61.

188. Gerke V, Moss S (2002) Annexins: form structure to function. ***Physiol Rev*** 82(2):331-71.

189. Madureira PA, Hill R, Miller VA, Giacomantonio C, Lee PW, Waisman DM (2011) AnnexinA2 is a novel cellular redox regulatory protein involved in tumorigenesis. ***Oncotarget*** 12:1075-93.

190. Santoro MG (2000) Heat shock factors and the control of the stress response. ***Biochem pharmacol*** 59(1):55-63.

191. Doherty GJ, McMahon HT (2008) Mediation, modulation, and consequences of membrane-cytoskeleton interactions. ***Annu Rev Biophys*** 37:65-95.

192. Mazzola JL, Sirover MA (2002) Alteration of intracellular structure and function of glyceraldehyde-3-phosphate dehydrogenase: a common phenotype of neuro-degenerative disorders? ***Neurotoxicol*** 23(4-5):603-9.

193. Ishitani R, Tanaka M, Sunaga K, Katsube N, Chuang DM (1998) Nuclear localization of neurons undergoing apoptosis. ***Mol Pharmacol*** 53(4):701-7.

194. Fukuhara Y, Takeshima T, Kashiwaya Y, Shimoda K, Ishitani R, Nakashima K (2001) GAPDH knockdown rescues mesencephalic dopaminergic neurons from $MPP^+$-induced apoptosis. ***Neuroreport*** 12(9):2049-52.

195. Feo S, Arcuri D, Piddini E, Passantino R, Giallongo A (2000) ENO1 gene product binds to the c-myc promoter and acts as a transcriptional repressor: relationship with Myc promoter-binding protein 1 (MBP-1). ***FEBS Lett*** 473(1):47-52.

196. Gupta V, Bamezai RN (2010) Human pyruvate kinase M2: A multifunctional protein. ***Protein Sci*** 19(11): 2031-44.

197. Ruiz-Ortega M, Ruperez M, Lorenzo O, Esteban V, Blanco J, Mezzano S, Egido J (2002) Angiotensin II regulates the synthesis of proinflammatory cytokines and chemokines in the kidney. ***Kidney Int Suppl*** 82:S12-22.

198. de Gasparo M, Catt KJ, Inagami T, Wright JW, Unger T (2000) International union of pharmacology. XXIII. The angiotensin II receptors. ***Pharmacol Rev*** 52(3):415-72.

199. Kunert-Radek J, Stepień H, Komorowski J, Pawlikowski M (1994) Stimulatory effect of angiotensin II on the proliferation of mouse spleen lymphocytes *in vitro* is mediated via both types of angiotensin II receptors. ***Biochem Biophys Res Commun*** 198(3):1034-9.

200. Pawlikowski M, Meleń-Mucha G, Mucha S (1999) The involvement of the renin-angiotensin system in the regulation of cell proliferation in the rat endometrium. ***Cell Mol Life Sci*** 55(3):506-10.

201. Pawlikowski M, Gruszka A, Mucha S, Melen-Mucha G (2001) Angiotensins II and IV stimulate the rat adrenocortical cell proliferation acting via different receptors. ***Endocr Regul*** 35(3):139-42.

202. Pawlikowski M, Mełén-Mucha G, Mucha S (2001) The involvement of angiotensins in the control of prostatic epithelial cell proliferation in the rat. ***Folia Histochem Cytobiol*** 39(4):341-3.

203. Bu L, Qu S, Gao X, Zou JJ, Tang W, Sun LL, Liu ZM (2011) Enhanced angiotensin-converting enzyme 2 attenuates angiotensin II-induced collagen production via AT1 receptor-phosphoinositide 3-kinase-Akt pathway. ***Endocrine*** 39(2):139-47.

204. Le Noble FA, Hekking JW, Van Straaten HW, Slaaf DW, Struyker Boudier HA (1991) Angiotensin II stimulates angiogenesis in the chorio-allantoic membrane of the chick embryo. ***Eur J Pharmacol*** 195(2):305-6.

205. Munzenmaier DH, Greene AS (1996) Opposing actions of angiotensin II on microvascular growth and arterial blood pressure. ***Hypertension*** 27(3 Pt 2):760-5.

206. Walsh DA, Hu DE, Wharton J, Catravas JD, Blake DR, Fan TP (1997) Sequential development of angiotensin receptors and angiotensin I converting enzyme during angiogenesis in the rat subcutaneous sponge granuloma. ***Br J Pharmacol*** 120(7):1302-11.

207. Chow L, Rezmann L, Catt KJ, Louis WJ, Frauman AG, Nahmias C, Louis SN (2009) Role of the renin-angiotensin system in prostate cancer. ***Mol Cell Endocrinol*** 302(2):219-29.

208. Ino K, Shibata K, Kajiyama H, Nawa A, Nomura S, Kikkawa F (2006) Manipulating the angiotensin system--new approaches to the treatment of solid tumors. ***Expert Opin Biol Ther*** 6(3):243-55.

209. Deshayes F, Nahmias C (2005) Angiotensin receptors: a new role in cancer? ***Trends Endocrinol Metab*** 16(7):293-9.

210. Li W, Ye Y, Fu B, Wang J, Yu L, Ichiki T, Inagami T, Ichikawa I, Chen X (1998) Genetic deletion of AT2 receptor antagonizes angiotensinII-induced apoptosis in fibroblasts of the mouse embryo. ***Biochem Biophys Res Commun*** 250(1):72-6.

211. Cigola E, Kajstura J, Li B, Meggs LG, Anversa P (1997) Angiotensin II activates programmed myocyte cell death *in vitro*. ***Exp Cell Res*** 231(2):363-71.

212. Bhaskaran M, Reddy K, Radhakrishanan N, Franki N, Ding G, Singhal PC (2003) Angiotensin II induces apoptosis in renal proximal tubular cells. ***Am J Physiol Renal Physiol*** 284(5):F955-65.

213. Bonner JC (2004) Regulation of PDGF and its receptors in fibrotic diseases. ***Cytokine Growth Factor Rev*** 15(4):255-73.

214. Ostendorf T, Rong S, Boor P, Wiedemann S, Kunter U, Haubold U, van Roeyen CR, Eitner F, Kawachi H, Starling G, Alvarez E, Smithson G, Floege J (2006) Antagonism of PDGF-D by human antibody CR002 prevents renal scarring in experimental glomerulonephritis. ***J Am Soc Nephrol*** 17(4):105410-62.

215. Boor P, Konieczny A, Villa L, Kunter U, van Roeyen CR, LaRochelle WJ, Smithson G, Arrol S, Ostendorf T, Floege J (2007) PDGF-D inhibition by CR002 ameliorates tubulointerstitial fibrosis following experimental glomerulonephritis. ***Nephrol Dial Transplant*** 22(5):1323-31.

216. Eitner F, Bücher E, van Roeyen C, Kunter U, Rong S, Seikrit C, Villa L, Boor P, Fredriksson L, Bäckström G, Eriksson U, Ostman A, Floege J, Ostendorf T (2008)

PDGF-C is a proinflammatory cytokine that mediates renal interstitial fibrosis. ***J Am Soc Nephrol*** 19(2):281-9.

217. Piastowska-Ciesielska AW, Dominska K, Nowakowska M, Gajewska M, Gajos-Michniewicz A, Ochedalski T (2013) Angiotensin modulates human mammary epithelial cell motility. ***J Renin Angiotensin Aldosterone Syst*** 15(4):419-29.

218. Greco S, Muscella A, Elia MG, Salvatore P, Storelli C, Marsigliante S (2002) Activation of angiotensin II type I receptor promotes protein kinase C translocation and cell proliferation in human cultured breast epithelial cells. ***J Endocrinol*** 174(2):205-14.

219. Zhao Y, Chen X, Cai L, Yang Y, Sui G, Fu S (2010) Angiotensin II/angiotensin II type I receptor (AT1R) signaling promotes MCF-7 breast cancer cells survival via PI3-kinase/Akt pathway. ***J Cell Physiol*** 225(1):168-73.

220. Hunyady L, Catt KJ (2006) Pleiotropic AT1 receptor signaling pathways mediating physiological and pathogenic actions of angiotensin II. ***Mol Endocrinol*** 20(5):953-70.

221. Haendeler J, Berk BC (2000) Angiotensin II mediated signal transduction. Important role of tyrosine kinases. ***Regul Pept*** 95(1-3):1-7.

222. Uemura H, Ishiguro H, Nakaigawa N, Nagashima Y, Miyoshi Y, Fujinami K, Sakaguchi A, Kubota Y (2003) Angiotensin II receptor blocker shows antiproliferative activity in prostate cancer cells: a possibility of tyrosine kinase inhibitor of growth factor. ***Mol Cancer Ther*** 2(11):1139-47.

223. AbdAlla S, Lother H, Abdel-tawab AM, Quitterer U (2001) The angiotensin II AT2 receptor is an AT1 receptor antagonist. ***J Biol Chem*** 276(43):39721-6.

224. Dinh DT, Frauman AG, Johnston CI, Fabiani ME (2001) Angiotensin receptors: distribution, signalling and function. ***Clin Sci (Lond)*** 100(5):481-92.

225. Levy BI (2005) How to explain the differences between renin angiotensin system modulators. ***Am J Hypertens*** 18(9 Pt 2):134S-41S.

226. Domińska K, Piastowska AW, Rebas E, Lachowicz-Ochedalska A (2009) The influence of peptides from the angiotensin family on tyrosine kinase activity and cell viability in a human hormone-dependent prostate cancer line. ***Endokrynol Pol*** 60(5):363-9.

227. Chow L, Rezmann L, Imamura K, Wang L, Catt K, Tikellis C, Louis WJ, Frauman AG, Louis SN (2008) Functional angiotensin II type2 receptors inhibit growth factor signaling in LNCaP and PC3 prostate cancer cell lines. ***Prostate*** 68(6):651-60.

228. Green RS, Lieb ME, Weintraub AS, Gacheru SN, Rosenfield CL, Shah S, Kagan HM, Taubman MB (1995) Identification of lysyl oxidase and other platelet-derived growth factor-inducible genes in vascular smooth muscle cells by differential screening. ***Lab Invest*** 73(4):476-82.

229. Patton WF, Erdjument-Bromage H, Marks AR, Tempst P, Taubman MB (1995) Components of the protein synthesis and folding machinery are induced in vascular smooth muscle cells by hypertrophic and hyperplastic agents. Identification by comparative protein phenotyping and microsequencing. ***J Biol Chem*** 270(36):21404-10.

230. Saridaki A, Panayotou G (2005) Identification of growth factor-regulated proteins using 2D electrophoresis and mass spectrometry. ***Growth Factors*** 23(3):223-32.

231. Yang F, Chung AC, Huang XR, Lan HY (2009) Angiotensin II induces connective tissue growth factor and collagen I expression via transforming growth factor-beta-dependent and-independent Smad pathways: the role of Smad3. ***Hypertension*** 54(4):877-84.

232. Rupérez M, Sánchez-López E, Blanco-Colio LM, Esteban V, Rodríguez-Vita J, Plaza JJ, Egido J, Ruiz-Ortega M (2005) The Rho-kinase pathway regulates angiotensin II-induced renal damage. ***Kidney Int Suppl*** (99):S39-45.

233. Rodríguez-Vita J, Sánchez-López E, Esteban V, Rupérez M, Egido J, Ruiz-Ortega M (2005) Angiotensin II activates the Smad pathway in vascular smooth muscle cells by a transforming growth factor-beta-independent mechanism. ***Circulation*** 111(19):2509-17.

234. Finch JL, Suarez EB, Husain K, Ferder L, Cardema MC, Glenn DJ, Gardner DG, Liapis H, Slatopolsky E (2012) Effect of combining an ACE inhibitor and a VDR activator on glomerulosclerosis, proteinuria, and renal oxidative stress in uremic rats. ***Am J Physiol Renal Physiol*** 302(1):F141-9.

235. Schieffer B, Luchtefeld M, Braun S, Hilfiker A, Hilfiker-Kleiner D, Drexler H (2000) Role of NAD(P)H oxidase in angiotensin II-induced JAK/STAT signaling and cytokine induction. ***Circ Res*** 87(12):1195-201.

236. Xie Z, Singh M, Singh K (2004) ERK1/2 and JNKs, but not p38 kinase, are involved in reactive oxygen species-mediated induction of osteopontin gene expression by angiotensin II and interleukin-1beta in adult rat cardiac fibroblasts. ***J Cell Physiol*** 198(3):399-407.

237. Suzuki H, Frank GD, Utsunomiya H, Higuchi S, Eguchi S (2006) Current understanding of the mechanism and role of ROS in angiotensin II signal transduction. ***Curr Pharm Biotechnol*** 7(2):81-6.

238. Haugen EN, Croatt AJ, Nath KA (2000) Angiotensin II induces renal oxidant stress *in vivo* and heme oxygenase-1 *in vivo* and *in vitro*. ***Kidney Int*** 58(1):144-52.

239. Wang D, Chen Y, Chabrashvili T, Aslam S, Borrego Conde LJ, Umans JG, Wilcox CS (2003) Role of oxidative stress in endothelial dysfunction and enhanced responses to angiotensin II of afferent arterioles from rabbits infused with angiotensin II. ***J Am Soc Nephrol*** 14(11):2783-9.

240. Wolf G, Neilson EG (1993) Angiotensin II as a renal growth factor**.** ***J Am Soc Nephrol*** 3(9):1531-40.

241. Hod Y (2004) Differential control of apoptosis by DJ-1 in prostate benign and cancer cells. ***J Cell Biochem*** 92(6):1221-33.

242. Zhang HY, Wang HQ, Liu HM, Guan Y, Du ZX (2008) Regulation of tumor necrosis factor-related apoptosis-inducing ligand-induced apoptosis by DJ-1 in thyroid cancer cells. ***Endocr Relat Cancer*** 15(2):535-44.

243. Waak J, Weber SS, Waldenmaier A, Görner K, Alunni-Fabbroni M, Schell H, Vogt-Weisenhorn D, Pham TT, Reumers V, Baekelandt V, Wurst W, Kahle PJ (2009) Regulation of astrocyte inflammatory responses by the Parkinson's disease-associated gene DJ-1. ***FASEB J*** 23(8):2478-89.

244. Souza AC, Tsuji T, Baranova IN, Bocharov AV2, Wilkins KJ, Street JM, Alvarez-Prats A, Hu X1, Eggerman T, Yuen PS, Star RA (2015) TLR4 mutant mice are protected from renal fibrosis and chronic kidney disease progression. ***Physiol Rep*** 3(9). pii: e12558.

245. Yokota T, Sugawara K, Ito K, Takahashi R, Ariga H, Mizusawa H (2003) Down regulation of DJ-1 enhances cell death by oxidative stress, ER stress, and proteasome inhibition. ***Biochem Biophys Res Commun*** 312(4):1342-8.

246. Wilson MA, Collins JL, Hod Y, Ringe D, Petsko GA (2003) The 1.1-A resolution crystal structure of DJ-1, the protein mutated in autosomal recessive early onset Parkinson's disease. ***Proc Natl Acad Sci USA*** 100(16):9256-61.

247. Wei Y, Ringe D, Wilson MA, Ondrechen MJ (2007) Identification of functional subclasses in the DJ-1 superfamily proteins. ***PLoS Comput Biol*** 3(1):e10.

248. Macedo MG, Anar B, Bronner IF, Cannella M, Squitieri F, Bonifati V, Hoogeveen A, Heutink P, Rizzu P (2003) The DJ-1 L166P mutant protein associated with early onset Parkinson's disease is unstable and forms higher-order protein complexes. ***Hum Mol Genet*** 12(21):2807-16.

249. Moore DJ, Zhang L, Dawson TM, Dawson VL (2003) A missense mutation (L166P) in DJ-1, linked to familial Parkinson's disease, confers reduced protein stability and impairs homo-oligomerization. ***J Neurochem*** 87(6):1558-67.

250. Lakshminarasimhan M, Maldonado MT, Zhou W, Fink AL, Wilson MA (2008) Structural impact of three Parkinsonism-associated missense mutations on human DJ-1. ***Biochem*** 47(5):1381-92.

251. Bitar MS, Liu C, Ziaei A, Chen Y, Schmedt T, Jurkunas UV (2012) Decline in DJ-1 and decreased nuclear translocation of Nrf2 in Fuchs endothelial corneal dystrophy. ***Invest Ophthalmol Vis Sci*** 53(9):5806-13.

252. Jurkunas UV, Bitar MS, Funaki T, Azizi B (2010) Evidence of oxidative stress in the pathogenesis of Fuchs endothelial corneal dystrophy. ***Am J Pathol*** 177:2278-89.

253. Liu C, Chen Y, Kochevar IE, Jurkunas UV (2014) Decreased DJ-1 leads to impaired Nrf2-regulated antioxidant defense and increased UV-A-induced apoptosis in corneal endothelial cells. ***Invest Ophthalmol Vis Sci*** 55(9):5551-60.

254. Cuevas S, Yang Y, Konkalmatt P, Asico LD, Feranil J, Jones J, Villar VA, Armando I, Jose PA (2015) Role of nuclear factor erythroid 2-related factor 2 in the oxidative stress-dependent hypertension associated with the depletion of DJ-1. ***Hypertension*** 65(6):1251-7.

255. Yan YF, Chen HP, Huang XS, Qiu LY, Liao ZP, Huang QR (2015) DJ-1 Mediates the Delayed Cardio protection of Hypoxic Preconditioning Through Activation of Nrf2 and Subsequent Upregulation of Antioxidative Enzymes. ***J Cardiovasc Pharmacol*** 66(2):148-58.

256. Sun Q, Shen ZY, Meng QT, Liu HZ, Duan WN, Xia ZY (2015) The role of DJ-1/Nrf2 pathway in the pathogenesis of diabetic nephropathy in rats. ***Ren Fail*** [Epub ahead of print]

257. Liu F, Nguyen JL, Hulleman JD, Li L, Rochet JC (2008) Mechanisms of DJ-1 neuroprotection in a cellular model of Parkinson's disease. ***J Neurochem*** 105(6):2435-53.

258. Irrcher I, Aleyasin H, Seifert EL, Hewitt SJ, Chhabra S, Phillips M, Lutz AK, Rousseaux MW, Bevilacqua L, Jahani-Asl A, Callaghan S, MacLaurin JG, Winklhofer KF, Rizzu P, Rippstein P, Kim RH, Chen CX, Fon EA, Slack RS, Harper ME, McBride HM, Mak TW, Park DS (2010) Loss of the Parkinson's disease-linked gene DJ-1perturbs mitochondrial dynamics. ***Hum Mol Genet*** 19(19):3734-46.

259. Kamp F, Exner N, Lutz AK, Wender N, Hegermann J, Brunner B, Nuscher B, Bartels T, Giese A, Beyer K, Eimer S, Winklhofer KF, Haass C(2010) Inhibition of mitochondrial fusion by α-synuclein is rescued by PINK1, Parkin and DJ-1. ***EMBO J*** 29(20):3571-89.

260. Li HM, Niki T, Taira T, Iguchi-Ariga SM, Ariga H (2005) Association of DJ-1 with chaperones and enhanced association and colocalization with mitochondrial Hsp70 by oxidative stress. ***Free Radic Res*** 39(10):1091-9.

261. de Nobel H, Lawrie L, Brul S, Klis F, Davis M, Alloush H, Coote P (2001) Parallel and comparative analysis of the proteome and transcriptome of sorbic acid-stressed *Saccharomyces cerevisiae*. ***Yeast*** 18(15):1413-28.

262. van Genderen HO, Kenis H, Hofstra L, Narula J, Reutelingsperger CP (2008) Extracellular annexin A5: functions of phosphatidyl serine-binding and two-dimensional crystallization. ***Biochim Biophys Acta*** 1783(6):953-63.

263. Oling F, Santos JS, Govorukhina N, Mazères-Dubut C, Bergsma-Schutter W, Oostergetel G, Keegstra W, Lambert O, Lewit-Bentley A, Brisson A (2000) Structure of membrane-bound annexin A5 trimers: a hybrid cryo-EM-X-ray crystallography study. ***J Mol Biol*** 304(4):561-73.

264. Arur S, Uche UE, Rezaul K, Fong M, Scranton V, Cowan AE, Mohler W, Han DK (2003) Annexin I is an endogenous ligand that mediates apoptotic cell engulfment. ***Dev Cell*** 4(4):587-98.

# Acknowledgements

In the name of Allah; the most merciful, the most gracious. I am so grateful to Almighty Allah for His aid, clemency, and guidance throughout my life.

I would like to thank all great people who helped me to achieve this goal.

First, I wish to express my deep sense of gratitude to **Prof. Dr. Ernst Wimmer** for his convenient and understandable personality, facilitating all obstacles that would have hindered the accomplishment of this work. His insightful conversations and endless support are considerably appreciated.

My sincere thanks are due to **Prof. Dr. Uwe Groß** for his keen interest, personal attention and ceaseless encouragement.

I am honored to have them as my supervisors and appreciate their noble kindness.

I wish to express my sincere gratitude to **Prof. Dr. Hassan Dihazi** for his splendid guidance, fruitful scientific discussions and helpful comments during the entire course of my PhD work.

My sincere thanks to the members of the thesis committee; **Prof. Dr. Heidi Hahn**, **Prof. Dr. Rolf Daniel**, **PD Dr. Roland Dosch**, and **PD Dr. Michael Hoppert** for taking time out from their busy schedule to serve as my examiners and for their critical reading of my thesis.

I am thankful to **Prof. Dr. Gerhard A. Müller**, for giving me the opportunity to work at the Department of Nephrology and Rheumatology, University Medical Center. His kind hospitality is greatly acknowledged.

No words can truly express my deepest gratitude to **Elke Brünst-Knoblich** for her constant enthusiastic and supportive assistance.

I am thankful to all my lab mates for their friendship, discussions, advices, help and fabulous working environment.

Very special thanks go to **Prof. Dr. Abdul-Rahman Asif** and the proteomics laboratory technicians from the department of Clinical Chemistry specially, **Christina Wiese**, **Christa Schultz**, and **Susanne Goldmann** for the technical guidance and support in spectrometric analysis.

I offer special thanks to my little sweet family; husband, son, and daughter for their everlasting emotional and moral support. I am deeply indebted for their warmest and priceless loving, endless shore, and encouragement. I am unduly blessed having them in my life.

# Curriculum Vitae

## PERSONAL DATA

Family name: Eltoweissy

First name: Marwa

Place and date of birth: Alexandria, Egypt, 17.03.1966

Country of origin: Egypt

Postal address in Germany: Landwacht 6a, 37075 Göttingen

Email: eltoweissymar@yahoo.com

Telephone: 0176/62650074

## EDUCATION

Primary, Middle and Secondary School: EGC, Elnasr girls college, Alexandria, Egypt

Bachelor of Science: Faculty of Science, Alexandria University, Egypt

## CURRENT STUDIES IN GERMANY

Intended degree: Doctor rerum naturalium **(Dr. rer. nat.)**

Main Subject: Proteomics

Host University: Georg-August University Göttingen, Germany

Department: Nephrology and Rheumatology

Title of thesis: **Oxidative stress pathways in the pathogenesis of renal fibrosis: Multiple cellular stress proteins as regulative molecules and therapeutic targets.**

First Supervisor: Prof. Dr. Ernst Wimmer

Second Supervisor: Prof. Dr. Uwe Groß

## ACADEMIC CAREER/DEDGREES HELD

**1st Degree:** Master of Science (M.Sc.)
Main Subject: Physiology
University: University of Alexandria, Faculty of Science, Zoology department, Egypt
Duration of studies: Four Years
Degree result: Distinction

**2nd Degree:** Diploma-Biologist
Main Subject: Electrophysiology
University: University of Bonn, Faculty of Medicine, Institute of Physiology II, Germany
Duration of studies: Three Years
Degree result: Very good

**3rdDegree:** Doctor of Philosophy (Ph.D.)
Main Subject: Physiology
University: 1- University of Alexandria, Faculty of Science, Zoology department, Egypt

2- University of Bonn, Faculty of Medicine, Institute of Physiology II, Germany

Duration of studies: Four Years
Degree result: Distinction

**4thDegree:** Assist. Prof**.** (Present position in Egypt)
Main Subject: Physiology
University: University of Alexandria, Faculty of Science, Zoology department, Egypt

## PROFESSIONAL EXPERIENCE

**Employer/Organization:** Faculty of Science, Zoology department, Alexandria University

Position/Type of work: Demonstrator

Duration: Five years

**Employer/Organization:** Faculty of Science, Zoology department, Alexandria University

Position/Type of work: Assistant lecturer

Duration: Four years

**Employer/Organization:** Faculty of Medicine, Institute of Physiology II, Medical Department, Rheinischen Friedrich-Wilhelms University Bonn, Germany

Position/Type of work: Granted Ph.D. student in Channel System Program

Duration: Three years

**Employer/Organization:** Faculty of Science, Zoology department, Alexandria University

Position/Type of work: Lecturer

Duration: Five years

**Employer/Organization:** Faculty of Medicine, Gastroenterology and Endocrinology department, Georg-August University Göttingen, Germany

Position/Type of Work: Post-doctor Guest

Duration: One year

**Employer/Organization:** Faculty of Medicine, Nephrology and Rheumatology department, Georg-August University Göttingen, Germany

Position/Type of Work: Ph.D. fellow + Post-doctor Guest

Duration: Five years

## TEACHING SKILLS

- General Physiology for Pre-Pharmacy, Pre-Dentistry and 1st Year Biology students, Egypt

- Comparative animal Physiology for Bachelor Biology students, Egypt

- Proteomics for Master and Ph.D. students, Germany

## LIST OF PUBLICATIONS

1. **Eltoweissy M,** Müller GA, Bibi A, Nguyen PV, Dihazi GH, Müller AC, Dihazi H **(2011)** Proteomics analysis identifies PARK7 as an important player for renal cell resistance and survival under oxidative stress. ***Mol BioSyst*** 7(4):1277-88.

2. Bibi A, Agarwal NK, Dihazi GH, **Eltoweissy M,** Nguyen PV, Müller GA, Dihazi H **(2011)** Calreticulin is crucial for calcium homeostasis mediated adaptation and survival of thick ascending limb of Henle's loop cells under osmotic stress. ***Int J Biochem Cell Biol*** 43(8):1187-97.

3. Dihazi H, Dihazi GH, Müller AC, Lahrichi L, Asif AR, Bibi A, **Eltoweissy M**, Vasko R, Müller GA **(2011)** Proteomics characterization of cell model with renal fibrosis phenotype: Osmotic stress as fibrosis triggering factor**.** ***J Proteomic*** 74:304-18.

4. Pesic I, Dihazi GH, Müller GA, Jahn O, Hoffmann M, **Eltoweissy M,** Koziolek M, Dihazi H **(2011)** Short-time increase of glucose concentration in PDS results in extensive removal and high glycation level of vital proteins during continuous ambulatory peritoneal dialysis. ***Nephrol Dial Transplant*** 0: 1-10.

5. Dihazi H, Dihazi GH, Bibi A, **Eltoweissy M**, Müller CA, Asif AR, Rubel D, Vasko R, Müller GA **(2013)** Secretion of ERP57 is important for extracellular matrix accumulation and progression of renal fibrosis, and is an early sign of disease onset. ***J Cell Sci*** 126(Pt 16):3649-63.

6. Buchmaier BS, Bibi A, Müller GA, Dihazi GH, **Eltoweissy M**, Kruegel J, Dihazi H **(2013)** Renal cells express different forms of vimentin: The independent expression alteration of these forms is important in cell resistance to osmotic stress and apoptosis. ***PLoS One*** 8(7):e68301.

7. Pesic I, Müller GA, Baumann C, Dihazi GH, , Koziolek M, **Eltoweissy M,** Bramlage C, Asif AR, Dihazi H **(2013)** Cellulose membranes are more effective in holding back vital proteins and exhibit less interaction with plasma proteins during hemodialysis. ***Biochimica et Biophysica Acta 1834:*** 754-62.

8. Dihazi GH, Müller GA, Asif AR, **Eltoweissy M,** Wessels JT, Dihazi H **(2015)** Proteomic characterization of adrenal gland embryonic development reveals early initiation of steroid metabolism and reduction of the retinoic acid pathway. ***Proteome Sci*** 13:6.

9. **Eltoweissy M,** Dihazi GH, Müller GA, Asif AR, Dihazi H **(2016)** Protein DJ-1 and its anti-oxidative stress function play an important role in renal cells response to profibrotic agents. ***Mol Biosyst [In press].***

10. Trivedi R, Dihazi GH, **Eltoweissy M,** Mishra DP, Müller GA, Dihazi H **(2016)** PARK7 act as an antioxidant protein in clear cell renal cell carcinoma and induces cell resistance to Cisplatin-induced apoptosis. ***J Biomed Sci [In press].***

## LIST OF MANUSCRIPTS IN SUBMISSION STAGE

1. **Eltoweissy M**, Müller GA, Asif AR, Dihazi H. Comparative secretome analysis of renal cells treated with profibrotic agents.

2. Bibi A, **Eltoweissy M**, Asif AR, Müller GA, Dihazi H. Reduced calreticulin level results in oxidative stress mediated mitochondrial damage and kidney injury.

3. Dihazi GH, Jahn O, Tampe B, Zeisberg M, Müller C, **Eltoweissy M,** Müller GA, Dihazi H. Proteomic analysis of embryonic kidney development.

## ATTENDED CONGRESSES

1. **23. Jahrestagung der GASL, German Association for the Study of the Liver**, January 26-27, 2007, Göttingen, Germany.

2. **1. Jahrestagung der Deutschen Gessellschaft für Nephrologie,** September 26-29, 2009, Göttingen, Germany.

3. **XLVII ERA-EDTA Congress–II DGfN Congress,** June 25-28, 2010, Munich, Germany.

4. **Onkologisches Forum, Patienten Kongress. Eine Initiative des Patientenbeirates der Deutschen Krebshilfe,** September 25, 2010, Göttingen, Germany.

5. **Göttingen Proteomic Forum,** November 18, 2010, Göttingen, Germany.

6. **90th Annual Meeting of the German Physiological Society (DPG),** March 26-29, 2011, Regensburg, Germany.

7. **6th International Meeting of the Stem Cell Network North Rhine Westphalia,** April 05-06, 2011, Essen, Germany.

8. **10th HUPO World Congress 2011,** September 04-07, 2011, Geneva, Switzerland.

9. **3. Jahrestagung der Deutschen Gesellschaft für Nephrologie,** September 10-13, 2011, Berlin, Germany.

10. **American Society of Nephrology (ASN). Kidney week 2011,** November 08-13, 2011, Philadelphia, USA.

11. **30. Deutscher Krebs Kongress (DKG),** February 22-23, 2012, Berlin, Germany.

12. **4. Jahrestagung der Deutschen Gesellschaft für Nephrologie,** October 06-09, 2012, Hamburg, Germany.

13. **92nd Annual Meeting of the German Physiological Society, (DPG),** March 02-05, 2013, Heidelberg, Germany.

14. **5. Jahrestagung der Deutschen Gesellschaft für Nephrologie,** October 05-08, 2013, Berlin, Germany.

15. **32. Deutscher Krebs Kongress (DKG),** February 19-22, 2014, Berlin, Germany.

16. **93rd Annual Meeting of the German Physiological Society, (DPG),** March 13-15, 2014, Mainz, Germany.

17. **3rd International Conference on Nephrology and Therapeutics,** June 26-27, 2014 Valencia, Spain.

18. **6. Jahrestagung der Deutschen Gesellschaft für Nephrologie,** September 06-09, 2014, Berlin, Germany.

19. **5th International Conference on Proteomics and Bioinformatics,** September 01-03, 2015, Valencia, Spain.

20. **7. Jahrestagung der Deutschen Gesellschaft für Nephrologie,** September 12-15, 2015, Berlin, Germany.

## CONGRESS PRESENTATIONS

1. **Eltoweissy M**, Müller GA, Dihazi H. Proteomics characterization of proteins involved in oxidative stress response in renal interstitial fibroblasts. 1. Jahrestagung der Deutschen Gessellscaft für Nephrologie, September 26-29, 2009, Nephro News 38/9, P240, Göttingen, Deutschland.

2. **Eltoweissy M**, Müller GA, Bibi A, Dihazi H: Oxidative stress pathways in the pathogenesis of renal fibrosis: The role of the vasoactive compound angiotensin II (ANG II) and the platelet derived growth factor (PDGF). XLVII ERA-EDTA Congress-II DGfN Congress, June, 25-28, 2010, Nephrol. Dial. Transpl. Vol.3 Supplement 3 iii314, Munich, Germany.

3. Bibi A., Dihazi, GH, Van Nguyen P, Müller GA, **Eltoweissy M**, Dihazi H. Role of calreticulin (CRT) by regulating calcium homeostasis in the osmotic stress adaptation of thick ascending limb of Henle's loop (TALH) cells. XLVII ERA-EDTA Congress-II DGfN Congress, June, 25-28, 2010, Nephrol. Dial. Transpl. Vol. 3 Supplement 3 iii315, Munich, Germany.

4. **Eltoweissy M,** Müller GA, Dihazi H. Proteomics characterization of proteins involved in oxidative stress response in human renal cell lines (TK173 and HK-2). Göttingen Proteomic Forum, 18 November 2010, Poster presentation, Göttingen, Germany.

5. **Eltoweissy M**, Müller GA, Bibi A, Dihazi H. Proteomics analysis identifies PARK7 as an important player for renal cell resistance and survival under oxidative stress. 90th Annual Meeting of the German Physiological Society (DPG), March 26-29, 2011, P143, Regensburg, Germany.

6. **Eltoweissy M**, Dihazi GH, Bibi A, Müller GA, Dihazi H. Proteomics characterization of cell model with renal fibrosis phenotype: Osmotic stress as fibrosis triggering factor. 90th Annual Meeting of the German Physiological Society (DPG), March 26-29, 2011, P144, Regensburg, Germany.

7. **Eltoweissy M**, Müller, GA, Bibi A, Van Nguyen P, Dihazi GH, Müller CA, Dihazi H. Functional proteomics analysis identify PARK7 as an important player for renal cell resistance and survival under oxidative stress. 10th HUPO World Congress 2011, September 04-07, 2011, P502, Geneva, Switzerland.

8. **Eltoweissy M**, Müller GA, Vasko R, Von Jaschke AK, Asif AR, Dihazi H. Impact of Cisplatin administration on protein expression levels in renal cell carcinoma: A proteomic analysis. 3. Jahrestagung der Deutchen Gessellschaft für Nephrologie, September 10-13, 2011, DGfN Heft 03/2011, P274, Berlin, Deutschland.

9. Bibi A, Buchmeier B, **Eltoweissy M**, Dihazi GH, Müller GA, Dihazi H. Expression and reorganization of vimentin play a vital role in osmotic stress resistance of renal cells. 3. Jahrestagung der Deutchen Gessellschaft für Nephrologie, September 10-13, 2011, DGfN Heft 03/2011, P273, Berlin, Deutschland.

10. Dihazi GH, Pesic I, **Eltoweissy M**, Müller GA, Koziolek M, Jahn O, Dihazi H. Identification of four urine proteins as marker for diabetic nephropthy. 3. Jahrestagung der Deutchen Gessellschaft für Nephrologie, September 10-13, 2011, DGfN Heft 03/2011, P196, Berlin, Deutschland.

11. Bibi A, Dihazi GH, **Eltoweissy M**, Müller GA, Dihazi H. Renal epithelial cells suppress calreticulin expression to increase free calcium and adaptation to osmotic stress. American Society of Nephrology (ASN). Kidney week 2011, Philadelphia, PA, November 08-13, 2011, Philadelphia, USA.

12. **Eltoweissy M**, Bibi A, Dihazi GH, Müller GA, Asif AR, Dihazi H. PARK7 and PRDX6 as important players in cytokine induced renal cell transformation. 4. Jahrestagung der Deutschen Gesellschaft für Nephrologie, October 06-09, 2012, Hamburg, Deutschland.

13. Bibi A, **Eltoweissy M**, Dihazi GH, Müller GA, Dihazi H. Role of calreticulin, a calcium binding ER protein deficiency in the progression of renal glomerulosclerosis. 4. Jahrestagung der Deutschen Gesellschaft für Nephrologie, October 06-09, 2012, Hamburg, Deutschland.

14. Dihazi H, Dihazi GH, Bibi A, **Eltoweissy M**, Müller CA, Müller GA. ERP57 secretion as an important step in ECM accumulation and renal fibrosis progression. 4. Jahrestagung der Deutschen Gesellschaft für Nephrologie, October 06-09, 2012, Hamburg, Germany.

15. Dihazi GH, Müller GA, Jahn O, **Eltoweissy M**, Bibi A, Dihazi H. Proteomic mapping of embryonic kidney development: Role of heterochromatin binding proteins in nephrogenesis. 4. Jahrestagung der Deutschen Gesellschaft für Nephrologie, October 06-09, 2012, Hamburg, Deutschland.

16. **Eltoweissy M**, Dihazi GH, Müller GA, Asif AR, Dihazi H. PARK7 in the pathogenesis of renal fibrosis: The role of the vasoactive compound angiotensin II (ANG II) and the platelet

derived growth factor (PDGF). 92nd Annual Meeting of the German Physiological Society (DPG), March 02-05, 2013, Heidelberg, Germany.

17. **Eltoweissy M.** PARK7 in the pathogenesis of renal fibrosis: The role of the vasoactive compound Angiotensin II (ANG II) and the Platelet Derived Growth Factor (PDGF). 3rd International Conference on Nephrology and Therapeutics, June 26-27, 2014, Oral presentation, Valencia, Spain.

18. **Eltoweissy M**, Müller GA, Asif AR, Dihazi H. Comparative secretome analysis of renal cells treated with profibrotic agents. 6. Jahrestagung der Deutschen Gesellschaft für Nephrologie, September 06-09, 2014, Berlin, Deutschland.

19. **Eltoweissy M,** Müller GA, Asif AR, Dihazi H. Secretome proteomic analysis of renal cells treated with the pro-fibrotic agents ANG II, TGFß1 and PDGF: A comparative study. 5th International Conference on Proteomics and Bioinformatics, September 01-03, 2015, J. of Proteomics and Bioinformatics, P02, Valencia, Spain.

20. **Eltoweissy M,** Trivedi R, Dihazi GH, Müller GA, Dihazi H. PARK7 acts as an antioxidant protein in clear cell renal cell carcinoma and induces cell resistance to Cisplatin-induced apoptosis. 7. Jahrestagung der Deutschen Gesellschaft für Nephrologie, September 12-15, 2015, DGfN Heft 07/2015, P103, Berlin, Germany.

21. Noman H, Dihazi GH, **Eltoweissy M,** Müller GA, Dihazi H. Calreticulin is an important player in calcium homeostasis in kidney.7. Jahrestagung der Deutschen Gesellschaft für Nephrologie, September 12-15, 2015, DGfN Heft 07/2015, P99, Berlin, Germany.

22. Dihazi GH, Tampe B, Tampe D, **Eltoweissy M,** Müller GA, Dihazi H. Heterochromatin binding proteins as important regulator of the nephrogenesis. 7. Jahrestagung der Deutschen Gesellschaft für Nephrologie, September 12-15, 2015, DGfN Heft 07/2015, P101, Berlin, Germany.

## WORKSHOPS AND SYMPOSIA

1. Proteomics 2.0 Initiative 2011 (Neue Entwicklungen und methodische Möglichkeiten in der Proteom-Analyse, 31st May 2011 Göttingen/ Deutschland.

2. Göttinger Transport days, 16th and 17th October 2010 Göttingen/Germany.

3. An Integrated Approach to the Physiology of Organic Cation Transporters, 15th October 2010 Göttingen/Germany.

4. Symposium Nephrologie 2010, 27th March 2010 Göttingen/ Deutschland.

5. Laborautomation, Rationalisierung, Innovation-Zukunft im Labor, 18th-20th March 2010 Bad Sooden-Allendorf/ Deutschland.

6. Optical Imaging Workshop, 26th and 27th November 2009 Göttingen/Germany.

7. Falk Research Workshop. Morphogenesis and Cancerogenesis of the Liver, 25th and 26th January 2007 Göttingen/Germany.

## COURSES

1. Introduction to MASCOT, 2nd December 2010 Göttingen, Germany.

2. Introduction to Laboratory Animal Science, 25th February-2nd March 2011, Central animal facility, University medical center, Göttingen, Germany.

3. Laser capture microdissection coupled with mass spectrometery, Eurokup Training School, May 25-27, 2011, Rotterdam, Netherlands.